DESIGN, SYNTHESIS, AND BIOLOGICAL EVALUATION OF NOVEL ANTIMICROBIALS FOR BIOFILM ERADICATION

by

Isurika Buddhini Wattegedara

A dissertation submitted in partial fulfillment
of the requirements for the degree

of

Master of Science

in

Chemistry

MONTANA STATE UNIVERSITY
Bozeman, Montana

July 2024

DEDICATION

I dedicated this dissertation to my parents, whose support and encouragement have been the foundation of my journey. Their love and belief in me made this achievement possible.

ACKNOWLEDGEMENTS

I would like to express my sincere gratitude to Dr. Tom Livinghouse for believing in my potential and for fostering an environment of learning and discovery. I am deeply thankful for the knowledge and skills I gained under his mentorship and his patience and encouragement throughout this journey.

A special thanks to Dr. Mary Cloninger for invaluable feedback and kind, supportive words of encouragement throughout this journey. I am also profoundly grateful to Dr. David Fialho for his unwavering support and inspiring guidance.

I would also like to thank my colleagues and fellow researchers in the lab for their support in making this happen. Lastly, I extend my heartfelt appreciation to my family and friends for their unwavering support and understanding throughout this journey.

TABLE OF CONTENTS

TABLE OF CONTENTS CONTINUED

LIST OF FIGURES

Figure Page

LIST OF FIGURES CONTINUED

LIST OF FIGURES CONTINUED

LIST OF FIGURES CONTINUED

LIST OF FIGURES CONTINUED

LIST OF FIGURES CONTINUED

LIST OF FIGURES CONTINUED

LIST OF FIGURES CONTINUED

ABSTRACT

The National Institutes of Health reports that biofilms account for 80% of all infections caused by microorganisms and play a substantial role in infections acquired in healthcare settings among humans. Considering the antimicrobial resistance observed toward commercially available antimicrobials, it is crucial to identify effective treatment alternatives for infections associated with biofilms. Small molecule adjuvants show promise in broadening the range of treatment options by enhancing effectiveness against both gram-positive and gram-negative bacteria. A new series of pyrimidotriazine derivatives have been synthesized as novel antimicrobial agents. Their antimicrobial efficacy was assessed against Methicillin-Resistant *Staphylococcus aureus* (MRSA USA300 LAC) and multidrug-resistant *Pseudomonas aeruginosa* (PA14) using Kirby-Bauer Disk Diffusion assays. Investigation of antibacterial screening data indicated that pyrimidotriazine compounds show higher inhibition against PA14 than MRSA at 100 mM in DMSO. An optimized synthetic route has been developed to prepare these compounds with high efficiency. Furthermore, tetrahydroimidazo[1,2-a]pyrimidinium derivatives, synthesized via the hydrogenation of imidazo[1,2-a]pyrimidinium salts, also exhibit high bioactivity against MRSA. 2-aminoimidazole heterocycle is a key pharmacophore that demonstrated its capabilities in inhibiting biofilm formation, dispersion, and resensitizes multi-drug-resistant bacterial strains to antibiotic treatments. A library of novel disubstituted 2-aminoimidazoles has been synthesized in excellent yields via an optimized route. The library was tested for the antibiofilm effect against Methicillin-resistant *Staphylococcus aureus* and *Pseudomonas aeruginosa* in Kirby-Bauer Disk Diffusion assays.

CHAPTER ONE

INTRODUCTION

The introductory chapter aims to establish the necessary foundation for this thesis. It emphasized the urgent need for new antimicrobial agents aimed at reducing the prevalence of infections caused by biofilms. Furthermore, it outlines the structure of the thesis, giving a brief overview of each chapter.

1.1 General Background

Biofilms are described as spatially organized multicellular clusters of microbes that adhere to solid biotic or abiotic surfaces.[1] The extracellular polymeric substances biofilms produce cause them to form tightly packed clusters. This disparate infrastructure is one of the main ways bacteria develop resistance to antibiotics. Furthermore, the dissemination of antibiotic-resistance genes among various pathogenic bacteria, combined with the absence of new antibiotics, has resulted in many infections becoming multidrug-resistant (MDR) and challenging to treat.[2] More than 80% of bacterial infectious diseases are related to biofilms, including wound infections, endocarditis, cystic fibrosis pneumonia, implant-related infections, and dental caries, which are recurrent and chronic threats caused by biofilms.[3–5] The Centers for Disease Control and Prevention (CDC) estimated that over 2 million people in the United States alone are infected with antibiotic-resistant bacteria, leading to approximately 35,000 deaths annually.[6] Due to the complexity and severity of biofilm infections, conventional antibiotics are very limited in their ability to eradicate bacteria within them.[7] Therefore, new strategies are imperative to treat biofilm-related infections.

1.1.1 Formation & Architecture of Biofilms

The formation and development of biofilms include a series of steps, including transforming bacteria from their planktonic state to their sessile biofilm-producing state.[8] This formation process is controlled by temperature, pH, surface characteristics, hydrodynamic forces, quorum sensing, secondary messengers, and other signaling compounds.[9] There are five main stages in which bacteria form biofilms attached to any surface or layer.[8] Initially, planktonic bacteria attach reversibly to a pre-conditioned surface. As a biofilm develops by synthesizing extracellular polysaccharide substances (EPS), this attachment changes from reversible to irreversible. In the aftermath of the maturation of microcolonies into a biofilm, cells begin to disperse into the environment.[3]

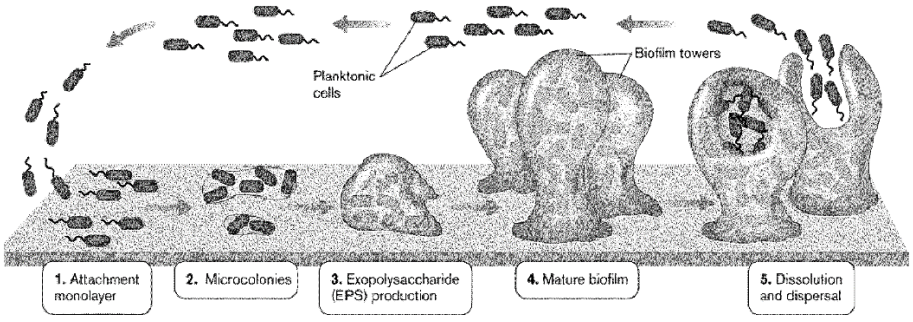

Figure 1: Five stages of biofilm development.[10]

The formation of biofilms begins with the adhesion of individual cells to material surfaces that are exposed to an aqueous medium, which leads to the formation of a conditioning layer. [11] In bacteria, external appendages like flagella, pili, and fimbriae help to overcome repulsive physical forces and reach the bulk lattice of the conditioning layer. This interaction stimulates chemical reactions and strengthens the bacteria-surface bond.[12] After initial interaction between bacteria and the surface has developed, weak interactions such as acid-base, hydrophobic, Van der Waals, and

electrostatic forces fuel this reversible adhesion.[13] At this stage, bacteria start secreting EPS facilitating microbial adhesion and forming bacterial cell aggregates on the substratum.[14] In the absence of physical or chemical intervention, the adhesion becomes irreversible.

Following irreversible attachment, bacterial cells proliferate and produce essential biofilm matrix components, forming micro-colonies.[15] These micro-colonies utilize nutrients from the surrounding fluid and conditioning film, which facilitate cell adhesion and maintain colony stability amidst environmental changes.[16] Concurrently, the necessity for motility of sessile cells decreases, leading to the inhibition of surface appendage production, while the expression of genes associated with cell surface proteins and secreted products increases.[17]

During the maturation stage of biofilm formation, initially adhered small colonies expand and accumulate debris and planktonic bacteria, leading to the development of a mature biofilm characteristic three-dimensional structure.[18] EPS is crucial in this phase, facilitating microbial adhesion, stabilizing the biofilm structure, binding cells, and protecting against stressors such as immune responses, antimicrobials, oxidative damage, and metallic cations. Quorum sensing (QS) is a cell signaling system used by biofilms in this stage enabling bacteria to coordinate group behavior.[3]

At the final phase, bacterial dispersal from biofilms occurs through cell shredding or detachment, influenced by factors such as nutrient limitation, fluid dynamics, shear effects in the bulk fluid, secretary proteins, changes in temperature and oxygen levels, metabolic accumulation, and the regulation of genes related to cell motility and EPS degradation.[3,9]

1.1.2 Biofilm-Related Infections

Biofilm-related infections can be acute or chronic, with chronic infections further categorized into device-related and non-device-related infections. Biofilm infections associated with the device were first demonstrated by Costerton et al. These infections are frequently seen in patients with medical implants such as urinary catheters, central venous catheters, and contact lenses.[19] In contrast, non-device-related infections are associated with areas like the respiratory system and are prevailing in immunocompromised patients[20]. According to National Institute of Health (NIH) statistics, microbial biofilms account for approximately 65 % of all microbiological infections in tissues and 80 % of persistent infections linked to medical implants.[9]

1.1.3 Biofilm Antibiotic Tolerance

Bacterial biofilm formation is associated with clusters of cells embedded in an extracellular polymeric matrix, providing bacteria a protective layer and shielding them from host defense mechanisms and some antibiotics.[21] Within biofilms, bacteria exhibit distinct phenotypic and gene expression profiles resulting in reduced metabolic rates and increased cell-to-cell communication.[22] Due to these adaptations, bacteria are less susceptible to chemical and physical stress, enhancing their potential to develop antibiotic resistance. The restricted oxygen diffusion within the biofilm creates an oxygen gradient, leading to anaerobic microenvironments.[23] The ESKAPE pathogens-*Enterobacter* species*, Staphylococcus aureus, Klebsiella pneumoniae, Acinetobacter baumannii, Pseudomonas aeruginosa,* and *Enterococcus faecium* are known for causing biofilm-mediated infections and are recognized as multi-drug resistant species.[24] Consequently, it has been reported that antibiotic resistance in biofilm-forming bacteria is 1000 times higher than in planktonic bacteria.[25] Due to the importance of biofilms in clinical settings,

there has been a focused effort within scientific and medical research to develop therapeutic strategies capable of mitigating biofilm formation.

1.1.4 Biofilm Control Strategies

Strategies to combat biofilms are primarily classified into two distinct approaches: biofilm inhibition to prevent their initial formation or dispersing mature biofilm. Anti-biofilm agents may either inhibit the transition of bacteria from a planktonic to a sessile state or destroy preformed biofilms via several mechanisms. (1) Inhibiting microbial adhesion to surfaces; (2) Inhibiting quorum sensing (QS) systems; (3) Hindering regulatory mechanisms such as nucleotide second messenger signaling system; and (4) Disrupting the architecture of existing biofilm communities.[26] To prevent microbial attachment one can, alter the surface by leaving unique 3D patterns or target physicochemical characteristics such as surface hydrophobicity.[27] Pre-conditioning the surfaces with chemicals like surfactants is a way to inhibit bacterial adherence.[28] Quorum sensing (QS) process is a chemical communication process that coordinates the collective behaviors of bacteria. It operates through a gene expression system regulated by self-produced signaling molecules called autoinducers.[26] Once these molecules accumulate to a threshold concentration, depending on cell density, bacterial communities activate genes associated with pathogenesis, including those involved in biofilm formation. Disabling the QS system with small molecules is considered a promising therapeutic strategy to inhibit bacterial pathogenicity.[26]

The second messenger cyclic di-GMP (C-di-GMP) plays a significant role in biofilm formation by stimulating the biosynthesis of adhesins, adhesive pili, and EPS substances and by inhibiting bacterial motility while Sortase A (SrtA) is a membrane transpeptidase critical for Gram-positive bacterial pathogenesis by anchoring surface-exposed proteins to the cell wall envelope,

facilitating adhesion, evasion of host defenses, and biofilm formation.[29] Hence, C-di-GMP and SrtA are promising targets for anti-infective drugs.

1.1.5 Current Therapeutic Applications for Biofilm Inhibition

The two primary techniques for biofilm eradication involve surgical debridement and antimicrobial therapy. These approaches do, however, have significant limitations. In clinical practice, antibiotic therapy is widely used; nevertheless, its efficacy is compromised by the emergence of antibiotic-resistant bacteria and the development of biofilms, both of which undermine their therapeutic potency.

1.1.6 Adjuvant Approach

Antibiotic adjuvants have emerged as a promising strategy to combat multi-drug-resistant bacteria. As a therapeutic strategy, molecules that inhibit and disperse biofilms through non-microbicidal mechanisms will be most likely to act as adjuvants to traditional antibiotics.[5] These anti-biofilm molecules will keep the bacteria in their susceptible planktonic state, allowing conventional antibiotics and immune response to eliminate the biofilm effectively. [30] Adjuvants help to lower the minimum inhibitory concentration of antibiotics, allowing for lower antibiotic doses and potentially reducing dose-dependent toxicity.[31,32]

Melander et al. developed an array of novel molecular scaffolds of 2-aminoimidazole (2-AI) derivatives as anti-biofilm agents which mimic guanidine found in various natural alkaloids including Bromoageliferin and Oroidin, both isolated from the marine sponge Agelas conifer. [33–37] These natural products are reported to inhibit and disperse bacterial biofilms via non-microbicidal mechanisms.[38,39] Subsequently, Melander et al. synthesized disubstituted analogues of 2-aminoimidazole/triazole conjugates (2-AIT) to improve antibiofilm activity. Despite enhanced

anti-biofilm activity against MRSA, many of these compounds also affected bacterial growth.[40] Roger et al. and Melander et al. introduced a novel group of hybrid anti-biofilm agents, incorporating 2-AI and methyl carbamate motifs. However, the introduction of carbamate functionality into 2-AI did not yield improvement in its biofilm modulation activity.[41] Steenackers et al. developed a library of anti-biofilm agents using the 5-aryl-2-aminoimidazole scaffold that was effective against Gram-positive and Gram-negative pathogens.[42] Recently, Kaur Gill et al. reported a library of polysubstituted 2-aminoimidazoles exhibiting potent anti-biofilm efficacy against the Gram-negative and Gram-positive bacteria with BIC_{50} values in the low micromolar range.[43] Frei and coworkers have shown that the 5,6-dimethoxy-2-aminoimidazole derivatives effectively inhibit and disperse *P. aeruginosa* biofilms.[44]

1.2 Project Overview

Over the last 60 years, only two new classes of antibiotics have been introduced to medical practice: lipopeptides and oxazolidinones, both targeting Gram-positive bacteria. Unfortunately, resistance to these drugs developed shortly after their introduction.[45,46] Gram-negative bacteria are naturally more resistant to many antibiotics, mainly due to the low permeability of their outer membrane. This has significantly contributed to the difficulty in discovering new antibiotics effective against Gram-negative in recent decades.[47] Our research aims to address these issues by developing a novel class of adjuvants targeting specific biochemical targets and designing new adjuvants that can potentially enhance the cell permeability of existing antibiotics for Gram-negative bacterial strains.

Methicillin-resistant *Staphylococcus aureus* (MRSA USA300 LAC) and multidrug-resistant *Pseudomonas aeruginosa* (PA14) are the two model bacterial strains used in our

biological studies as they are involved in biofilm formation and antibiotic resistance.[48] MRSA and PA14 are facultative anaerobes where MRSA is a Gram-positive bacterium, and PA14 is a Gram-negative bacterium.[49] These species possess antibiotic resistance due to low cell permeability, multiple efflux pumps, antibiotic-modifying enzymes, and resistance through mutational changes.[48]

In the initial study, a new series of pyrimidotriazines were synthesized, and their biological activity was evaluated against MRSA and PA14. Results have shown that pyrimidotriazine compounds show high potency against multidrug-resistant *Pseudomonas aeruginosa*. In the second study, we found a novel compound series of tetrahydroimidazo[1,2-a]pyrimidinium tetrafluororoborate salts effective against MRSA. In the third study, a new library of disubstituted 2-aminoimidazoles (2-AI) was synthesized. These 2-AI compounds were found to be effectively causing biofilms to disperse back into a more vulnerable planktonic phenotype.

CHAPTER TWO

DESIGN AND SYNTHESIS OF PYRIMIDOTRIAZINE DERIVATIVES: PROMISING CANDIDATES FOR NOVEL ANTIMICROBIAL AGENTS

Contribution of Authors and Co-Authors

Manuscript in Chapter 2

Author: Isurika B. Wattegedara

Contributions: Prepared manuscript and performed compound synthesis.

Co-Author: Amethyst R. Demeritte

Contributions: Performed biological evaluation studies and edited manuscript.

Co-Author: Heidi N. Koenig

Contributions: Performed compound synthesis.

Co-Author: Tom Livinghouse

Contributions: Directed compound design and synthesis, prepared manuscript, corresponding author.

Co-Author: Philip S. Stewart

Contributions: Designed biological evaluation experiments and provided laboratory space.

Co-Author: Garth A. James

Contributions: Designed biological evaluation experiments and provided laboratory space.

Manuscript Information

Isurika B. Wattegedara, Amethyst R. Demeritte, Heidi Koenig, Tom Livinghouse, Phil Stewart and Garth James.

Status of Manuscript:
☒ Manuscript in preparation
☐ Officially submitted to a peer-reviewed journal
☐ Accepted by a peer-reviewed journal
☐ Published in a peer-reviewed journal

2.1 Abstract

A new series of novel antimicrobial pyrimidotriazine derivatives were designed, synthesized, and evaluated. Their antimicrobial efficacy was assessed against multidrug-resistant *Pseudomonas aeruginosa* (PA14) and Methicillin-resistant *Staphylococcus aureus* (MRSA USA300 LAC) using Kirby-Bauer disk diffusion assays. The results from the antibacterial screening data indicate that the pyrimidotriazine compounds show higher inhibition against PA14 than MRSA at 100 mM in DMSO. An optimized synthetic route has been developed to prepare these compounds with high efficiency.

2.2 Introduction

The emergence of multidrug-resistant pathogenic bacteria poses a serious global health risk. According to the Centers for Disease Control and Prevention (CDC), over two million people in the United States acquire antibiotic-resistant infections every year, resulting in more than 23,000 deaths. Among ESKAPE pathogens (*Enterococcus faecium, Staphylococcus aureus, Klebsiella pneumoniae, Acinetobacter baumannii, Pseudomonas aeruginosa,* and *Enterobacter*) that are considered the greatest threat to human health, multidrug-resistant Gram-negative bacteria are a particular concern due to the current lack of efficacious treatments.[24] Current research focuses on developing small molecular adjuvants to overcome antibiotic resistance mechanisms. This approach offers an alternative strategy to developing new front-line antimicrobials.[50,51]

While the pyrimidotriazine class has not been explored as an antimicrobial agent, previous studies by Farghaly and coworkers involved the synthesis of pyrimidotriazines and assessing their efficacy as antihypertensive agents.[52] Additionally, Glover et al. outlined a synthetic route for

pyrimidotriazines, starting from 2-hydrazinopyrimidine and bromoacetone.[53] Here, we describe the use of pyrimidotriazines as potential antimicrobial agents. Preliminary data obtained from Kirby-Bauer disk diffusion (KBDD) assays indicate that these compounds exhibit significant activity against multidrug-resistant *Pseudomonas aeruginosa*. Structure-activity relationship (SAR) studies were subsequently conducted by varying substitution at the 5-position.

2.2.1 Antimicrobial Design and Synthesis

We previously developed a flexible synthetic route for the preparation of imidazo[1,2-a]pyrimidinium chlorides as intermediates for the synthesis of 2-aminoimidazoles. This route involved the preparation of imidazo[1,2-a]pyrimidinium bromide **3** by treating 2-aminopyrimidine **1** with the α-bromo ketone **2**, followed by subsequent dehydration with HCl in dioxane to yield the corresponding imidazo[1,2-a]pyrimidinium chloride **4** (Scheme 1). However, under the same conditions, the reaction of imidazo[1,2-a]pyrimidinium bromide **3a-f** unexpectedly gave 1,4-dihydropyrimidotriazinium chloride **6a-f** as the product (Scheme 2). We subsequently found that direct treatment of 2-hydrazinylpyrimidine with the appropriate 2-bromoaetophenones **2a-f** in 2-isopropanol directly led to a series of novel derivatives.

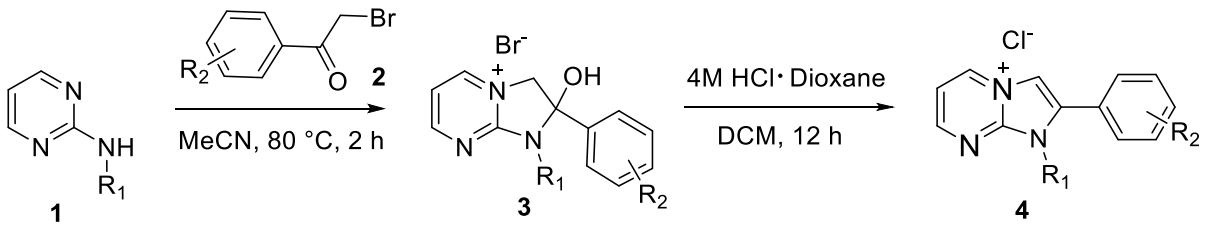

Scheme 1: Previous synthetic route to imidazo[1,2-a]pyrimidinium chloride, with varying R1 and R2 substituents.

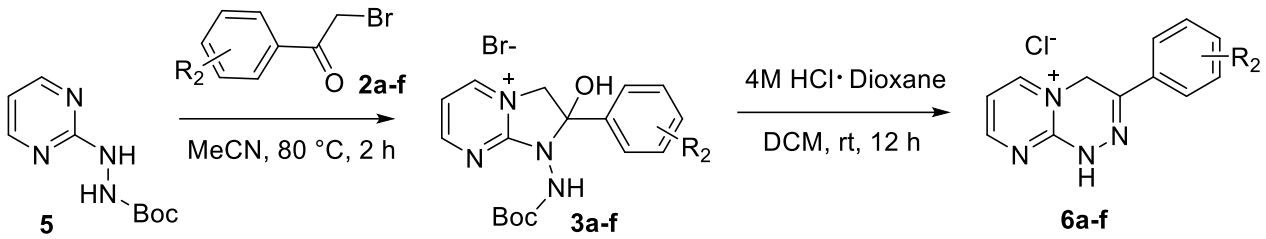

Scheme 2: Synthesis of 1,4-dihydropyrimidotriazinium salt using Boc-protected hydrazinylpyrimidine, R2 is shown in Figure 1.

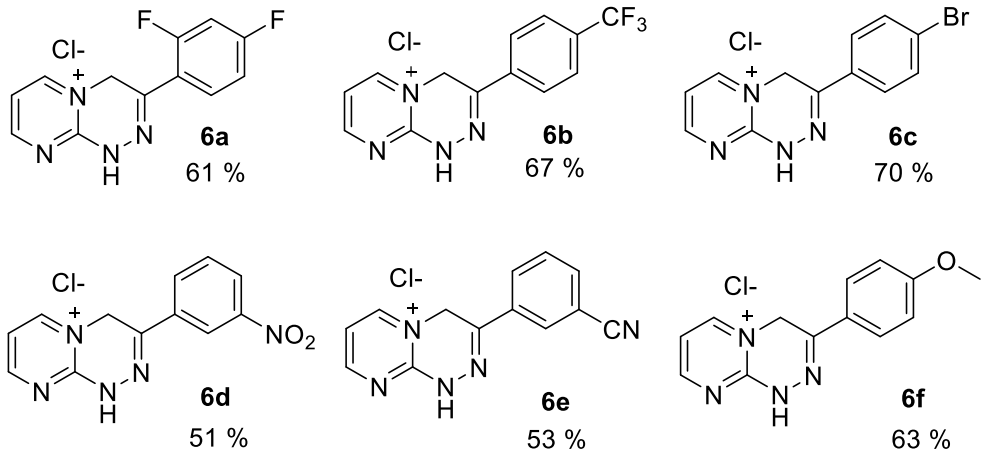

Figure 2.1: Synthesized 1,4-dihydropyrimidotriazinium chloride derivatives.

Glover et al. and Farghaly et al. earlier reported the synthesis of 1,4-dihydropyrimidotriazinium salts by treating 2-hydrazinopyrimidine with bromoacetone in ethanol in a single step.[52,53] We further explored using aprotic solvents, such as acetonitrile (MeCN) and tetrahydrofuran (THF). However, these attempts were unsuccessful. Our optimization results confirm that alkylation selectivity towards the desired core pyrimidine nitrogen is favored in protic solvents, enhancing the overall efficiency of the synthesis. Compared to the route previously used via imidazo[1,2-a]pyrimidinium hydroxy bromide salt intermediate, this new synthetic route comprises one step, which is more efficient.

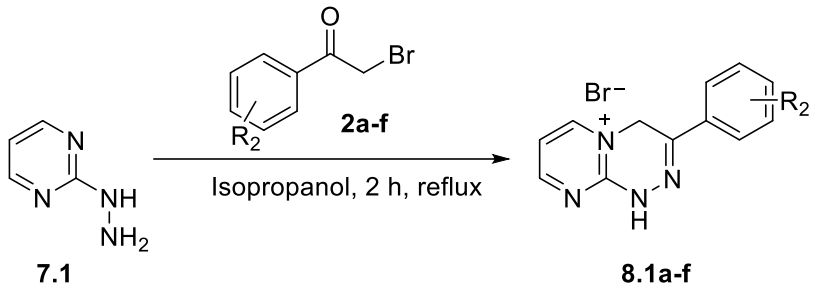

Scheme 3: Synthetic route to 1,4-dihydropyrimidotriazinium bromide, R_2 is shown in Figure 2.

To study the structure-activity relationship (SAR), we modified the N1 position of the pyrimidotraizine scaffold to create more analogues for screening. This approach is based on our experience with the 2-aminoimidazole scaffold, where functionalization of the N1 position of 2-aminoimidazoles led to enhanced potency against Gram-positive bacteria.

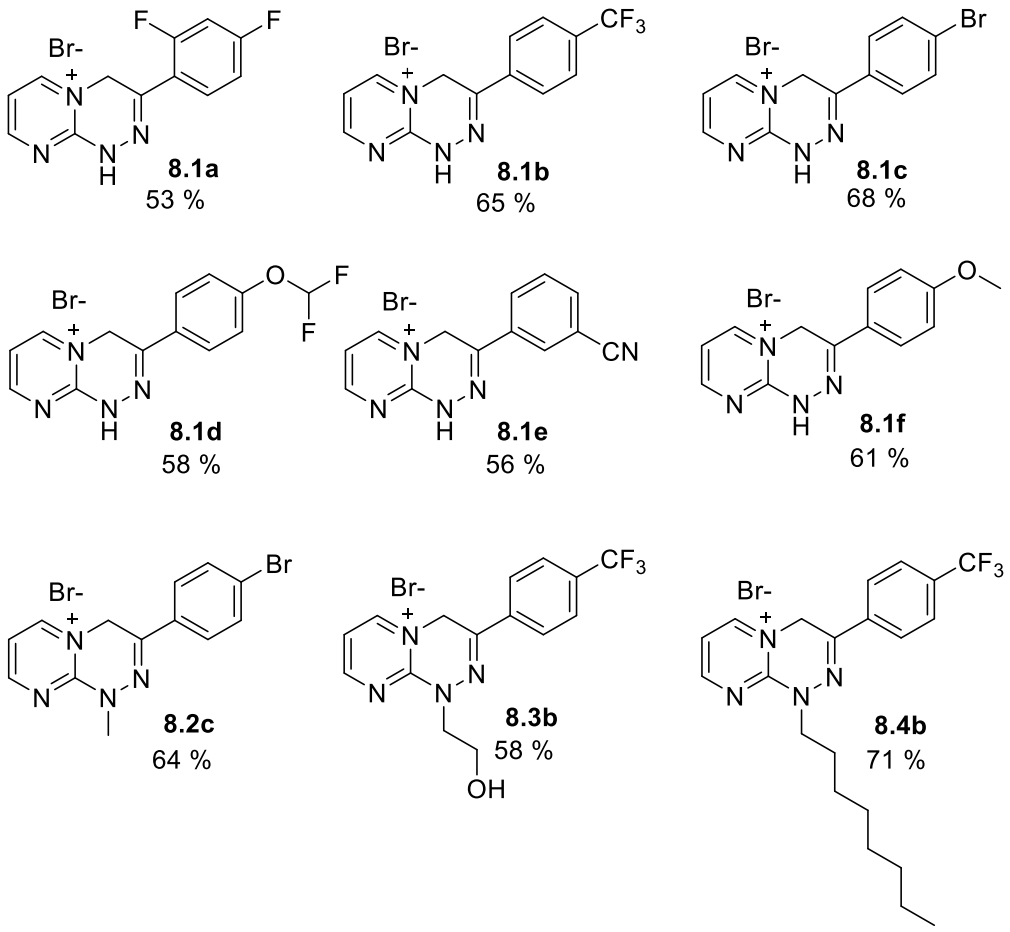

Figure 2.2: Synthesized 1,4-dihydropyrimidotriazinium bromide derivatives.

2.2.2. Biological Screening

Subsequently, the potential adjuvants were screened for their ability to inhibit biofilms of the medically relevant bacteria methicillin-resistant *Staphylococcus aureus* (MRSA) and multidrug-resistant *Pseudomonas aeruginosa* (PA14) via Kirby-Bauer disk diffusion assays.

2.3. Research Materials and Methods

2.3.1 Chemistry

All chemical reagents were purchased from commercially available sources (TCI America, Portland, OR, USA; Ambeed, Arlington Heights, IL, USA; and Sigma Aldrich, Burlington, NC, USA) and used without further purification, Moisture-sensitive reagents were distilled from CaH_2. Solvents utilized in filtrations, transfers, and chromatography were certified ACS grade. Thin-layer chromatography was performed on Silicycle Glass Backed TLC Extra Hard Layer, 60Å plates (thickness; 250 μm, indicator; F-254), and visualization was accomplished with UV light (254 nm), or potassium permanganate.

2.3.1.1 General Bromination for the Preparation of α-Brominated Acetophenones: A 100 mL round-bottomed flask equipped with a magnetic stirring bar and Polyseal cap was charged with the requisite acetophenone (16.6 mmol) and chloroform (30 mL) and stirred at room temperature. N-bromosuccinimide (3.25 g, 16.6 mmol) was added portion-wise, followed by TsOH (0.57 g, 3.32 mmol) and stirred at room temperature for 12 h. Water (20 mL) was added, and the organic layer was extracted with dichloromethane (3× 10 mL). The collected organic layer was dried over anhydrous Na2SO4, filtered, and concentrated. The obtained crude product was purified by column chromatography to yield α-bromoacetophenone as a crystalline solid.

2.3.1.2 General N-Alkylation Procedure for the Preparation of imidazo[1,2-a]pyrimidinium Hydroxy Bromide Salts: A 5 mL round-bottomed flask equipped with a magnetic stirring bar and reflux condenser was charged with the requisite aminopyrimidine (1 mmol), the requisite 2-bromoaceteophenone (1.2 mmol) and anhydrous MeCN (1 mL). The reaction mixture

was heated under reflux for 2 h. The product mixture was then diluted with diethyl ether (5 mL), filtered, and dried to provide the imidazo[1,2-a]pyrimidinium hydroxy bromide salt as a crystalline solid.

2.3.1.3 General Dehydration Procedure for the Preparation of imidazo[1,2-a]pyrimidinium chloride: A 10 mL round-bottomed flask equipped with a magnetic stirring bar and Polyseal cap was charged with the requisite imidazo[1,2-a]pyrimidinium hydroxy bromide salt (1 mmol) and DCM (2 mL). 4M HCl in dioxane (0.5 mL) was added, and the resultant reaction mixture was stirred at rt for 24 h. After completion, the solvent was removed in vacuo, followed by azeotropic drying with methanol to provide the imidazo[1,2-a]pyrimidinium chloride salt as a crystalline solid.

2.3.1.4 General Nucleophilic Aromatic Substitution for the Preparation of hydrazinylpyrimidine: A 50 mL round-bottom flask, equipped with a magnetic stirring bar and a Polyseal cap, was charged with the requisite hydrazine (10 mmol) and triethylamine (1.67 mL, 12 mmol) in methanol (6 mL), followed by the addition of 2-chloropyrimidine (1.32 g, 11.5 mmol). The reaction mixture was stirred at 23 °C for 20 h and then heated to 50 °C for an additional 3 h. 3 M NaOMe in methanol (3.83 mL, 11.5 mmol) was added, and the volatiles were evaporated. Subsequently, 1,4-dioxane (10 mL) was added, and the mixture was filtered, washed with 1,4-dioxane (2 × 2.5 mL), and dried to yield the product as a viscous liquid.

2.3.1.5. General N-alkylation procedure for the preparation of 1,4-dihydropyrimidotriazinium bromide: A 10 mL round-bottomed flask equipped with a magnetic stirring bar and reflux condenser was charged with 2-hydrazinylpyrimidine (1 mmol) and

deoxygenated isopropanol (5 mL). The requisite 2-bromoaceteophenone (1.2 mmol) was added to the reaction mixture and heated under reflux for 2 h. The progress of the reaction was monitored by TLC. After reaction completion, the resultant mixture was concentrated to half of its volume and then left to cool to rt. The obtained precipitate was filtered, washed with isopropanol, and dried to obtain the product as a crystalline solid.

2.3.2 Microbiology

2.3.2.1 Strains and Media Growth for Kirby-Bauer Assays: Biological evaluation was conducted against Pseudomonas aeruginosa (PA14) and Staphylococcus aureus (MRSA USA300 LAC). Overnight cultures were prepared by transferring single colonies from the plates into 25 mL tryptic soy broth (TSB) in Erlenmeyer flasks and incubating at 37 °C, 150 rpm for 16 h. Then, 10 µL of overnight cultures were transferred into 50 mL of TSB, vortexed, and standardized to 105–106 CFU/mL via absorbance readings at 600 nm for Pseudomonas aeruginosa (PA14). While 625 µL of overnight cultures were transferred into 50 mL of TSB, vortexed, and standardized to 108 CFU/mL (0.5 McFarland Standard) via absorbance readings at 600 nm for Staphylococcus aureus (MRSA USA300 LAC).

2.3.2.2 Kirby-Bauer Disk Diffusion (KBDD) Assays: Sterile 6 mm filter disks were impregnated with 20 µL of antimicrobial working concentrations diluted in DMSO. A 5-minute wait allowed for full absorption of the solutions. Polystyrene petri dishes (100 mm x 15 mm) were prepped as Mueller-Hinton (MH) agar plates to a level of 4 mm. The MH agar plates were inoculated (200 µL) with uniformity using a glass spreader. Once a confluent lawn of growth was attained, the plate was allowed to dry. Within 15 minutes, impregnated antimicrobial disks were

dispensed evenly (no less than 20 mm) from each other using sterile forceps. MH agar plates were incubated at 37 °C for 24 h under static conditions. Zones of inhibition were measured (in mm), and qualitative observations of the biofilm were recorded.

2.4 Results and Discussion

2.4.1 Chemistry

The synthesis of 1,4-dihydropyrimidotriazinium chloride follows a two-step route (Scheme 2). First, N-alkylation of α-brominated acetophenones is conducted, followed by a subsequent dehydration step using HCl in dioxane. During the dehydration step, Boc-deprotection occurs initially, followed by ring opening, making terminal nitrogen in the hydrazine more susceptible to nucleophilic attack. This rearrangement promotes the formation of a more stable pyrimidotriazine. Notably, the dehydration step is straightforward, requiring no additional workup, as the product obtained is pure and free of byproducts.

We developed a one-step protocol for synthesizing pyrimidotriazine salts by [54] (Scheme 3). This method significantly simplifies the synthesis, offering a more efficient pathway than the two-step route in Scheme 2. However, an additional recrystallization step with diethyl ether was necessary to optimize the yield.

2.4.2 Microbiology

Our preliminary screening of compounds via Kirby-Bauer disk diffusion assays revealed significantly higher bioactivity against multidrug-resistant *Pseudomonas aeruginosa* (PA14) than MRSA. Structure-activity relationships (SAR) studies facilitated the identification of lead

compounds within this batch, providing valuable insights into the molecular features contributing to their bioactivity.

In the chloride series, 2,4-difluorophenyl substituent **6a** at the 5-position of pyrimidotriazine exhibited the highest activity against PA14, with an inhibition zone of 20 mm (Graph 2.1). This series' next most effective salt was the para trifluoromethyl substituent **6b**, which demonstrated an inhibition zone of 19 mm. However, compound **6a** exhibited reduced bioactivity against MRSA, giving an inhibition zone of 12 mm, whereas **6b** demonstrated a more substantial inhibition zone of 18 mm. Compound **6e**, with meta-cyano functionalization, exhibited the lowest bioactivity against both bacterial strains.

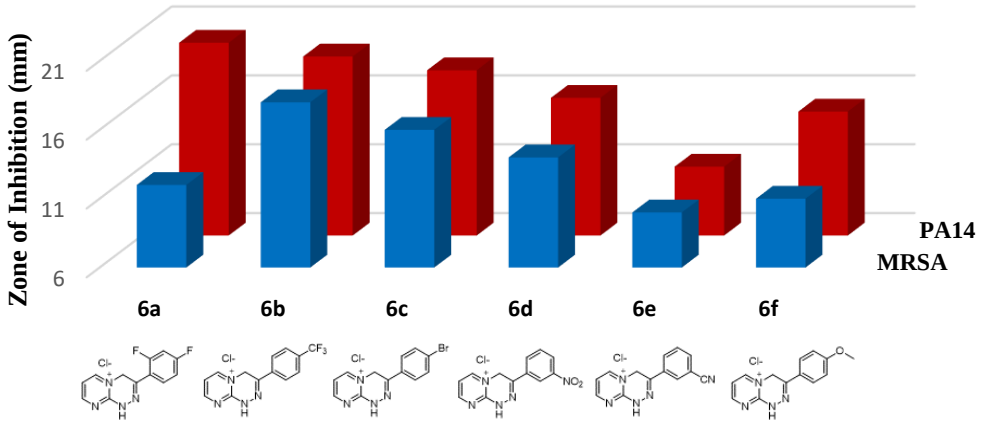

Figure 2.3: Correlation of 1,4-dihydropyrimido[1,2-a]triazinium chloride versus MRSA and P. aeruginosa biofilm inhibition. Diameters of the zones of inhibition were measured in mm and averaged across biological triplicates.

For the bromide series (Graph 2.2), the R_2 substituents did not follow the same SAR trends as the best of this series against PA14 was the para trifluoromethyl substituent **8.1b**, resulting in the remarkably high zone of inhibition of 26 mm. The para difluoromethoxy substituent **8.1d**

exhibited the highest activity against MRSA in this series, while the second highest against PA14 was observed. A methyl group at the N1 position **8.2c** resulted in a twofold decrease in bioactivity against PA14, while no significant change in bioactivity against MRSA was observed. Further tuning the length of the aliphatic chain at N1 did not result in a substantial increase in activity against PA14 but led to a drastic decrease in activity against MRSA.

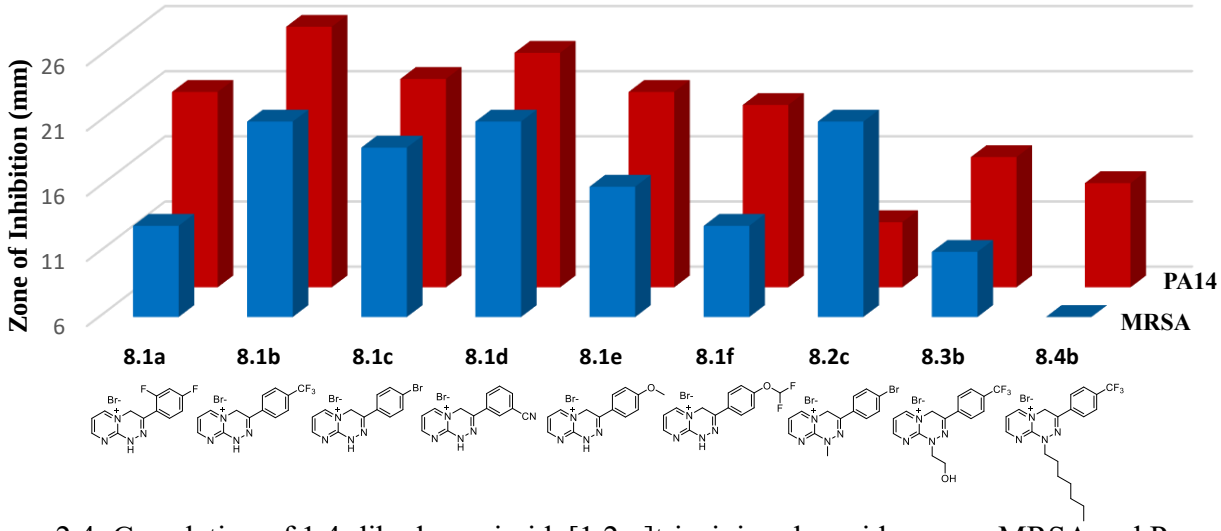

Figure 2.4: Correlation of 1,4-dihydropyrimido[1,2-a]triazinium bromide versus MRSA and P. aeruginosa biofilm inhibition. Diameters of the zones of inhibition were measured in mm and averaged across biological triplicates.

Overall, the Br- salts of pyrimidotriazine compounds showed higher activity against both bacterial strains than their chloride salts, indicating that bromide is a more effective counterion for antimicrobials. Additionally, almost all of our lead compounds contain fluorine substituents, demonstrating the significant potency of fluorine in enhancing antimicrobial efficacy.

2.5 Conclusions

We have introduced a new class of pyrimidotriazine agents that can inhibit biofilm formation. We have also developed a one-step synthetic route for forming these compounds in good yields. Given the promising antibiofilm activity displayed by these, we are continuing to develop additional derivatives based on the pyrimidotriazine core motif. Also, in future studies, identified lead compounds will be subjected to dose-response assays, including minimum inhibitory concentration (MIC) and minimum biofilm eradication concentration (MBEC) tests, to determine their IC_{50} values.

2.6 Conflicts of Interest

The authors declare no conflicts of interest.

2.7 Acknowledgements

This research was funded through generous external donations from Professor Tom Livinghouse.

CHAPTER THREE

CURRENT AND FUTURE STUDIES

3.1 SAR Studies of imidazo[1,2-a]pyrimidinium tetrafluoroborate salts

Steenackers and coworkers previously reported a method for synthesizing N1-substituted 2-aminoimidazoles from 2-aminopyrimidines through the formation of N1-substituted imidazo[1,2-a]pyrimidinium salts.[55] They utilized a microwave-assisted synthetic method followed by dehydration with polyphosphoric and perchloric acids to obtain the corresponding N1-substituted imidazo[1,2-a]pyrimidinium perchlorate salt.[55] Due to the strenuous reaction conditions and toxicity effects of perchlorate counterion in the human body, we modified the dehydration step by employing tetrafluoroboric acid diethyl etherate complex, resulting in the corresponding N1-substituted imidazo[1,2-a]pyrimidinium tetrafluoroborate salt (Scheme 1).

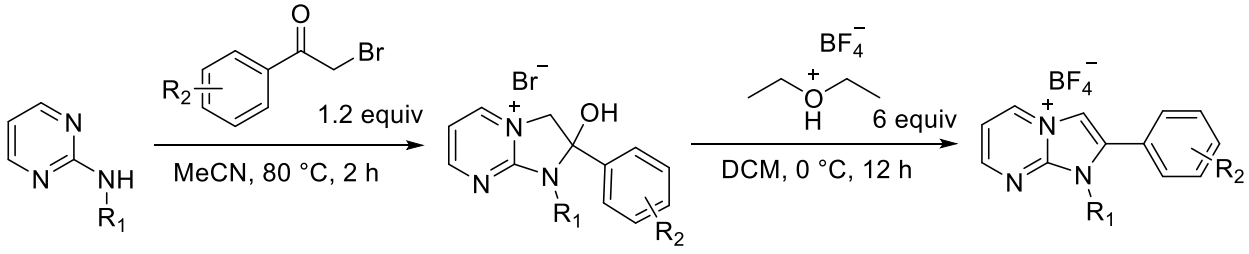

Scheme 1: Synthetic route of imidazo[1,2-a]pyrimidinium tetrafluoroborate salt.

As our previous work demonstrated that imidazo[1,2-a]pyrimidinium tetrafluoroborate salts possess antibacterial activity and variation at the N1 position can enhance bioactivity, we thought to continue exploring bioactivity by incorporating new R1 substituents at the N1 position (Figure 3.1.1).

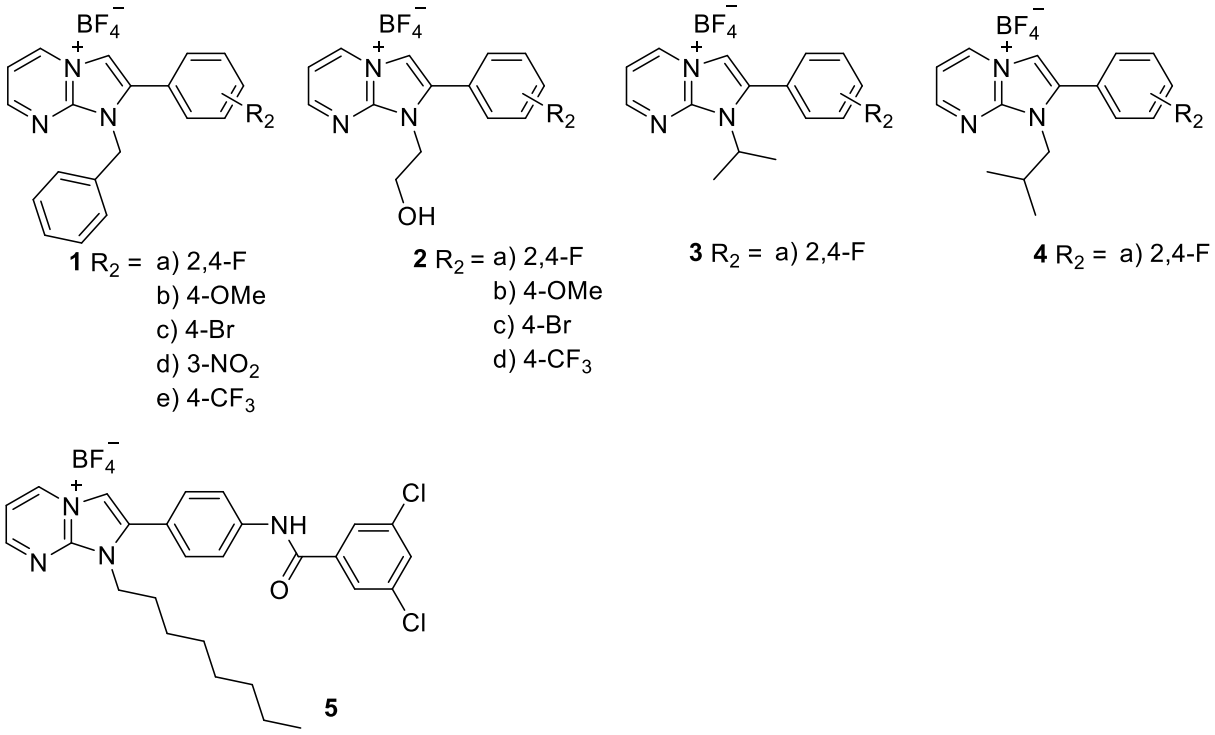

Figure 3.1.1: Imidazo[1,2-a]pyrimidinium tetrafluoroborate salts synthesized.

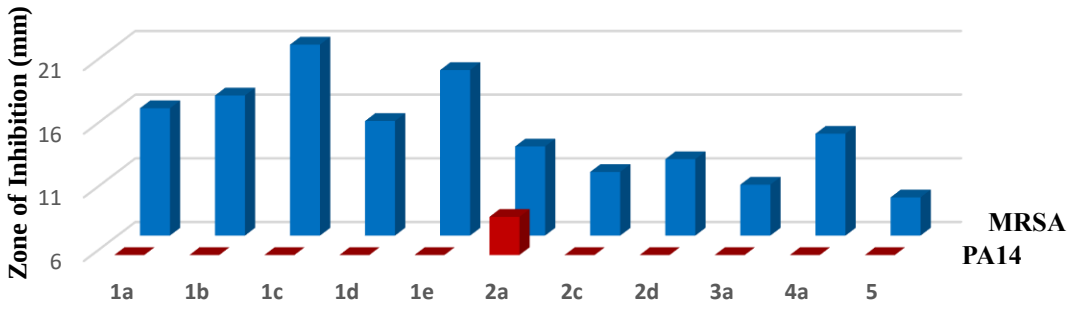

Figure 3.1.2: imidazo[1,2-a]pyrimidinium tetrafluoroborate salts versus MRSA and *P. aeruginosa* biofilm inhibition.

Subsequently, we refined the dehydration step by employing 4M HCl in dioxane to form the corresponding chloride salts directly. The resultant imidazo[1,2-a]pyrimidinium salt with chloride counterion was then evaluated for bioactivity, and it found that chloride salts are more potent against our bacterial strains than BF_4^- salts.

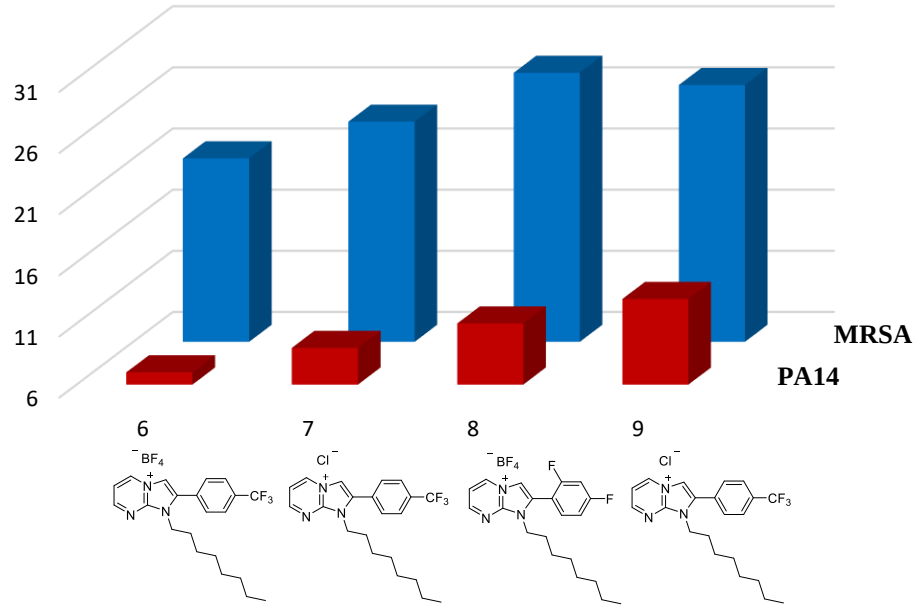

Figure 3.1.3: Correlation of tetrafluoroborate and chloride counterparts of imidazo[1,2-a]pyrimidinium salt versus MRSA and P. aeruginosa.

As no additional workup is required after the reaction completion, the product yield is comparatively higher than the chloride salt metathesis. These findings established the use of HCl in dioxane as a preferred dehydration agent in our subsequent synthesis of imidazo[1,2-a]pyrimidinium salts.

3.2 Tetrahydroimidizo[1,2-a]pyrimidinium tetrafluoroborate salts as antimicrobial agents

Inspired by Melander and coworkers' synthesis of dimeric 2-aminoimidazoles, which exhibit higher bioactivity compared to monomeric 2-aminoimidazoles, we are focusing on synthesizing the precursor for dimerization.[56] We aimed to produce a meta-substituted NH_2 derivative of imidazo[1,2-a]pyrimidinium salt via hydrogenation with palladium on carbon. In addition to the reduction of the meta-nitro group, the aromatic ring of the pyrimidinium was also reduced, leading to the discovery of a novel series of tetrahydroimidazo[1,2-a]pyrimidinium compounds (Scheme 2).

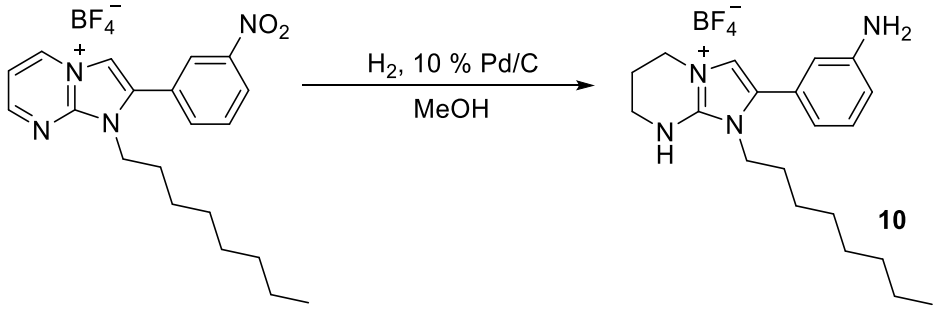

Scheme 2: Synthetic route of tetrahydroimidazo[1,2-α]pyrimidinium tetrafluoroborate salts.

Subsequent studies have involved modifying the aryl substituents and biologically evaluating these compounds against MRSA USA300 LAC using KBDD assays (Figure 3.2.1). The results indicated that the bioactivity of tetrahydroimidazo[1,2-α]pyrimidinium derivatives is slightly lower than that of the parent imidazo[1,2-α]pyrimidinium salt (Figure 3.2.2). Our ongoing work aims to expand this series by altering the N1 substituent to explore the SAR of these novel compounds.

Unlike their parent counterparts, the non-aromatic nature of tetrahydroimidazo[1,2-α]pyrimidinium derivatives has the potential to lower toxicity and improve tolerability in humans. Also, these derivatives could offer different mechanisms of action with potentially lower resistance development despite their slightly reduced potency. Therefore, we hypothesized that tetrahydroimidazo[1,2-a]pyrimidinium derivatives could serve as promising antimicrobial agents for controlling biofilm formation.

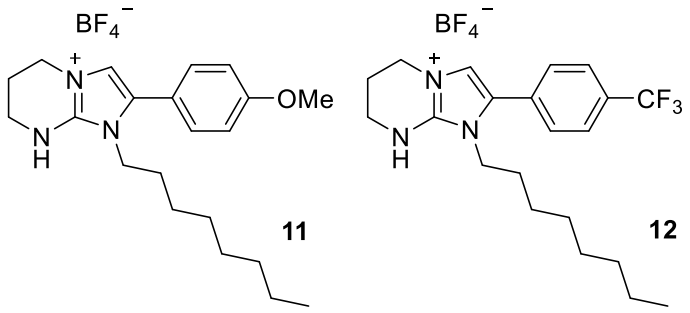

Figure 3.2.1: Synthesized tetrahydroimidazo[1,2-a]pyrimidinium tetrafluoroborate salts.

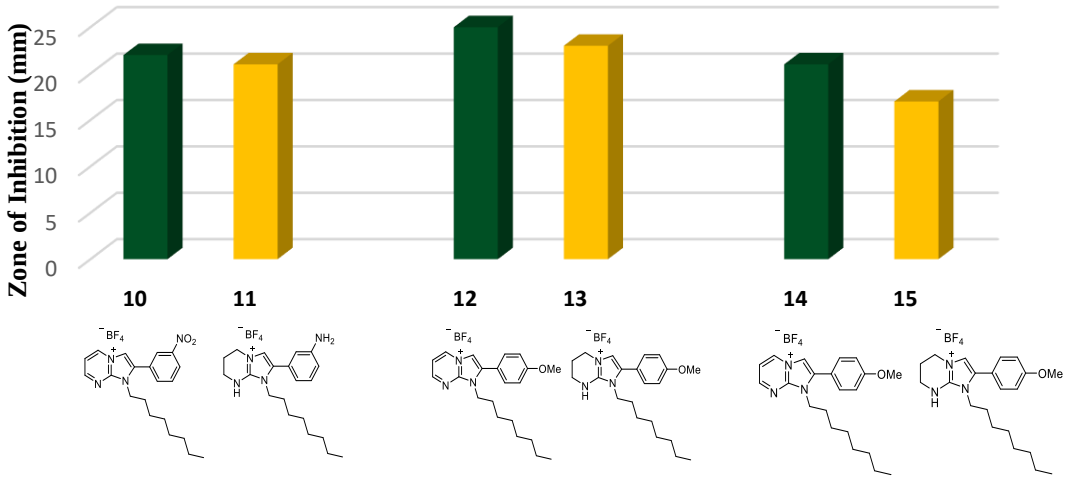

Figure 3.2.2: Correlation of imidazo[1,2-a]pyrimidinium and tetrahydroimidazole[1,2-a]pyrimidinium salts versus MRSA biofilm inhibition.

3.3 Novel imidazo[1,2-a]pyrimidinium Dimers

Drawing inspiration from the dimeric nature of 2-AI in the oroidin family, as seen for Bromoageliferin in Figure 3.3, Steenackers and Melander groups investigated the potential of dimers of the 2-AI derivatives as biofilm inhibitors.[56,57]

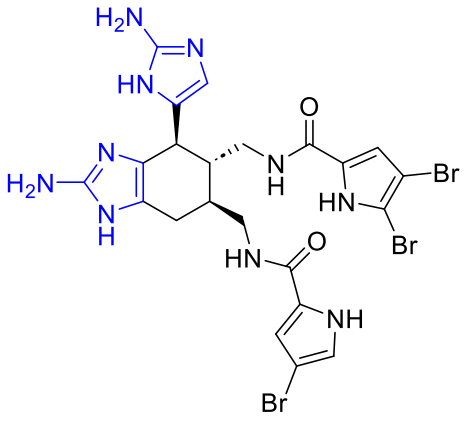

Figure 3.3: Structure of Bromoageliferin, a sponge-derived marine alkaloid with anti-biofilm properties.

Since the established synthetic route to dimerizing 2-AI proved unsuitable for our imidazo[1,2-α]pyrimidinium tetrafluoroborate salts, we designed a new route (Scheme 3).

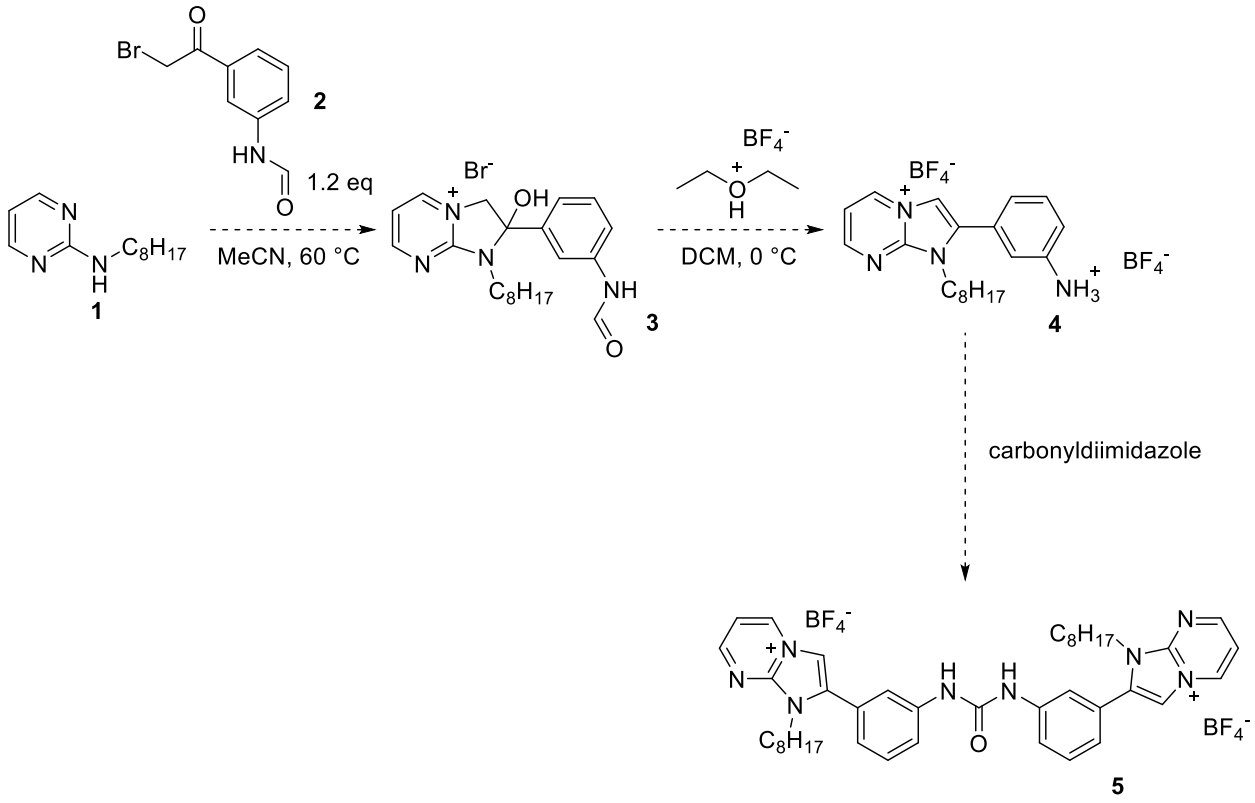

Scheme 3: Synthetic route to imidazo[1,2-a]pyrimidinium tetrafluoroborate salt dimers.

These new dimers will be employed in KBDD synergism assays in combination with conventional antibiotics to determine their effectiveness in resensitizing resistant bacterial strains.[56]

3.4 Studying synergistic effects between conventional antibiotics and pyrimidotriazine-derived antibiofilm agents.

As a therapeutic strategy, molecules that manage bacterial biofilms through non-microbicidal mechanisms are likely to work synergistically with conventional antibiotics,

effectively overcoming infections that would persist if treated with either agent alone.[58] KBDD assays were conducted for conventional antibiotics: Vancomycin, Novobiocin, and Tetracycline against MRSA and Ciprofloxacin and Colistin against PA14 at 100 mM concentrations. Future work will address studying the synergistic effect of lead pyrimidotriazine compounds with conventional antibiotics to re-sensitize bacteria to the antibiotic.

REFERENCES CITED

1. Laws, M.; Shaaban, A.; Rahman, K. M. Antibiotic Resistance Breakers: Current Approaches and Future Directions. *FEMS Microbiology Reviews*. Oxford University Press June 10, 2019, pp 490–516.

2. Doron, S. *B Bacterial Infections: Overview*.

3. Alotaibi, G. F. Factors Influencing Bacterial Biofilm Formation and Development. *Am J Biomed Sci Res* **2021**, *12* (6), 617–626.

4. Jensen, P.; Moser, C.; Kharazmi, A.; Presler, T.; Koch, C.; Høiby, N. Increased Serum Concentration of G-CSF in Cystic Fibrosis Patients with Chronic Pseudomonas Aeruginosa Pneumonia. *Journal of Cystic Fibrosis* **2006**, *5* (3), 145–151.

5. Davies, D. Understanding Biofilm Resistance to Antibacterial Agents. *Nature Reviews Drug Discovery*. February 2003, pp 114–122.

6. *Antibiotic Resistance Threats in the United States, 2019*; Atlanta, Georgia, 2019.

7. LewisOscar, F.; MubarakAli, D.; Nithya, C.; Priyanka, R.; Gopinath, V.; Alharbi, N. S.; Thajuddin, N. One Pot Synthesis and Anti-Biofilm Potential of Copper Nanoparticles (CuNPs) against Clinical Strains of Pseudomonas Aeruginosa. *Biofouling* **2015**, *31* (4), 379–391.

8. Srinivasan, R.; Santhakumari, S.; Poonguzhali, P.; Geetha, M.; Dyavaiah, M.; Xiangmin, L. Bacterial Biofilm Inhibition: A Focused Review of Recent Therapeutic Strategies for Combating the Biofilm Mediated Infections. *Frontiers in Microbiology*. Frontiers Media S.A. May 12, 2021.

9. Rather, M. A.; Gupta, K.; Mandal, M. Microbial Biofilm: Formation, Architecture, Antibiotic Resistance, and Control Strategies. *Brazilian Journal of Microbiology*. Springer Science and Business Media Deutschland GmbH December 1, 2021, pp 1701–1718.

10. US20240156788A1.

11. Donlan, R. M. *Biofilms: Microbial Life on Surfaces*; 2002; Vol. 8.

12. Garrett, T. R.; Bhakoo, M.; Zhang, Z. Bacterial Adhesion and Biofilms on Surfaces. *Progress in Natural Science*. Science Press 2008, pp 1049–1056.

13. Zhu, T.; Yang, C.; Bao, X.; Chen, F.; Guo, X. Strategies for Controlling Biofilm Formation in Food Industry. *Grain and Oil Science and Technology*. KeAi Communications Co. December 1, 2022, pp 179–186.

14. Dunne, W. M. Bacterial Adhesion: Seen Any Good Biofilms Lately? *Clinical Microbiology Reviews*. 2002, pp 155–166.

15. Singh, S.; Datta, S.; Narayanan, K. B.; Rajnish, K. N. Bacterial Exopolysaccharides in Biofilms: Role in Antimicrobial Resistance and Treatments. *Journal of Genetic Engineering and Biotechnology*. Springer Science and Business Media Deutschland GmbH December 1, 2021.

16. Sonnleitner, D.; Sommer, C.; Scheibel, T.; Lang, G. Approaches to Inhibit Biofilm Formation Applying Natural and Artificial Silk-Based Materials. *Materials Science and Engineering C* **2021**, *131*.

17. Sivadon, P.; Barnier, C.; Urios, L.; Grimaud, R. Biofilm Formation as a Microbial Strategy to Assimilate Particulate Substrates. *Environmental Microbiology Reports*. Wiley-Blackwell December 1, 2019, pp 749–764.

18. Han, A.; Lee, S. Y. An Overview of Various Methods for in Vitro Biofilm Formation: A Review. *Food Science and Biotechnology*. The Korean Society of Food Science and Technology October 1, 2023, pp 1617–1629.

19. Khatoon, Z.; McTiernan, C. D.; Suuronen, E. J.; Mah, T.-F.; Alarcon, E. I.; Alarcon Bacterial, E. I. Bacterial Biofilm Formation on Implantable Devices and Approaches to Its Treatment and Prevention. *Heliyon* **2018**, *4*, 1067.

20. Sauer, K.; Stoodley, P.; Goeres, D. M.; Hall-Stoodley, L.; Burmølle, M.; Stewart, P. S.; Bjarnsholt, T. The Biofilm Life Cycle: Expanding the Conceptual Model of Biofilm Formation. *Nature Reviews Microbiology*. Nature Research October 1, 2022, pp 608–620.

21. Payne, D. J. Microbiology: Desperately Seeking New Antibiotics. *Science*. September 19, 2008, pp 1644–1645.

22. Botto, M.; Fong, K. Y.; So, A. K.; Koch, C.; Costerton, J. W.; Stewart, P. S.; Greenberg, E. P. *Bacterial Biofilms: A Common Cause of Persistent Infections*; Walport, 1998; Vol. 64.

23. Stewart, P. S.; Franklin, M. J. Physiological Heterogeneity in Biofilms. *Nature Reviews Microbiology*. March 2008, pp 199–210.

24. Mulani, M. S.; Kamble, E. E.; Kumkar, S. N.; Tawre, M. S.; Pardesi, K. R. Emerging Strategies to Combat ESKAPE Pathogens in the Era of Antimicrobial Resistance: A Review. *Front Microbiol* **2019**, *10* (APR).

25. Mirghani, R.; Saba, T.; Khaliq, H.; Mitchell, J.; Do, L.; Chambi, L.; Diaz, K.; Kennedy, T.; Alkassab, K.; Huynh, T.; Elmi, M.; Martinez, J.; Sawan, S.; Rijal, G. Biofilms: Formation, Drug Resistance and Alternatives to Conventional Approaches. *AIMS Microbiology*. AIMS Press 2022, pp 240–278.

26. Shrestha, L.; Fan, H. M.; Tao, H. R.; Huang, J. D. Recent Strategies to Combat Biofilms Using Antimicrobial Agents and Therapeutic Approaches. *Pathogens*. MDPI March 1, 2022.

27. Kim, S.; Jung, U. T.; Kim, S. K.; Lee, J. H.; Choi, H. S.; Kim, C. S.; Jeong, M. Y. Nanostructured Multifunctional Surface with Antireflective and Antimicrobial Characteristics. *ACS Appl Mater Interfaces* **2015**, *7* (1), 326–331.

28. Pereira, M. O., Maia Machado, I., Simões, M., & Vieira, M. J. (2007). *Preventing biofilm formation using surfactants*.

29. Dsouza, F. P.; Dinesh, S.; Sharma, S. Understanding the Intricacies of Microbial Biofilm Formation and Its Endurance in Chronic Infections: A Key to Advancing Biofilm-Targeted Therapeutic Strategies. *Archives of Microbiology*. Springer Science and Business Media Deutschland GmbH February 1, 2024.

30. Gill, E. E.; Franco, O. L.; Hancock, R. E. W. Antibiotic Adjuvants: Diverse Strategies for Controlling Drug-Resistant Pathogens. *Chem Biol Drug Des* **2015**, *85* (1), 56–78.

31. Melander, R. J.; Melander, C. The Challenge of Overcoming Antibiotic Resistance: An Adjuvant Approach? *ACS Infect Dis* **2017**, *3* (8), 559–563.

32. Boyd, N. K.; Teng, C.; Frei, C. R. Brief Overview of Approaches and Challenges in New Antibiotic Development: A Focus on Drug Repurposing. *Frontiers in Cellular and Infection Microbiology*. Frontiers Media S.A. May 17, 2021.

33. Rogers, S. A.; Melander, C. Construction and Screening of a 2-Aminoimidazole Library Identifies a Small Molecule Capable of Inhibiting and Dispersing Bacterial Biofilms across Order, Class, and Phylum. *Angewandte Chemie - International Edition* **2008**, *47* (28), 5229–5231.

34. Minvielle, M. J.; Bunders, C. A.; Melander, C. Indole-Triazole Conjugates Are Selective Inhibitors and Inducers of Bacterial Biofilms. *Medchemcomm* **2013**, *4* (6), 916–919.

35. Richards, J. J.; Ballard, T. E.; Melander, C. Inhibition and Dispersion of Pseudomonas Aeruginosa Biofilms with Reverse Amide 2-Aminoimidazole Oroidin Analogues. *Org Biomol Chem* **2008**, *6* (8), 1356–1363.

36. Reyes, S.; Huigens, R. W.; Su, Z.; Simon, M. L.; Melander, C. Synthesis and Biological Activity of 2-Aminoimidazole Triazoles Accessed by Suzuki-Miyaura Cross-Coupling. *Org Biomol Chem* **2011**, *9* (8), 3041–3049.

37. Yeagley, A. A.; Su, Z.; McCullough, K. D.; Worthington, R. J.; Melander, C. N-Substituted 2-Aminoimidazole Inhibitors of MRSA Biofilm Formation Accessed through Direct 1,3-Bis(Tert-Butoxycarbonyl)Guanidine Cyclization. *Org Biomol Chem* **2013**, *11* (1), 130–137.

38. Yamada, A., Kitamura, H., Yamaguchi, K., Fukuzawa, S., Kamijima, C., Yazawa, K., Kuramoto, M., Wang, G. Y. S., Fujitani, Y., & Uemura, D. (1997). Development of Chemical Substances Regulating Biofilm Formation. *Bulletin of the Chemical Society of Japan*, *70*(12), 3061–3069.

39. Kelly, S., Jensen, P., Henkel, T., Fenical, W., & Pawlik, J. (2003). Effects of Caribbean sponge extracts on bacterial attachment. *Aquatic Microbial Ecology*, *31*, 175–182.

40. Su, Z.; Yeagley, A. A.; Su, R.; Peng, L.; Melander, C. Structural Studies on 4,5-Disubstituted 2-Aminoimidazole-Based Biofilm Modulators That Suppress Bacterial Resistance to β-Lactams. *ChemMedChem* **2012**, *7* (11), 2030–2039.

41. Rogers, S. A.; Lindsey, E. A.; Whitehead, D. C.; Mullikin, T.; Melander, C. Synthesis and Biological Evaluation of 2-Aminoimidazole/Carbamate Hybrid Anti-Biofilm and Anti-Microbial Agents. *Bioorg Med Chem Lett* **2011**, *21* (4), 1257–1260.

42. Steenackers, H. P. L.; Ermolat'Ev, D. S.; Savaliya, B.; Weerdt, A. De; Coster, D. De; Shah, A.; Van Der Eycken, E. V.; De Vos, D. E.; Vanderleyden, J.; De Keersmaecker, S. C. J. Structure-Activity Relationship of 2-Hydroxy-2-Aryl-2,3-Dihydro-Imidazo[1, 2-

a]Pyrimidinium Salts and 2N-Substituted 4(5)-Aryl-2-Amino-1H-Imidazoles as Inhibitors of Biofilm Formation by Salmonella Typhimurium and Pseudomonas Aeruginosa. *Bioorg Med Chem* **2011**, *19* (11), 3462–3473.

43. Gill, R. K.; Kumar, V.; Robijns, S. C. A.; Steenackers, H. P. L.; Van der Eycken, E. V.; Bariwal, J. Polysubstituted 2-Aminoimidazoles as Anti-Biofilm and Antiproliferative Agents: Discovery of Potent Lead. *Eur J Med Chem* **2017**, *138*, 152–169.

44. Frei, R.; Breitbach, A. S.; Blackwell, H. E. 2-Aminobenzimidazole Derivatives Strongly Inhibit and Disperse Pseudomonas Aeruginosa Biofilms. *Angewandte Chemie - International Edition* **2012**, *51* (21), 5226–5229.

45. Clatworthy, A. E.; Pierson, E.; Hung, D. T. Targeting Virulence: A New Paradigm for Antimicrobial Therapy. *Nature Chemical Biology*. Nature Publishing Group 2007, pp 541–548.

46. Coates, A. R.; Halls, G.; Hu, Y. Novel Classes of Antibiotics or More of the Same? LINKED ARTICLES. **2011**.

47. Hay, M., Thomas, D. W., Craighead, J. L., Economides, C., & Rosenthal, J. (2014). Clinical development success rates for investigational drugs. *Nature Biotechnology*, *32*(1), 40–51.

48. Krell, T.; Matilla, M. A. Pseudomonas Aeruginosa. *Trends in Microbiology*. Elsevier Ltd February 1, 2024, pp 216–218.

49. Rajkumari, N.; Mathur, P.; Bhardwaj, N.; Gupta, G.; Dahiya, R.; Behera, B.; Misra, M. C. Resistance Pattern of Mupirocin in Methicillin-Resistant Staphylococcus Aureus in Trauma Patients and Comparison between Disc Diffusion and E-Test for Better Detection of Resistance in Low Resource Countries. *J Lab Physicians* **2014**, *6* (02), 091–095.

50. Taylor, P. L.; Rossi, L.; De Pascale, G.; Wright, G. D. A Forward Chemical Screen Identifies Antibiotic Adjuvants in Escherichia Coli. *ACS Chem Biol* **2012**, *7* (9), 1547–1555.

51. Brackett, C. M.; Melander, R. J.; An, I. H.; Krishnamurthy, A.; Thompson, R. J.; Cavanagh, J.; Melander, C. Small-Molecule Suppression of β-Lactam Resistance in Multidrug-Resistant Gram-Negative Pathogens. *J Med Chem* **2014**, *57* (17), 7450–7458.

52. Farghaly, A. M.; AboulWafa, O. M.; Elshaier, Y. A. M.; Badawi, W. A.; Haridy, H. H.; Mubarak, H. A. E. Design, Synthesis, and Antihypertensive Activity of New Pyrimidine Derivatives Endowing New Pharmacophores. *Medicinal Chemistry Research* **2019**, *28* (3), 360–379.

53. Doughty, D. G.; Glover, E. E.; Vaughan, K. D. *N-Amination and Subsequent Oxidation of Imidazo[l,2-a]Pyrimidines*.

54. Steenackers, H. P. L.; Ermolatev, D. S.; Savaliya, B.; De Weerdt, A.; De Coster, D.; Shah, A.; Van Der Eycken, E. V.; De Vos, D. E.; Vanderleyden, J.; De Keersmaecker, S. C. J. Structure-Activity Relationship of 4(5)-Aryl-2-Amino-1 H -Imidazoles, N 1-Substituted 2-Aminoimidazoles and Imidazo[1,2- a]Pyrimidinium Salts as Inhibitors of Biofilm Formation by Salmonella Typhimurium and Pseudomonas Aeruginosa. *J Med Chem* **2011**, *54* (2).

55. Marrujo, S. A.; Hubble, V. B.; Yang, J.; Wang, M.; Nemeth, A. M.; Barlock, S. L.; Juarez, D.; Smith, R. D.; Melander, R. J.; Ernst, R. K.; Chang, M.; Melander, C. Dimeric 2-Aminoimidazoles Are Highly Active Adjuvants for Gram-Positive Selective Antibiotics against Acinetobacter Baumannii. *Eur J Med Chem* **2023**, *253*.

56. Trang, T. T. T.; Dieltjens, L.; Hooyberghs, G.; Waldrant, K.; Ermolat'ev, D. S.; Van der Eycken, E. V.; Steenackers, H. P. L. Enhancing the Anti-Biofilm Activity of 5-Aryl-2-Aminoimidazoles through Nature Inspired Dimerisation. *Bioorg Med Chem* **2018**, *26* (8), 1470–1480.

57. Rogers, S. A.; Huigens, R. W.; Cavanagh, J.; Melander, C. Synergistic Effects between Conventional Antibiotics and 2-Aminoimidazole-Derived Antibiofilm Agents. *Antimicrob Agents Chemother* **2010**, *54* (5), 2112–2118.

APPENDICES

APPENDIX A

FULL EXPERIMENTAL

All chemical reagents and conventional antibiotics were purchased from commercial sources (TCI America, Portland, OR, USA and Sigma Aldrich, Burlington, NC, USA) and used as received without further purification. Solvents utilized in filtrations, transfers, and chromatography were certified ACS grade. Thin-layer chromatography was performed on Silicycle Glass Backed TLC Extra Hard Layer, 60 Å plates (thickness; 250 µm, indicator; F-254) and visualization was accomplished with UV light (254 nm), and/or potassium permanganate. All synthesized compounds were characterized on a Bruker 500 MHz NMR Ascend Avance III HD (actively shielded) Spectrometer and a Bruker 600 MHz NMR Avance III NMR (actively shielded) Spectrometer. J values were depicted in hertz (Hz) and spin multiplicities were described as singlet (s), doublet (d), triplet (t), quartet (q), multiplet (m), and broad (b). Chemical shifts were reported in parts per million (δ), employing the solvent resonance as the internal standard.

Preparation of compounds in Chapter 2

2.1 A Preparation 1,4-dihydropyrimidotriazinium chloride derivatives

General procedure for dehydration

A 10 mL round-bottomed flask equipped with a magnetic stirring bar and Polyseal cap was charged with the requisite imidazo[1,2-a]pyrimidinium hydroxy bromide salt (1 mmol) and DCM (2 mL). To the reaction mixture 4M HCl in dioxane (0.5 mL) was added. The resultant reaction mixture was allowed to stir at rt for 24 h. After completion, the solvent was removed in vacuo followed by azeotropic drying with MeOH to provide the imidazo[1,2-a]pyrimidinium chloride salt as a crystalline solid.

2.1.1A Preparation of 3-(2,4-difluorophenyl)-1,4-dihydropyrimido[2,1-c][1,2,4]triazin-5-ium chloride de [**6a**]. The title compound was prepared according to the representative procedure on a 0.36 mmol scale, and **6a** was obtained as a yellow crystalline solid (0.061 g, 61 %); ^{1}H NMR (500 MHz, MeOD) δ 9.06 (dd, J = 4.6, 2.1 Hz, 1H), 8.56 (dd, J = 6.6, 4.5 Hz, 1H), 7.58 (m, 2H), 7.47 (dd, J = 6.6, 4.5 Hz, 1H), 7.20 (m, 2H), 5.53 (d, J = 1.8 Hz, 2H); ^{13}C NMR (126 MHz, MeOD) δ 116.7, 148.9, 147.9, 141.5, 130.7 (dd, J = 9.6, 3.2 Hz), 115.5, 112.3 (d, J = 3.6 Hz), 112.2 (d, J = 2.8 Hz), 104.4 (t, J = 27.3 Hz), 49.6 (d, J = 14.5 Hz); ^{19}F NMR (471 MHz, MeOD) δ -106.17 (p, J = 8.6 Hz), -109.93 (q, J = 10.4 Hz).

2.1.2A Preparation of 3-(4-(trifluoromethyl)phenyl)-1,4-dihydropyrimido[2,1-c][1, 2,4] tr iazin-5-ium chloride [**6b**]. The title compound was prepared according to the representative procedure on a 0.36 mmol scale, and **6b** was obtained as a yellow crystalline solid (0.076 g, 67 %); ^{1}H NMR (500 MHz, MeOD) δ 9.08 (dd, J = 4.4, 1.6 Hz, 1H), 8.65 (dd, J = 6.7, 1.6 Hz, 1H), 8.13 (d, J = 8.4 Hz, 2H), 7.88 (d, J = 8.4 Hz, 2H), 7.49 (dd, J = 6.7, 4.6 Hz, 1H), 5.65 (s, 2H); ^{13}C NMR (126 MHz, MeOD) δ 166.9, 148.7, 147.9, 143.2, 135.5, 132.4 (d, J = 34.0 Hz), 126.5, 125.5 (q, J = 4.5 Hz), 123.9 (d, J = 271 Hz), 115.4.

2.1.3A Preparation of 3-(4-bromophenyl)-1,4-dihydropyrimido[2,1-c][1,2,4]triazin-5-ium chloride [**6c**]. The title compound was prepared according to the representative procedure on a 0.22 mmol scale, and **6c** was obtained as a yellow crystalline solid (0.050 g, 70 %); ^{1}H NMR (500 MHz, MeOD) δ 9.05 (dd, J = 4.5, 2.0 Hz, 1H), 8.56 (dd, J = 6.5, 1.8 Hz, 1H), 7.85 (d, J = 8.7 Hz, 2H), 7.74 (d, J = 8.8 Hz, 2 H), 7.46 (dd, J = 6.5, 4.2 Hz, 1 H), 5.58 (s, 2H); ^{13}C NMR (126 MHz, MeOD) δ 166.7, 147.8, 143.6, 131.9, 130.9, 127.5, 125.6.

2.1.4A Preparation of 3-(3-nitrophenyl)-1,4-dihydropyrimido[2,1-c][1,2,4]triazin-5-ium chloride [**6d**]. The title compound was prepared according to the representative procedure on a 0.36 mmol scale, and **6d** was obtained as a yellow crystalline solid (0.054 g, 51 %); ^{1}H NMR (500 MHz, DMSO-d_6) δ 9.11 (dd, J = 4.4, 2.0 Hz, 1H), 8.67 (dd, J = 6.4, 1.8 Hz, 1H), 8.59 (t, J = 1.8 Hz, 1H), 8.42 (m, 1H), 8.25 (m, 1H), 7.88 (t, J = 7.9 Hz, 1 H), 7.57 (dd, J = 6.5, 4.6 Hz, 1H), 5.68 (s, 2H); ^{13}C NMR (126 MHz, MeOD) δ 167.1, 149.3, 148.8, 148.6, 143.4, 134.1, 132.7, 131.2, 126.1, 121.0, 116.2, 48.9.

2.1.5A Preparation of 3-(3-cyanophenyl)-1,4-dihydropyrimido[2,1-c][1,2,4]triazin-5-ium chloride [**6e**]. The title compound was prepared according to the representative procedure on a 0.78 mmol scale, and **6e** was obtained as a yellow crystalline solid (0.112 g, 53 %); ^{1}H NMR (500 MHz, (MeOD) δ 9.06 (dd, J = 4.6, 2.0 Hz, 1H), 8.57 (dd, J = 6.6, 1.8 Hz, 1H), 8.27 (s, 1H), 8.23 (m, 1H), 7.94 (m, 1H), 7.75 (t, J = 8.1 Hz, 1H), 7.48 (dd, J = 6.5, 4.4 Hz, 1H), 5.61 (s, 2H); ^{13}C NMR (126 MHz, MeOD) δ 166.8, 148.7, 147.9, 142.8, 134.2, 133.3, 130.1, 129.9, 129.5, 117.5, 115.4, 113.1.

2.2 A Preparation of 1,4-dihydropyrimidotriazinium bromide derivatives

2.2.1A Preparation of 3-(2,4-difluorophenyl)-1,4-dihydropyrimido[2,1-c][1,2,4]triazin-5-ium bromide [**8.1a**]. A 10 mL round-bottomed flask equipped with a magnetic stirring bar and reflux condenser was charged with 2-hydraznylpyrimidine (0.111 g, 1.0 mmol) and deoxygenated isopropanol (5 mL). The 2-bromo-1-(2,4-difluorophenyl)ethanone (0.282 g, 1.2 mmol) was added to the reaction mixture and heated under reflux for 2 h. The progress of the reaction was monitored by TLC. After reaction completion, the resultant mixture was concentrated to half of its volume and then left to cool to rt. The obtained precipitate was filtered, washed with isopropanol, and dried

to provide the bromide salt as a yellow crystalline solid (0.173 g, 53 %); ^{1}H NMR (500 MHz, MeOD) δ 9.05 (dd, J = 4.5, 1.9 Hz, 1H), 8.56 (dd, J = 6.5, 1.9 Hz, 1H), 7.97 (m, 1H), 7.46 (dd, J = 6.5, 4.5 Hz, 1H), 7.18 (m, 2H), 5.55 (s, 2H); ^{13}C NMR (126 MHz, MeOD) δ 116.7, 166.0 (d, J = 12.9 Hz), 163.9 (d, J = 12.9 Hz), 163.0 (d, J = 12.4 Hz), 161.0 (J = 11.9 Hz), 148.9, 147.9, 141.5 (d, J = 2.3 Hz), 130.7 (dd, J = 9.7, 4.4 Hz), 117.2 (dd, J = 11.3, 4.1 Hz), 115.6, 112.3 (d, J = 2.7 Hz), 112.2 (d, J = 3.4), 104.4 (t, J = 26.9 Hz), 49.6 (d, 13.9 Hz); ^{19}F NMR (471 MHz, MeOD) δ -106.18 (p, J = 8.6 Hz), -109.89 (q, J = 9.1 Hz).

2.2.2A Preparation of 3-(4-(trifluoromethyl)phenyl)-1,4-dihydropyrimido[2,1-c][1,2,4] tri azin-5-ium bromide [**8.1b**]. A 10 mL round-bottomed flask equipped with a magnetic stirring bar and reflux condenser was charged with 2-hydraznylpyrimidine (0.111 g, 1.0 mmol) and deoxygenated isopropanol (5 mL). The 2-bromo-1-(4-(trifluoromethyl)phenyl)ethanone (0.320 g, 1.2 mmol) was added to the reaction mixture and heated under reflux for 2 h. The progress of the reaction was monitored by TLC. After reaction completion, the resultant mixture was concentrated to half of its volume and then left to cool to rt. The obtained precipitate was filtered, washed with isopropanol, and dried to provide the bromide salt as a yellow crystalline solid (0.233 g, 65 %); ^{1}H NMR (500 MHz, MeOD) δ 9.06 (dd, J = 4.6, 2.0 Hz, 1H), 8.59 (dd, J = 6.6, 1.0 Hz, 1H), 8.12 (d, J = 8.3 Hz, 2H), 7.87 (d, J = 8.3 Hz, 2H), 7.48 (dd, J = 6.4, 4.4 Hz, 1H), 5.65 (s, 2H); ^{13}C NMR (126 MHz, MeOD) δ 166.9, 148.7, 147.9, 143.2, 135.5, 132.5, 132.2, 127.7, 126.5, 125.5 (q, J = 4.0 Hz), 124.9, 122.8, 115.4; ^{19}F NMR (471 MHz, MeOD) δ -64.52.

2.2.3A Preparation of 3-(4-bromophenyl)-1,4-dihydropyrimido[2,1-c][1,2,4]triazin-5-ium bromide [**8.1c**]. A 10 mL round-bottomed flask equipped with a magnetic stirring bar and reflux condenser was charged with 2-hydraznylpyrimidine (0.111 g, 1.0 mmol) and deoxygenated

isopropanol (5 mL). The 2-bromo-1-(4- bromophenyl)ethanone (0.333 g, 1.2 mmol) was added to the reaction mixture and heated under reflux for 2 h. The progress of the reaction was monitored by TLC. After reaction completion, the resultant mixture was concentrated to half of its volume and then left to cool to rt. The obtained precipitate was filtered, washed with isopropanol, and dried to provide the bromide salt as a yellow crystalline solid (0.252 g, 68 %); ^{1}H NMR (500 MHz, MeOD) δ 9.04 (dd, J = 4.4, 2.0 Hz, 1H), 8.57 (dd, J = 6.4, 1.8 Hz, 1H), 7.85 (m, 2H), 7.73 (m, 2H), 7.45 (dd, J = 6.6, 4.6 Hz, 1H), 5.59 (s, 2H); ^{13}C NMR (126 MHz, MeOD) δ 166.7, 148.7, 147.9, 143.6, 131.9, 131.0, 127.6, 125.6, 115.1.

2.2.4A Preparation of 3-(4-(difluoromethoxy)phenyl)-1,4-dihydropyrimido[2,1-c][1,2,4] triazin-5-ium bromide [8.1d]. A 10 mL round-bottomed flask equipped with a magnetic stirring bar and reflux condenser was charged with 2-hydraznylpyrimidine (0.111 g, 1.0 mmol) and deoxygenated isopropanol (5 mL). The 2-bromo-1-(4-(difluoromethoxy)phenyl)ethanone (0.318 g, 1.2 mmol) was added to the reaction mixture and heated under reflux for 2 h. The progress of the reaction was monitored by TLC. After reaction completion, the resultant mixture was concentrated to half of its volume and then left to cool to rt. The obtained precipitate was filtered, washed with isopropanol, and dried to provide the bromide salt as a yellow crystalline solid (0.207 g, 58 %); ^{1}H NMR (500 MHz, MeOD) δ 9.03 (dd, J = 4.4, 2.0 Hz, 1H), 8.57 (dd, J = 6.6, 2.0 Hz, 1H), 7.98 (m, 2H), 7.43 (dd, J = 6.4, 4.4 Hz, 1H), 7.31 (m, 2H), 6.99 (t, J = 73.6 Hz, 1H), 5.59 (s, 2H); ^{13}C NMR (126 MHz, MeOD) δ 116.6, 153.9, 148.7, 147.8, 143.6, 128.7, 127.8, 118.7, 118.0, 114.9 (t, J = 127.2 Hz)); ^{19}F NMR (471 MHz, MeOD) δ -84.44 (d, J = 72.9 Hz).

2.2.5A Preparation of 3-(3-cyanophenyl)-1,4-dihydropyrimido[2,1-c][1,2,4]triazin-5-ium bromide [**8.1e**]. A 10 mL round-bottomed flask equipped with a magnetic stirring bar and reflux

condenser was charged with 2-hydraznylpyrimidine (0.111 g, 1.0 mmol) and deoxygenated isopropanol (5 mL). The 2-bromo-1-(4-cyanophenyl)ethanone (0.269 g, 1.2 mmol) was added to the reaction mixture and heated under reflux for 2 h. The progress of the reaction was monitored by TLC. After reaction completion, the resultant mixture was concentrated to half of its volume and then left to cool to rt. The obtained precipitate was filtered, washed with isopropanol, and dried to provide the bromide salt as a yellow crystalline solid (0.177 g, 56 %); ^{1}H NMR (500 MHz, MeOD) δ 9.05 (dd, J = 4.5, 2.0 Hz, 1H), 8.55 (dd, J = 6.6, 2.0 Hz, 1H), 8.25 (m, 1H), 8.20 (m, 1H), 7.92 (m, 1H), 7.73 (t, 7.9 Hz, 1H), 7.47 (dd, J = 6.6, 4.5 Hz, 1H), 5.59 (s, 2H).

2.2.6A Preparation of 3-(4-methoxyphenyl)-1,4-dihydropyrimido[2,1-c][1,2,4]triazin-5-ium bromide [**8.1f**]. A 10 mL round-bottomed flask equipped with a magnetic stirring bar and reflux condenser was charged with 2-hydraznylpyrimidine (0.111 g, 1.0 mmol) and deoxygenated isopropanol (5 mL). The 2-bromo-1-(4- methoxyphenyl)ethanone (0.275 g, 1.2 mmol) was added to the reaction mixture and heated under reflux for 2 h. The progress of the reaction was monitored by TLC. After reaction completion, the resultant mixture was concentrated to half of its volume and then left to cool to rt. The obtained precipitate was filtered, washed with isopropanol, and dried to provide the bromide salt as a yellow crystalline solid (0.196 g, 61 %); ^{1}H NMR (500 MHz, MeOD) δ 8.99 (dd, J = 4.3, 2.0 Hz, 1H), 8.51 (dd, J = 6.6, 1.9 Hz, 1H), 7.89 (m, 2H), 7.38 (dd, J = 6.6, 4.5 Hz, 1H), 7.10 (m, 2H), 5.52 (s, 2H), 3.89 (s, 2H); ^{13}C NMR (126 MHz, MeOD) δ 166.4, 162.6, 148.6, 147.6, 144.3, 129.2, 127.7, 124.2, 114.6, 114.1, 54.7.

2.2.7A Preparation of 3-(4-bromophenyl)-1-methyl-1,4-dihydropyrimido[2,1-c][1,2,4] triazin-5-ium bromide. [8.2c]. A 10 mL round-bottomed flask equipped with a magnetic stirring bar and reflux condenser was charged with 2-(1-methylhydrazinyl)pyrimidine (0.124 g, 1.0 mol)

and deoxygenated isopropanol (5 mL). The 2-bromo-1-(4- bromophenyl)ethanone (0.333 g, 1.2 mmol) was added to the reaction mixture and heated under reflux for 2 h. The progress of the reaction was monitored by TLC. After reaction completion, the resultant mixture was concentrated to half of its volume and then left to cool to rt. The obtained precipitate was filtered, washed with isopropanol, and dried to provide the bromide salt as a yellow crystalline solid (0.246 g, 64 %); ^{1}H NMR (500 MHz, MeOD) δ 9.10 (m, 1H), 8.63 (m, 1H), 7.87 (m, 2H), 7.49 (m, 1H), 5.60 (d, J = 1.3 Hz, 2H), 3.89 (d, J = 1.6 Hz, 3H); ^{13}C NMR (126 MHz, MeOD) δ 166.2, 148.6, 147.9, 144.0, 131.9, 130.5, 127.8, 126.0, 114.7, 38.8, 23.8.

2.2.8A Preparation of 1-(2-hydroxyethyl)-3-(4-(trifluoromethyl)phenyl)-1,4-dihydro pyrimido[2,1-c][1,2,4]triazin-5-ium bromide [**8.3b**]. A 10 mL round-bottomed flask equipped with a magnetic stirring bar and reflux condenser was charged with the requisite 2-(1-methylhydrazinyl)pyrimidine (0.124 g, 1.0 mmol) and deoxygenated isopropanol (5 mL). The 2-bromo-1-(4- bromophenyl)ethanone (0.334 g, 1.2 mmol) was added to the reaction mixture and heated under reflux for 2 h. The progress of the reaction was monitored by TLC. After reaction completion, the resultant mixture was concentrated to obtain the crude product. The resulting crude mixture was purified by flash chromatography on silica gel (MeOH/ DCM = 10 : 90, v/v) to afford the title product as a white solid (0.223 g, 58 %); ^{1}H NMR (500 MHz, DMSO- d_6) δ 9.15 (dd, J = 4.1, 1.5 Hz, 1H), 8.80 (m, 1H), 8.09 (d, J = 7.7 Hz, 2H), 7.97 (d, J = 8.4 Hz, 2H), 7.59 (dd, J = 6.5, 4.5 Hz, 1H), 7.15 (t, J = 51.2 Hz, 1H), 5.70 (s, 2H), 4.29 (t, 5.8 Hz, 2H), 3.83 (t, J = 5.6 Hz, 2H); ^{13}C NMR (126 MHz, MeOD) δ 166.6, 150.1, 148.0, 144.2, 127.6, 126. 4, 115.9, 58.1, 53.9, 48.7.

2.3 A Preparation of α-Brominated Acetophenones

2.3.1A Preparation of 2-bromo-1-(2,4-difluorophenyl)ethanone [2a]. A 100 mL round-bottomed flask equipped with a magnetic stirring bar and Polyseal cap was charged with 2,4-fluoroacetophenone (10.000 g, 7.58 mL, 64 mmol) and acetic acid (15 mL) and stirred at room temperature. A solution of bromine (3.3 mL, 64 mmol) in acetic acid (25 mL) was prepared. A small portion of the bromine in acetic acid solution (2 mL) was added and stirred at room temperature until the red color discharged (15-20 min). The remaining bromine in acetic acid solution was added dropwise with stirring, and the reaction mixture was allowed to stir for an additional 1 h at room temperature. A 250 mL round-bottomed flask equipped with a magnetic stirring bar and ice water bath was charged with 100 mL of ice water and the reaction mixture was added dropwise. A solid precipitated out as it was allowed to stir. This solid was then filtered and washed with water (3 × 30 mL) to provide the product as a white crystalline solid (7.880 g, 52%); ^{1}H NMR (500 MHz, $CDCl_3$) δ 7.99 (m, 1H), 7.01 (m, 1H), 6.91 (m, 1H), 4.47 (d, J = 2.4 Hz, 2H), 161.5 (d, J = 12.7 Hz), 133.6 (dd, J = 3.7, 10.9 Hz); ^{13}C NMR (126 MHz, $CDCl_3$) δ 187.7 (d, J = 4.4 Hz), 167.5 (d, J = 12.5 Hz), 165.4 (12.7 Hz), 163.5 (d, J = 12.5 Hz, 161.5 (d, J = 12.7), 133.6 (dd, J = 3.7, 10.9 Hz), 119.3 (dd, J = 3.5, 12.7 Hz), 112.8 (3.9, 22.0 Hz), 104.9 (dd, J = 25.2, 27.2 Hz), 35.5 (d, J = 10.2 Hz); ^{19}F NMR (471 MHz, $CDCl_3$) δ -99.6 (m), -103.7 (q, 10.5 Hz).

2.3.2A Preparation of 3-(2-bromoacetyl)benzonitrile [2e]. A 25 mL round-bottomed flask equipped with a magnetic stirring bar and Polyseal cap was charged with 3-cyanoacetophenone (1.452 g, 10 mmol) and acetic acid (10 mL) and stirred at room temperature. A solution of bromine (0.5 mL, 10 mmol) in acetic acid (4 mL) was prepared. A small portion of bromine in acetic acid solution (0.25 mL) was added and stirred at room temperature until the red color discharged (15-

20 min). The remaining bromine in acetic acid solution was added dropwise with stirring and the reaction mixture was allowed to stir for an additional 1 h at room temperature. A 50 mL round-bottomed flask equipped with a magnetic stirring bar and ice water bath was charged with 25 mL of ice water and the reaction mixture was added dropwise. A solid precipitated out as it was allowed to stir. This solid was then filtered and washed with water (3 × 10 mL) to provide the product as a white crystalline solid (1.568 g, 70%); ^{1}H NMR (500 MHz, $CDCl_3$) δ 8.29 (m, 1H), 8.24 (dt, J = 1.3, 7.9 Hz, 1H), 7.92 (dt, J = 1.3, 7.6 Hz, 1H), 7.68 (t, 7.9 Hz, 1H), 4.44 (s, 2H); ^{13}C NMR (126 MHz, $CDCl_3$) δ 189.5, 136.7, 134.7, 132.9, 132.6, 129.9, 117.6, 113.6, 29.7.

2.3.3A Preparation of 2-bromo-1-(4-(difluoromethoxy)phenyl)ethanone [2d]. A 50 mL round-bottomed flask equipped with a magnetic stirring bar and Polyseal cap was charged with 4-difluoromethoxyacetophenone (5.000 g, 27 mmol) and acetic acid (10 mL) and stirred at room temperature. A solution of bromine (1.38 mL, 27 mmol) in acetic acid (10 mL) was prepared. A small portion of the bromine in acetic acid solution (1 mL) was added and stirred at room temperature until the red color discharged (15-20 min). The remaining bromine in acetic acid solution was added dropwise with stirring and the reaction mixture was allowed to stir for an additional 1h at room temperature. A 100 mL round-bottomed flask equipped with a magnetic stirring bar and ice water bath was charged with 30 mL of ice water, and the reaction mixture was added dropwise. A solid precipitated out as it was allowed to stir. This solid was then filtered and washed with water (3 × 20 mL) to provide the product as a crystalline yellow solid (5.457 g, 76%). ^{1}H NMR (500 MHz, $CDCl_3$) δ 8.04 (m, 2H), 7.23 (m, 2H), 6.64 (t, J = 72.7 Hz, 1H), 4.43 (s, 2H); ^{13}C NMR (126 MHz, $CDCl_3$) δ 189.9, 155.3 (t, J = 2.8 Hz), 131.2, 130.8, 118.9, 117.3, 115.2, 113.1, 30.4; ^{19}F NMR (471 MHz, MeOD) δ -82.0 (d, 73.4 J).

2.3.4A Preparation of 2-bromo-1-(4-methoxyphenyl)ethanone [2f]. A 100 mL round-bottomed flask equipped with a magnetic stirring bar and Polyseal cap was charged with 4-methoxyacetophenone (2.5 g, 16.6 mmol) and $CHCl_3$ (30 mL) and stirred at room temperature. NBS (3.250 g, 18.2 mmol) was added followed by TsOH (0.570 g, 3.3 mmol) and stirred at room temperature overnight. Water was added (20 mL) and the organic layer was extracted with DCM (3 × 10 mL). The collected organic layer was dried in vacuo to yield the crude product. Minor impurities were removed via silica gel column (DCM/ Hexane = 60 : 40, v/v) to afford the title product as a white solid (3.522 g, 93%). ^{1}H NMR (500 MHz, $CDCl_3$) δ 7.99 (m, 2H), 6.98 (m, 2H), 4.42 (s, 2H), 3.90 (s, 3H); ^{13}C NMR (126 MHz, $CDCl_3$) δ 189.9, 164.2, 131.4, 126.9, 114.1, 55.6, 30.7.

Preparation of compounds in Chapter 3

3.1 A Preparation of substituted 2-aminopyrimidines

3.1.1A Preparation of N-benzylpyrimidin-2-amine [1]. A 25 mL round-bottomed flask equipped with a magnetic stirring bar and reflux condenser was charged with 2-chloropyrimidine (1.145 g, 10 mmol, 1.0 eq.), benzylamine (2.2 mL, 11 mmol, 1.1 eq.), anhydrous finely powdered potassium carbonate (2.073 g, 15 mmol, 1.5 eq.) and anhydrous acetonitrile (10 mL). The reactant mixture was stirred at reflux overnight. Upon cooling the reactant mixture to room temperature, water (20 mL) was added, and the mixture was subsequently extracted with dichloromethane (2 × 20 mL). The combined organic layers were dried over Na_2SO_4, filtered, and concentrated in vacuum to give the title product as a yellow solid (1.759 g, 95%); ^{1}H NMR (500 MHz, $CDCl_3$) δ 8.28 (d, J = 4.7

Hz, 2H), 7.32 (m, 5H), 6.54 (t, J = 4.8 Hz, 1H), 5.52 (s, 1H), 4.64 (d, 6.0 Hz, 2H); ^{13}C NMR (126 MHz, $CDCl_3$) δ 162.8, 158.0, 139.1, 128.6, 127.5, 127.3, 110.9, 45.4.

3.1.2A Preparation of 2-(pyrimidin-2-ylamino)ethanol [2]. A 25 mL round-bottomed flask equipped with a magnetic stirring bar and reflux condenser was charged with 2-chloropyrimidine (1.145 g, 10 mmol, 1.0 eq.), 2-aminoethanol (0.6719 g, 11 mmol, 1.1 eq.), anhydrous finely powdered potassium carbonate (2.073 g, 15 mmol, 1.5 eq.) and anhydrous acetonitrile (10 mL). The reactant mixture was stirred at reflux overnight. Upon cooling the reactant mixture to room temperature, water (20 mL) was added, and the mixture was subsequently extracted with dichloromethane (2 × 20 mL). The combined organic layers were dried over Na_2SO_4, filtered, and concentrated in vacuum. The resulting crude mixture was purified by flash chromatography on silica gel (MeOH/ CH_2Cl_2 = 10 : 90, v/v) to afford the title product as a white solid (1.184 g, 87%); ^{1}H NMR (500 MHz, $CDCl_3$) δ 8.27 (dd, *J* = 4.8, 1.4 Hz, 2H), 6.56 (m, H), 5.7 (s, 1H), 4.03 (s, 1H), 3.83 (m, 2H), 3.59 (m, 2H); ^{13}C NMR δ (126 MHz, $CDCl_3$) δ 162.3, 158.0, 110.9, 63.4, 44.7.

3.1.3A Preparation of N-octylpyrimidin-2-amine [6]. A 25 mL round-bottomed flask equipped with a magnetic stirring bar and reflux condenser was charged with 2-chloropyrimidine (1.145 g, 10 mmol, 1.0 eq.), octan-1-amine (1.422 g, 11 mmol, 1.1 eq.), anhydrous finely powdered potassium carbonate (2.073 g, 15 mmol, 1.5 eq.) and anhydrous acetonitrile (10 mL). The reactant mixture was stirred at reflux overnight. Upon cooling the reactant mixture to room temperature, water (20 mL) was added, and the mixture was subsequently extracted with dichloromethane (2 × 20 mL). The combined organic layers were dried over Na_2SO_4, filtered, and concentrated in vacuum to give the title product as a yellow solid (1.995 g, 96%); ^{1}H NMR (500 MHz, $CDCl_3$) δ 8.26 (d, *J* = 4.9 Hz, 2H), 6.49 (t, *J* = 5.0 Hz, 1H), 5.19 (s, 1H), 3.39 (q, *J* = 7.0 Hz, 2H), 2.89 (t, *J*

= 7.5 Hz, 1H), 1.64 (m, 3H), 1.32 (m, 10H), 0.88 (m, 4H); ^{13}C NMR (126 MHz, $CDCl_3$) δ 162.5, 158.0, 110.3, 41.5, 31.8, 29.6, 29.3, 29.2, 27.0, 22.6, 14.1(residual water masked the peaks at δ 1.32 in ^{1}H NMR).

3.2 A Preparation of 2-hydroxy-1*H*-imidazo[1,2-a]pyrimidinium bromide salts

3.2.1A Preparation of 1-benzyl-2-(2,4-difluorophenyl)-2-hydroxy-2,3-dihydro-1H-imidazo [1,2-a]pyrimidin-4-ium bromide [1a′]. A 5 mL round-bottomed flask equipped with a magnetic stirring bar was charged with N-benzylpyrimidin-2-amine (0.1852 g, 1 mmol), 2-bromo-1-(2,4-difluorophenyl)ethanone (0.2820 g, 1.2 mmol) and anhydrous MeCN (1 mL). The reactant mixture was stirred at reflux for 2 h. The product mixture was then diluted with ethylene ether (5 mL), filtered, and dried to provide the hydroxy salt as white crystalline solid (0.2734 g, 65%); ^{1}H NMR (400 MHz, $CDCl_3$) δ 9.16 (dd, *J* = 6.3, 1.7 Hz, 1H), 8.85 (dd, *J* = 4.5, 1.8 Hz, 1H), 7.89 (m, 2H), 7.10 (m, 4H), 6.91 (m, 3H), 6.36 (m, 1H), 5.56 (dd, *J* = 14.2, 2.9 Hz, 1H), 4.99 (d, *J* = 15.5 Hz, 1H), 4.7 (d, *J* = 14.6 Hz, 1H), 4.47 (d, *J* = 15.2 Hz, 1H).

3.2.2A Preparation of 1-benzyl-2-(4-bromophenyl)-2-hydroxy-2,3-dihydro-1H-imidazo[1,2-a]pyrimidin-4-ium bromide [1c′]. A 5 mL round-bottomed flask equipped with a magnetic stirring bar was charged with N-benzylpyrimidin-2-amine (0.1852 g, 1 mmol), 2-bromo-1-(4-bromophenyl)ethanone (0.3335 g, 1.2 mmol) and anhydrous MeCN (1 mL). The reactant mixture was stirred at reflux for 2 h. The product mixture was then diluted with ethylene ether (5 mL), filtered, and dried to provide the hydroxy salt as a white crystalline solid (0.2381 g, 51%); ^{1}H NMR (500 MHz, DMSO-d_6) δ 9.16 (d, *J* = 4.5, 1H), 9.03 (d, *J* = 6.1 Hz, 1H), 8.49 (s, 1H), 8.25 (m, 4H), 7.63 (t, *J* = 8.1 Hz, 1H), 7.48 (m, 3H), 7.09 (m, 5H), 4.98 (d, *J* = 7.7 Hz, 2H), 4.79 (d, *J* = 16.1 Hz, 1H), 4.46 (d, *J* = 15.8 Hz, 1H), 4.08 (s, 1H).

3.2.3A Preparation of 1-benzyl-2-hydroxy-2-(3-nitrophenyl)-2,3-dihydro-1H-imidazo[1,2-a]pyrimidin-4-ium bromide [1d′]. A 5 mL round-bottomed flask equipped with a magnetic stirring bar was charged with N-benzylpyrimidin-2-amine (0.1852 g, 1 mmol), 2-bromo-1-(3-nitrophenyl)ethanone (0.2760 g, 1.2 mmol) and anhydrous MeCN (1 mL). The reactant mixture was stirred at reflux for 2 h. The product mixture was then diluted with ethylene ether (5 mL), filtered, and dried to provide the hydroxy salt as a pale yellow crystalline solid (0.2327 g, 54%); ^{1}H NMR (500 MHz, DMSO-d_6) δ 9.13 (dd, J = 4.6, 1.6 Hz, 1H), 8.99 (dd, J = 6.5, 1.4 Hz, 1H), 8.47 (s, 1H), 8.29 (s, 1H), 8.15 (dd, J = 8.6, 2.9 Hz, 2H), 7.61 (t, J = 8.6 Hz, 1 H), 7.45 (m, 2H), 3.86 (m, 4H), 4.95 (dd, J = 22.5, 14.7 Hz, 1H), 4.76 (d, J = 16.1 Hz, 1H), 4.42 (d, J = 16.1 Hz, 1 H), 4.05 (q, J = 5.4 Hz, 1H).

3.2.4A Preparation of 1-benzyl-2-hydroxy-2-(4-(trifluoromethyl)phenyl)-2,3-dihydro-1H-imidazo[1,2-a]pyrimidin-4-ium bromide [3e′]. A 5 mL round-bottomed flask equipped with a magnetic stirring bar and reflux condenser was charged with N-benzylpyrimidin-2-amine (0.1852 g, 1 mmol), 2-bromo-1-(4-(trifluoromethyl)phenyl)ethanone (0.3205 g, 1.2 mmol) and anhydrous MeCN (1 mL). The reactant mixture was stirred at reflux for 2 h. The product mixture was then diluted with ethylene ether (5 mL), filtered, and dried to provide the hydroxy salt as a pale yellow crystalline solid (0.3401 g, 75%); ^{1}H NMR (400 MHz, DMSO-d_6) δ 9.13 (d, J = 3.6 Hz, 1H), 9.01 (d, J = 5.6 Hz, 1H), 8.20 (s, 1H), 7.94 (d, J = 7.8 Hz, 2H), 7.70 (d, J = 8.5 Hz, 2H), 7.47 (m, 2H), 7.13 (m, 4H), 4.98 (s, 1H), 4.57 (dd, J = 71.31, 15.9 Hz, 2H), 4.07 (s, 1H).

3.2.5A Preparation of 2-(2,4-difluorophenyl)-2-hydroxy-1-(2-hydroxyethyl)-2,3-dihydro-1H-imidazo[1,2-a]pyrimidin-4-ium bromide [2a′]. A 5 mL round-bottomed flask equipped with a magnetic stirring bar was charged with 2-(pyrimidin-2-ylamino)ethanol (0.1392 g, 1 mmol), 2-

bromo-1-(2,4-difluorophenyl)ethanone (0.2820 g, 1.2 mmol) and anhydrous MeCN (1 mL). The reactant mixture was stirred at reflux for 2 h. The product mixture was then diluted with ethylene ether (5 mL), filtered, and dried to provide the hydroxy salt as a beige crystalline solid (0.355 g, 95%); ^{1}H NMR (500 MHz, CD_3CN) δ 8.91 (dd, J = 4.6, 1.9 Hz, 1H), 8.46 (dd, J = 6.5, 1.8 Hz, 1H), 7.96 (m, 2H), 7.12 (m, 3H), 5.03 (d, J = 14.2 Hz, 1H).

3.2.6A Preparation of 2-(4-bromophenyl)-2-hydroxy-1-(2-hydroxyethyl)-2,3-dihydro-1H-imidazo [1,2-a]pyrimidin-4-ium bromide [1c′]. A 5 mL round-bottomed flask equipped with a magnetic stirring bar was charged with 2-(pyrimidin-2-ylamino)ethanol (0.1392 g, 1 mmol), 2-bromo-1-(4-bromophenyl)ethanone (0.3335 g, 1.2 mmol) and anhydrous MeCN (1 mL). The reactant mixture was stirred at reflux for 2 h. The product mixture was then diluted with ethylene ether (5 mL), filtered, and dried to provide the hydroxy salt as a yellow crystalline solid (0.4029 g, 97%); ^{1}H NMR (500 MHz, DMSO-d_6) δ 9.09 (dd, J = 4.5, 1.9 Hz, 1H), 8.92 (dd, J = 6.2, 1.7 Hz, 1H), 7.94 (s, 1H), 7.74 (s, 1H), 7.38 (dd, J = 6.3, 4.8 Hz, 1H), 4.85 (dd, J = 37.9, 14.9 Hz, 2H), 3.3 (m, 4H).

3.2.7A Preparation of 2-hydroxy-1-(2-hydroxyethyl)-2-(4-(trifluoromethyl)phenyl)-2,3-dihydro-1H-imidazo[1,2-a]pyrimidin-4-ium bromide [2d′]. A 5 mL round-bottomed flask equipped with a magnetic stirring bar was charged with 2-(pyrimidin-2-ylamino)ethanol (0.1392 g, 1 mmol), 2-bromo-1-(4-(trifluoromethyl)phenyl)ethanone (0.3205 g, 1.2 mmol) and anhydrous MeCN (1 mL). The reactant mixture was stirred at reflux for 2 h. The product mixture was then diluted with ethylene ether (5 mL), filtered, and dried to provide the hydroxy salt as a white crystalline solid (0.397 g, 98%); ^{1}H NMR (500 MHz, DMSO-d_6) δ 9.08 (m, 1H), 8.92 (d, J = 6.2

Hz, 1H), 7.95 (m, 5H), 7.38 (dd, *J* = 6.1, 4.7 Hz, 1H), 4.87 (dd, *J* = 37.0, 14.6 Hz, 3H), 3.33 (m, 7H).

3.2.8A Preparation of 2-hydroxy-1-(2-hydroxyethyl)-2-(3-nitrophenyl)-2,3-dihydro-1H-imidazo[1,2-a]pyrimidin-4-ium bromide [2e′]. A 5 mL round-bottomed flask equipped with a magnetic stirring bar was charged with 2-(pyrimidin-2-ylamino)ethanol (0.1392 g, 1 mmol), 2-bromo-1-(3-nitrophenyl)ethanone (0.2760 g, 1.2 mmol) and anhydrous MeCN (1 mL). The reactant mixture was stirred at reflux for 2 h. The product mixture was then diluted with ethylene ether (5 mL), filtered, and dried to provide the hydroxy salt as a pale yellow crystalline solid (0.351 g, 91%); ^{1}H NMR (400 MHz, CD_3CN) δ 9.09 (d, *J* = 3.7 Hz, 1H), 8.95 (d, *J* = 5.9 Hz, 1H), 8.65 (s, 1H), 8.35 (d, *J* = 8.3 Hz, 1H), 8.25 (d, *J* = 7.7 Hz, 1H), 8.17 (s, 1H), 7.82 (t, *J* = 7.9 Hz, 1H), 7.39 (t, *J* = 5.06 Hz, 1H), 4.9 (dd, *J* = 29.1, 14.2 Hz, 2H), 3.36 (m, 4H).

3.2.9A Preparation of 2-(4-chlorophenyl)-2-hydroxy-1-octyl-2,3-dihydro-1H-imidazo[1,2-a]pyrimidin-4-ium bromide [6a]. A 5 mL round-bottomed flask equipped with a magnetic stirring bar was charged with N-octylpyrimidin-2-amine (0.207 g, 1 mmol), 2-bromo-1-(4-methoxyphenyl)ethanone (0.2749 g, 1.2 mmol) and anhydrous MeCN (1 mL). The reactant mixture was stirred at reflux for 2 h. The product mixture was then diluted with ethylene ether (5 mL), filtered, and dried to provide the hydroxy salt as a white crystalline solid (0.250 g, 57%); ^{1}H NMR (400 MHz, $CDCl_3$) δ 8.87 (dd, *J* = 6.4, 1.9 Hz, 1H), 8.78 (dd, *J* = 4.5, 1.9 Hz, 1H), 7.51 (m, 2H), 6.99 (m, 3H), 5.49 (d, *J* = 14.1 Hz, 1H), 4.61 (d, *J* = 14.0 Hz, 1H), 3.81 (s, 3H), 3.39 (m, 2H), 1.21 (m, 10 H), 0.85 (t, *J* = 6.4 Hz, 3H).

3.2.10A Preparation of 2-(4-chlorophenyl)-2-hydroxy-1-octyl-2,3-dihydro-1H-imidazo[1,2-a]pyrimidin-4-ium bromide [6b]. A 5 mL round-bottomed flask equipped with a magnetic

stirring bar was charged with N-octylpyrimidin-2-amine (0.207 g, 1 mmol), 2-bromo-1-(4-chlorophenyl)ethanone (0.2802 g, 1.2 mmol) and anhydrous MeCN (1 mL). The reactant mixture was stirred at reflux for 2 h. The product mixture was then diluted with ethylene ether (5 mL), filtered, and dried to provide the hydroxy salt as a white crystalline solid (0.299 g, 68%); ^{1}H NMR (400 MHz, $CDCl_3$) δ 8.99 (dd, *J* = 6.4, 2.2 Hz, 1H), 8.73 (dd, *J* = 4.8, 1.9 Hz, 1H), 7.56 (s, 1H), 7.48 (d, *J* = 8.8 Hz, 2H), 7.36 (d, *J* = 8.8 Hz, 2H), 6.99 (dd, *J* = 6.4, 4.6 Hz, 1H), 5.47 (d, *J* = 14.3 Hz, 1H), 4.57 (d, *J* = 14.3 Hz, 1H), 3.32 (m, 2H), 1.14 (m, 10H), 0.79 (t, *J*= 7.1 Hz, 3H).

3.2.11A Preparation of 2-hydroxy-2-(4-nitrophenyl)-1-octyl-2,3-dihydro-1H-imidazo[1,2-a]pyrimidin-4-ium bromide [6c]. A 5 mL round-bottomed flask equipped with a magnetic stirring bar was charged with N-octylpyrimidin-2-amine (0.207 g, 1 mmol), 2-bromo-1-(4-nitrophenyl)ethanone (0.2930 g, 1.2 mmol) and anhydrous MeCN (1 mL). The reactant mixture was stirred at reflux for 2 h. The product mixture was then diluted with ethylene ether (5 mL), filtered, and dried to provide the hydroxy salt as a white crystalline solid (0.250 g, 56%); ^{1}H NMR (400 MHz, $CDCl_3$) δ 9.00 (dd, *J* = 6.3, 1.6 Hz, 1H), 8.83 (dd, *J* = 4.3, 1.9 Hz, 1H), 7.68 (s, 1H), 7.51 (m, 4H), 7.08 (dd, *J* = 6.3, 4.7 Hz, 1H), 5.56 (d, *J* = 14.1 Hz, 1H), 4.64 (d, *J* = 14.3 Hz, 1H), 3.41 (m, 2H), 1.24 (m, 10 H), 0.88 (t, *J* = 6.9 Hz, 3H).

3.2.12A Preparation of 2-(4-cyanophenyl)-2-hydroxy-1-octyl-2,3-dihydro-1H-imidazo[1,2-a]pyrimidin-4-ium bromide [6d]. A 5 mL round-bottomed flask equipped with a magnetic stirring bar was charged with N-octylpyrimidin-2-amine (0.207 g, 1 mmol), 2-bromo-1-(4-cyanophenyl)ethanone (0.2690 g, 1.2 mmol) and anhydrous MeCN (1 mL). The reactant mixture was stirred at reflux for 2 h. The product mixture was then diluted with ethylene ether (5 mL), filtered, and dried to provide the hydroxy salt as a white crystalline solid (0.2808 g, 65%); ^{1}H

NMR (400 MHz, $CDCl_3$) δ 9.15 (dd, *J* = 6.5, 1.8 Hz, 1H), 8.82 (dd, *J* = 4.3, 1.8 Hz, 1H), 7.52 (m, 5H), 7.09 (dd, *J* = 6.2, 4.7 Hz, 1H), 5.54 (d, *J* = 14.5 Hz, 1H), 4.68 (d, *J* = 14.5 Hz, 1H), 3.40 (m, 2H), 1.23 (m, 10H), 0.88 (t, *J* = 7.4 Hz, 3H).

3.2.13A Preparation of 2-(4-bromophenyl)-2-hydroxy-1-octyl-2,3-dihydro-1H-imidazo[1,2-a]pyrimidin-4-ium bromide [6e]. A 5 mL round-bottomed flask equipped with a magnetic stirring bar was charged with N-octylpyrimidin-2-amine (0.207 g, 1 mmol), 2-bromo-1-(4-bromophenyl)ethanone (0.3335 g, 1.2 mmol) and anhydrous MeCN (1 mL). The reactant mixture was stirred at reflux for 2 h. The product mixture was then diluted with ethylene ether (5 mL), filtered, and dried to provide the hydroxy salt as a white crystalline solid (0.299 g, 62%); ^{1}H NMR (500 MHz, $CDCl_3$) δ 9.02 (dd, *J* = 6.4, 1.9 Hz, 1H), 8.82 (dd, *J* = 4.6, 2.0 Hz, 1H), 7.68 (s, H), 7.61 (d, *J* = 8.5 Hz, 2H), 7.51 (d, *J* = 8.6 Hz, 2H), 7.08 (dd, *J* = 6.3, 4.8 Hz, 1H), 5.56 (d, *J* = 14.2 Hz, 1H), 4.46 (d, *J* = 14.2, 1H), 3.41 (m, 2H), 1.24 (m, 10 H), 0.88 (t, *J* = 7.8 Hz, 3H).

3.3 A Preparation of 1*H*-imidazo[1,2-a]pyrimidinium tetrafluoroborate salts

General Procedure

A 10 mL round-bottomed flask equipped with a magnetic stirring bar and Polyseal cap was charged with the requisite hydroxy salt (1 mmol) and dichloromethane (2 mL). The flask was then placed in an ice bath and tetra fluoroboric acid diethyl ether complex (0.8 mL, 6 mmol) was added with vigorous stirring. The reaction was maintained at 0 ˚C for 2.5 h before quenching with 2 mL of saturated aqueous sodium tetrafluoroborate. The resultant mixture was extracted with dichloromethane (3 x 2 mL) and the solvent was removed by rotary evaporation to yield the imidazo[1,2-α]pyrimidinium salt as a crystalline solid.

3.3.1A Preparation of 1-benzyl-2-(2,4-difluorophenyl)-1H-imidazo[1,2-a]pyrimidin-4-ium tetrafluoroborate [1a]. The title compound was prepared according to the representative procedure on a 0.54 mmol scale, and **1a** was obtained as a beige crystalline solid (0.1606 g, 73%); ^{1}H NMR (500 MHz, $CDCl_3$) δ 9.42 (dd, *J* = 6.9, 1.6 Hz, 1H), 9.03 (dd, *J* = 4.3, 1.4 Hz, 1H), 8.4 (s, 1H), 7.69 (dd, *J* = 6.7, 4.4 Hz, 1H), 7.51 (m, 1H), 7.24 (m, 3H), 7.03 (m, 4H), 5.62 (s, 2H); ^{13}C NMR (126 MHz, $CDCl_3$) δ 166.2 (d, *J* = 11.6 Hz), 164.2 (d, *J* = 11.9 Hz), 161.6 (d, *J* = 12.3 Hz), 159.6 (d, *J* = 12.7 Hz), 157.8, 142.9, 139.1, 134.0 (dd, *J* = 10.3, 2.4 Hz), 132.9, 131.5, 129.0 (d, *J* = 14.5 Hz), 127.6, 115.0, 114.2, 113.0 (dd, *J* = 22.5, 4.0 Hz), 109.2 (dd, *J* = 14.5, 3.4 Hz), 104.9 (t, *J* = 25.8 Hz); ^{19}F NMR (471 MHz, $CDCl_3$) δ -102.26 (m, 1F), -107.08 (m, 1F), -151.98.

3.3.2A Preparation of 1-benzyl-2-(4-bromophenyl)-1H-imidazo[1,2-a]pyrimidin-4-ium tetrafluoroborate [1c]. The title compound was prepared according to the representative procedure on a 0.44 mmol scale, and **1c** was obtained as a pale yellow crystalline solid (0.180 g, 90%); ^{1}H NMR (500 MHz, CD_3CN) δ 9.14 (dd, *J* = 4.5, 1.7 Hz, 1H), 9.11 (dd, *J* = 6.8, 1.7 Hz, 1H), 8.44 (dd, *J* = 8.2, 0.9 Hz, 1H), 8.25 (s, 1H), 8.23 (m, 1H), 7.79 (m, 3H), 7.29 (m, 3H), 7.07 (d, *J* = 6.8 Hz, 2H), 5.70 (s, 2H); ^{13}C NMR (126 MHz, CD_3CN) δ 158.8, 138.3, 136.1, 135.8, 134.0, 130.8, 128.9, 128.5, 127.4, 126.4, 125.8, 124.8, 47.8; ^{19}F NMR (471 MHz, $CDCl_3$) δ -151.84.

3.3.3A Preparation of 1-benzyl-2-(3-nitrophenyl)-1H-imidazo[1,2-a]pyrimidin-4-ium tetrafluoroborate [1d]. The title compound was prepared according to the representative procedure on a 0.54 mmol scale, and **1d** was obtained as a yellow crystalline solid (0.1118 g, 50%); ^{1}H NMR (500 MHz, CD_3CN) δ 9.15 (dd, *J* = 4.4, 1.7 Hz, 1H), 9.12 (dd, *J* = 6.8, 1.8 Hz, 1H), 8.44 (m, 1H), 8.26 (s, 1H), 8.22 (t, *J* = 2.0 Hz, 1H), 7.80 (m, 3H), 7.30 (m, 3H), 7.08 (m, 2H), 5.71 (s,

2H); ^{13}C NMR (126 MHz, CD_3CN) δ 158.8, 138.3, 136.1, 135.8, 134.0, 130.8, 128.9, 128.5, 128.5, 127.4, 126.4, 125.8, 124.9, 115.2, 112.6, 47.8; ^{19}F NMR (471 MHz, $CDCl_3$) δ -151.79.

3.3.4A Preparation of 1-benzyl-2-(4-(trifluoromethyl)phenyl)-1H-imidazo[1,2-a]pyrimidin-4-ium tetrafluoroborate [1e]. The title compound was prepared according to the representative procedure on a 0.66 mmol scale, and **1e** was obtained as a pale yellow crystalline solid (0.254 g, 87%); ^{1}H NMR (500 MHz, CD_3CN) δ 9.11 (m, 2H), 8.22 (s, 1H), 7.86 (d, J = 8.4 Hz, 2H), 7.72 (dd, J = 6.8, 4.4 Hz, 1H), 7.66 (d, J = 8.3 Hz, 2H), 7.28 (m, 3H), 7.18 (m, 5H), 5.71 (s, 2H); ^{13}C NMR (126 MHz, CD_3CN) δ 158.6, 143.4, 138.3, 136.6, 134.1, 132.2 (q, J = 30.9 Hz), 130.8, 128.9, 128.8, 128.4, 127.3, 126.2 (q, J = 3.6 Hz), 125.0, 122.8, 115.2, 112.2, 47.7; ^{19}F NMR (471 MHz, $CDCl_3$) δ -63.58, -151.78.

3.3.5A Preparation of 2-(2,4-difluorophenyl)-1-(2-hydroxyethyl)-1H-imidazo[1,2-a]pyrimidin-4-ium tetrafluoroborate [2a]. The title compound was prepared according to the representative procedure on a 0.80 mmol scale, and **2a** was obtained as a beige crystalline solid (0.1804 g, 62%); ^{1}H NMR (500 MHz, CD_3CN) δ 9.08 (dd, J = 4.3, 1.6 Hz, 1H), 9.05 (dd, J = 6.8, 1.8 Hz, 1H), 8.17 (s, 1H), 7.71 (m, 2H), 7.29 (m, 2H), 4.49 (t, J = 5.1 Hz, 2H), 3.80 (q, J = 5.5 Hz, 2H), 2.97 (t, J = 5.2 Hz, 1H); ^{13}C NMR (126 MHz, CD_3CN) δ 158.0, 137.9, 134.3 (dd, J = 9.9, 2.6 Hz), 131.8, 114.8, 112.8 (m), 112.6 (d, J = 4.0 Hz), 109.6, 58.8, 47.4; ^{19}F NMR (471 MHz, $CDCl_3$) δ -105.79 (m, 1F), -109.33 (m, 1F), -151.88.

3.3.6A Preparation of 2-(4-bromophenyl)-1-(2-hydroxyethyl)-1H-imidazo[1,2-a]pyrimidin-4-ium tetrafluoroborate [2c]. The title compound was prepared according to the representative procedure on a 0.72 mmol scale, and **2c** was obtained as a pale yellow crystalline solid (0.1864 g, 64%); ^{1}H NMR (500 MHz, CD_3CN) δ 9.05 (dd, J = 4.4, 0.7 Hz, 1H), 9.03 (dd, J = 6.7, 0.9 Hz,

1H), 8.12 (s, 1H), 7.74 (m, 5H), 4.54 (t, *J* = 5.3 Hz, 2H), 3.86 (q, *J* = 5.6 Hz, 2H), 3.05 (t, *J* = 6.0 Hz, 1H); ^{13}C NMR (126 MHz, CD_3CN) δ 157.7, 143.1, 137.8, 132.5, 132.1, 125.3, 124.4, 114.8, 111.2, 58.8, 47.2; ^{19}F NMR (471 MHz, CD_3CN) δ -151.84.

3.3.7A Preparation of 1-(2-hydroxyethyl)-2-(4-(trifluoromethyl)phenyl)-1H-imidazo[1,2-a] pyrimidin-4-ium tetrafluoroborate [2d]. The title compound was prepared according to the representative procedure on a 0.78 mmol scale, and **2d** was obtained as a pale yellow crystalline solid (0.219 g, 71%); ^{1}H NMR (500 MHz, CD_3CN) δ 9.07 (m, 2H), 8.19 (s, 1H), 7.95 (m, 4H), 7.69 (dd, *J* = 6.7, 4.5 Hz, 1H), 4.56 (t, *J* = 5.5 Hz, 2H), 3.87 (m, 2H), 3.09 (s, 1H); ^{13}C NMR (126 MHz, CD_3CN) δ 157.9, 143.2, 138.0, 137.4, 132.1 (q, *J* = 29.1 Hz), 131.2, 129.3, 126.2 (q, *J* = 3.6 Hz), 125.1, 122.9, 114.9, 111.7, 58.8, 47.3; ^{19}F NMR (471 MHz, $CDCl_3$) δ -63.48, -151.82.

3.3.8A Preparation of 1-(2-hydroxyethyl)-2-(3-nitrophenyl)-1H-imidazo[1,2-a]pyrimidin-4-ium tetrafluoroborate [2e]. The title compound was prepared according to the representative procedure on a 0.86 mmol scale, and **2e** was obtained as a yellow crystalline solid (0.2150 g, 67%); ^{1}H NMR (500 MHz, MeOD) δ 9.22 (dd, *J* = 6.8, 1.8 Hz, 1H), 9.07 (dd, *J* = 4.5, 1.6 Hz, 1H), 8.65 (s, 1H), 8.42 (m, 2H), 8.11 (d, *J* = 8.2 Hz, 1H), 7.82 (t, *J* = 8.2 Hz, 1H), 7.68 (dd, *J* = 7.3, 4.7 Hz, 1H), 4.55 (t, *J* = 5.1 Hz, 2H), 3.85 (t, *J* = 5.5 Hz, 2H); ^{13}C NMR (126 MHz, $CDCl_3$) δ 158.2, 148.6, 138.0, 136.7, 136.6, 130.8, 126.8, 125.7, 125.5, 144.9, 111.9, 58.8, 47.3; ^{19}F NMR (471 MHz, $CDCl_3$) δ -152.88.

3.3.9A Preparation of 2-(4-methoxyphenyl)-1-octyl-1H-imidazo[1,2-a]pyrimidin-4-ium tetrafluoroborate [6a]. The title compound was prepared according to the representative procedure on a 0.57 mmol scale, and **6a** was obtained as a white crystalline solid (0.214 g, 89%); ^{1}H NMR (500 MHz, $CDCl_3$) δ 9.34 (d, *J* = 6.4 Hz, 1H), 8.89 (d, *J* = 3.9 Hz, 1H), 8.28 (s, 1H),

7.56 (dd, *J* = 6.5, 4.5 Hz, 1H), 7.51 (d, *J* = 8.6 Hz, 2H), 7.08 (d, *J* = 8.5, 2H),4.45 (t, *J* = 7.6 Hz, 2H), 3.89 (s, 3H), 1.76 (p, *J* = 7.3 Hz, 2H), 1.22 (m, 10H), 0.86 (t, *J* = 7.0 Hz, 3H); ^{13}C NMR (126 MHz, $CDCl_3$) δ 161.9, 156.3, 142.2, 138.3, 131.2, 116.6, 115.1, 114.5, 111.7, 55.6, 44.8, 31.6, 29.1, 28.9, 28.7, 26.3, 22.6, 14.0; ^{19}F NMR (471 MHz, $CDCl_3$) δ -149.31, -151.92.

3.3.10A Preparation of -(4-chlorophenyl)-1-octyl-1H-imidazo[1,2-a]pyrimidin-4-ium tetra fluoroborate [6b]. The title compound was prepared according to the representative procedure on a 0.68 mmol scale, and **6b** was obtained as a white crystalline solid (0.4346 g, 98%); ^{1}H NMR (500 MHz, $CDCl_3$) δ 9.22 (dd, *J* = 6.7, 1.6 Hz, 1H), 8.84 (dd, *J* = 4.4, 1.6 Hz, 1H), 8.23 (s, 1H), 7.63 (d, *J* = 8.4 Hz, 2H), 7.48 (dd, *J* = 6.8, 4.5 Hz, 1H), 7.41 (d, *J* = 8.3 Hz, 2H), 4.37 (t, *J* = 7.7 Hz, 2H), 1.66 (m, 2H), 1.15 (m, 10H), 0.79 (t, *J* = 6.8 Hz, 3H); ^{13}C NMR (126 MHz, $CDCl_3$) δ 156.9, 142.4, 138.8, 137.9, 136.9, 131.1, 129.9, 123.3, 114.6, 112.3, 44.9, 31.6, 29.1, 28.9, 28.7, 26.3, 22.5, 14.0; ^{19}F NMR (471 MHz, $CDCl_3$) δ -152.18.

3.3.11A Preparation of -(4-nitrophenyl)-1-octyl-1H-imidazo[1,2-a]pyrimidin-4-ium tetra fluoroborate [6c]. The title compound was prepared according to the representative procedure on a 0.52 mmol scale, and **6c** was obtained as a beige crystalline solid (0.221 g, 97%); ^{1}H NMR (500 MHz, $CDCl_3$) δ 9.25 (dd, *J* = 6.9, 1.7 Hz, 1H), 8.93 (dd, *J* = 4.5, 1.6 Hz, 1H), 8.35 (s, 1H), 7.82 (m, 4H), 7.58 (dd, *J* = 6.6, 4.3 Hz, 1H), 4.45 (t, *J* = 7.7 Hz, 2H), 1.72 (m, 3H), 1.18 (m, 10H), 0.85 (t, *J* = 7.0 Hz, 3H); ^{13}C NMR (126 MHz, $CDCl_3$) δ 157.4, 142.7, 138.8, 135.9, 133.1, 130.6, 129.6, 117.6, 115.1, 114.8, 112.9, 45.0, 31.6, 29.1, 28.9, 28.7, 26.3, 22.5, 14.0; ^{19}F NMR (471 MHz, $CDCl_3$) δ -152.06.

3.3.12A Preparation of 2-(4-cyanophenyl)-1-octyl-1H-imidazo[1,2-a]pyrimidin-4-ium tetra fluoroborate [6d]. The title compound was prepared according to the representative procedure on

a 0.63 mmol scale, and **6d** was obtained as a white crystalline solid (0.2601 g, 98%); ^{1}H NMR (500 MHz, $CDCl_3$) δ 9.29 (dd, *J* = 6.9, 1.7 Hz, 1H), 8.91 (dd, *J* = 4.3, 1.7 Hz, 1H), 8.30 (s, 1H), 7.55 (m, 5H), 4.44 (t, *J* = 7.6 Hz, 2H), 1.72 (p, *J* = 7.2 Hz, 2H), 1.18 (m, 10H), 0.85 (t, *J* = 7.2 Hz, 3H); ^{13}C NMR (126 MHz, $CDCl_3$) δ 156.9, 142.5, 138.8, 137.9, 136.9, 123.4, 114.6, 112.3, 44.8, 31.6, 29.0, 28.9, 28.7, 26.3, 22.5, 14.0; ^{19}F NMR (471 MHz, $CDCl_3$) δ -152.38.

3.3.13A Preparation of 2-(4-bromophenyl)-1-octyl-1H-imidazo[1,2-a]pyrimidin-4-ium tetra fluoroborate [6e]. The title compound was prepared according to the representative procedure on a 0.58 mmol scale, and product **6e** was obtained as a yellow crystalline solid (0.2470 g, 90%); ^{1}H NMR (500 MHz, $CDCl_3$) δ 9.24 (dd, *J* = 6.7, 1.7 Hz, 1H), 8.93 (dd, *J* = 4.4, 1.7 Hz, 1H), 8.39 (m, 3H), 7.86 (m, 2H), 7.59 (dd, *J* = 6.7, 4.4 Hz, 1H), 4.46 (t, *J* = 7.9 Hz, 2H), 1.72 (p, *J* = 6.8 Hz, 2H), 1.20 (m, 10H), 0.84 (t, *J* = 7.3 Hz, 3H); ^{13}C NMR (126 MHz, $CDCl_3$) δ 157.5, 149.3, 142.8, 138.8, 135.5, 131.3, 131.1, 124.5, 114.8, 113.1, 45.0, 31.6, 29.1, 28.9, 28.7, 26.3, 22.5, 14.0; ^{19}F NMR (471 MHz, $CDCl_3$) δ -152.13.

APPENDIX B

SPECTRAL DATA

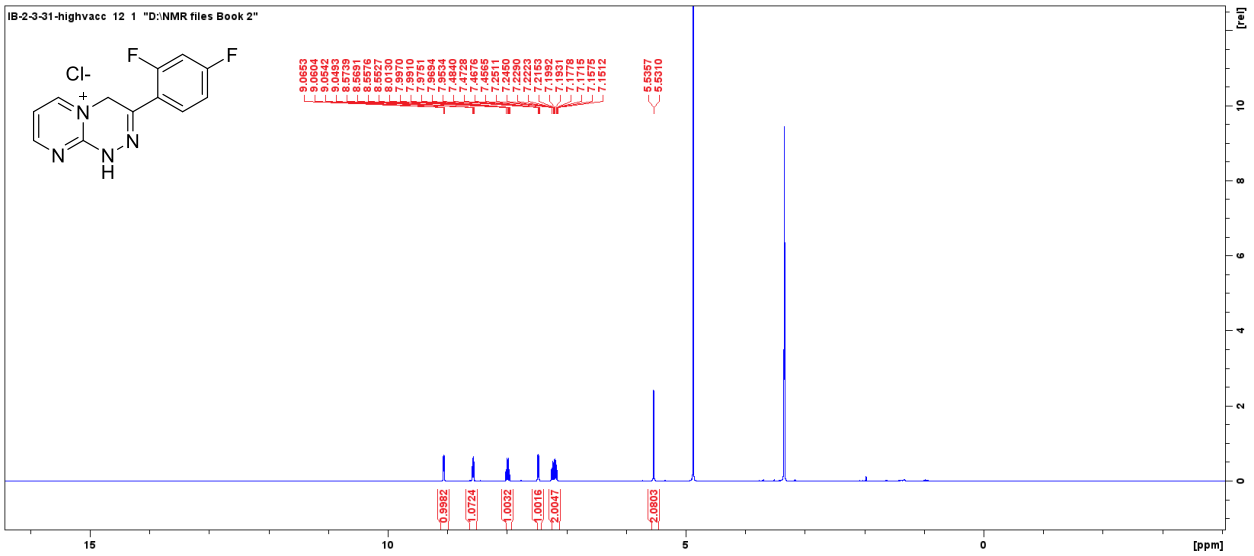

Figure 2.1.1 B: ^{1}H NMR Spectra of 3-(2,4-difluorophenyl)-1,4-dihydropyrimido[2,1-c][1,2,4] triazin-5-ium chloride [6a].

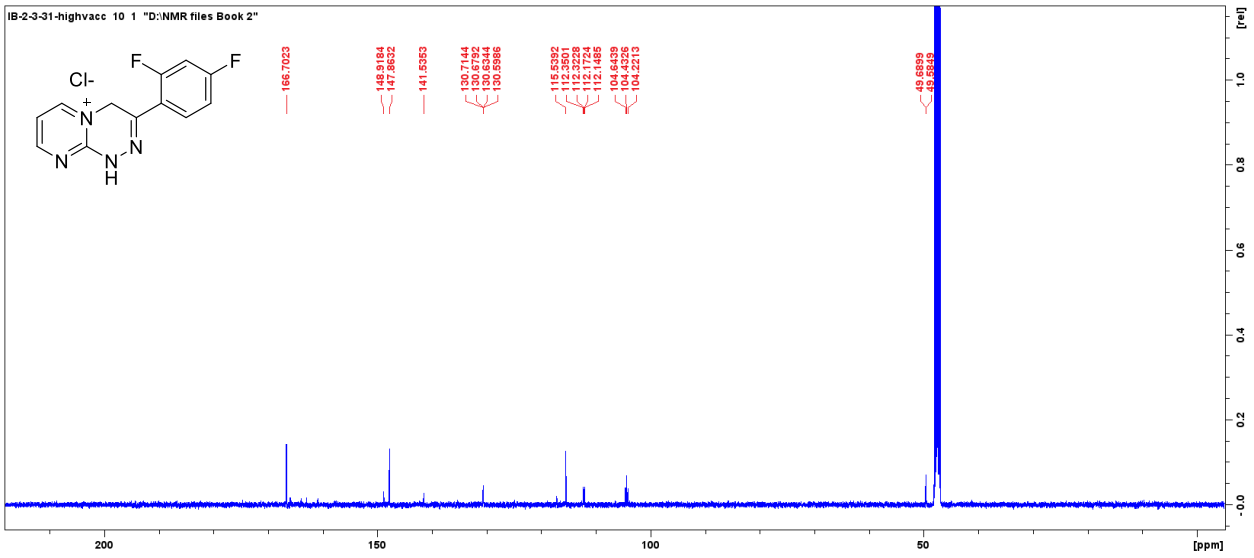

Figure 2.1.2 B: ^{13}C NMR Spectra of 3-(2,4-difluorophenyl)-1,4-dihydropyrimido[2,1-c][1,2,4] triazin-5-ium chloride [6a].

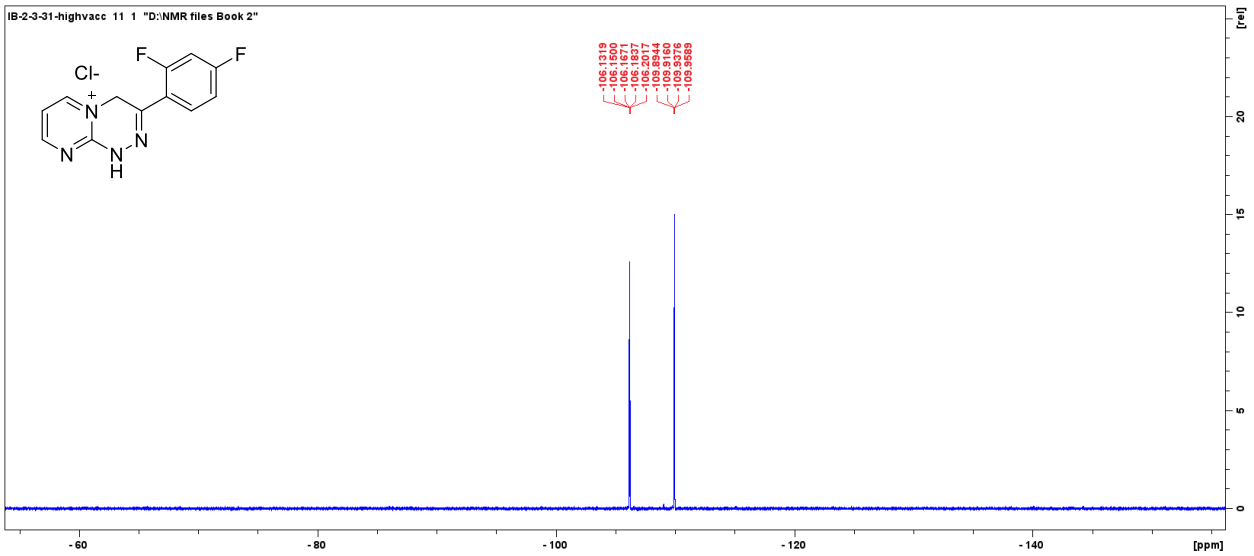

Figure 2.1.3 B: ^{19}F NMR Spectra of 3-(2,4-difluorophenyl)-1,4-dihydropyrimido[2,1-c][1,2,4] triazin-5-ium chloride [6a].

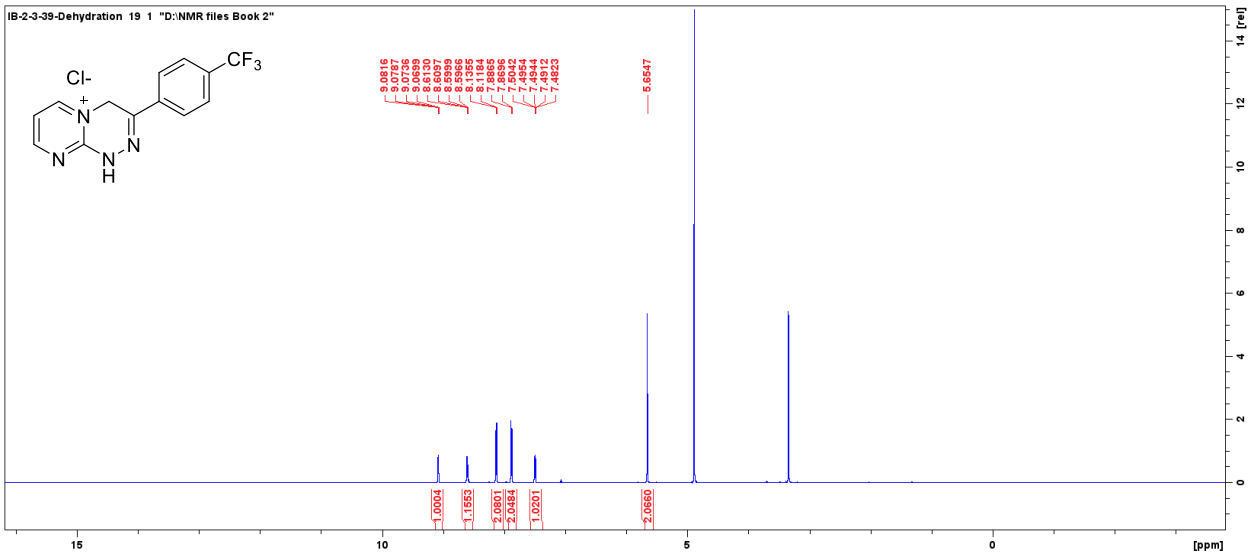

Figure 2.1.4 B: ^{1}H NMR Spectra of 3-(4-(trifluoromethyl)phenyl)-1,4-dihydropyrimido[2,1-c][1,2,4]triazin-5-ium chloride [6b].

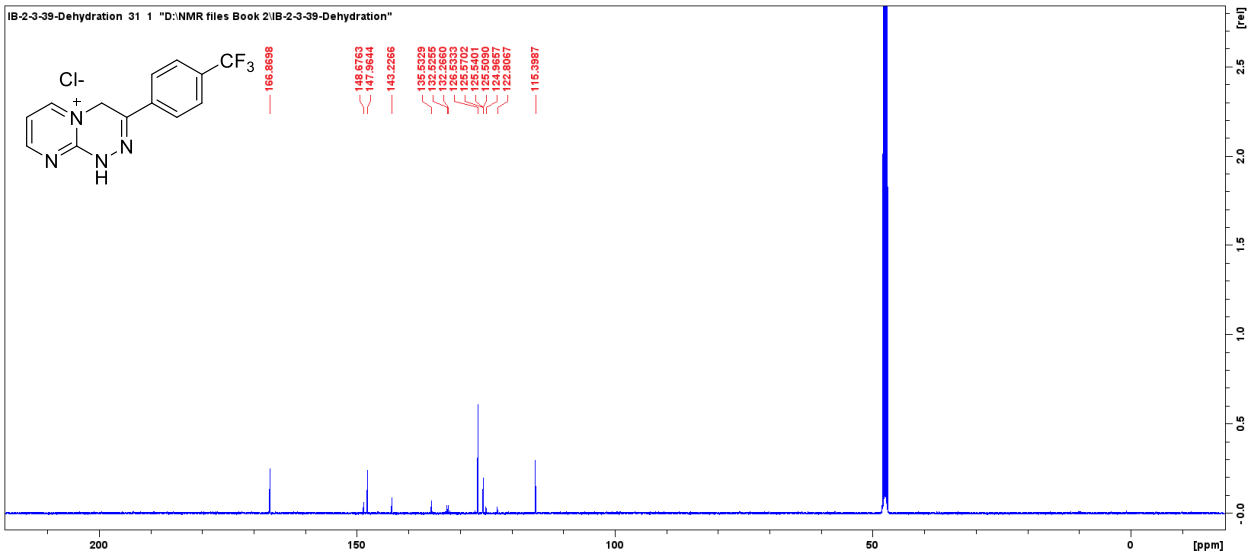

Figure 2.1.5 B: ^{13}C NMR Spectra of 3-(4-(trifluoromethyl)phenyl)-1,4-dihydropyrimido[2,1-c] [1,2,4]triazin-5-ium chloride [6b].

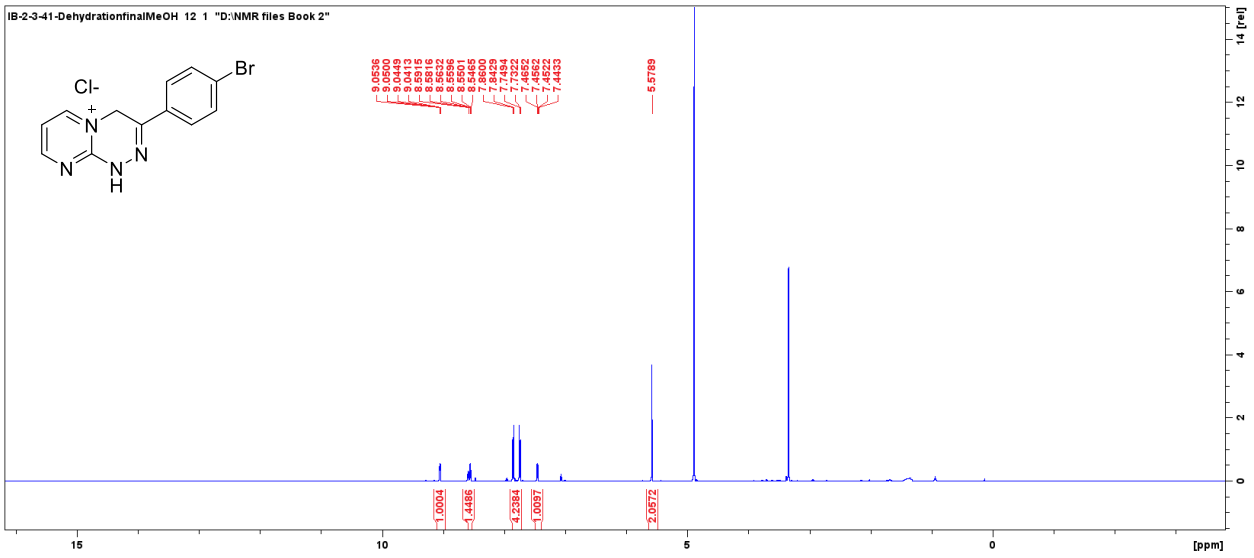

Figure 2.1.6 B: ^{1}H NMR Spectra of 3-(4-bromophenyl)-1,4-dihydropyrimido[2,1-c][1,2,4] triazin-5-ium chloride [6c].

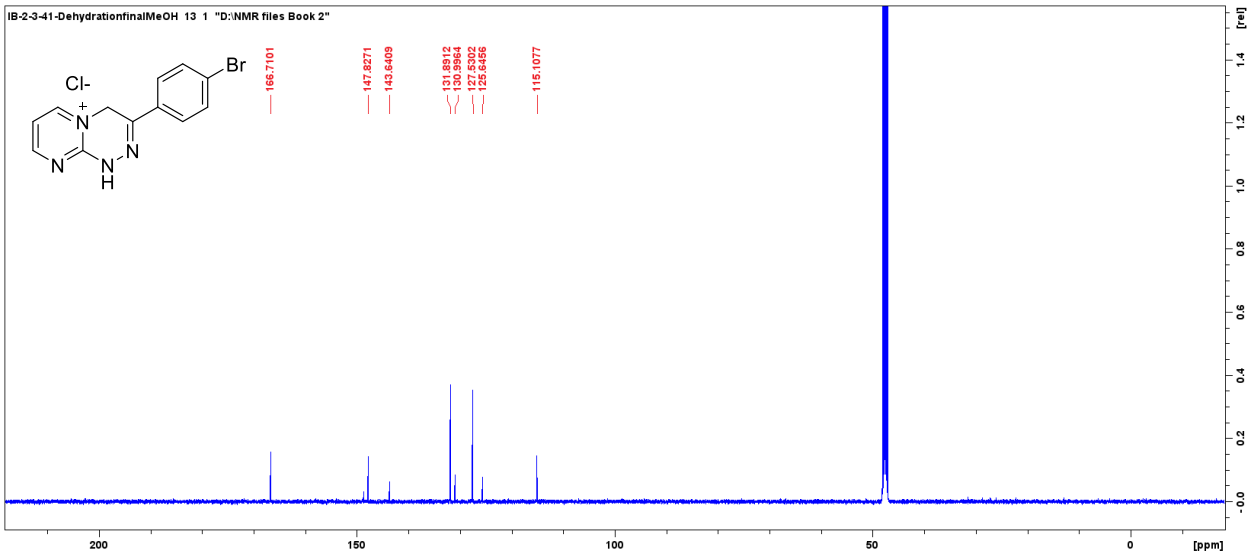

Figure 2.1.7 B: ^{13}C NMR Spectra of 3-(4-bromophenyl)-1,4-dihydropyrimido[2,1-c] [1,2,4] triazin-5-ium chloride [3].

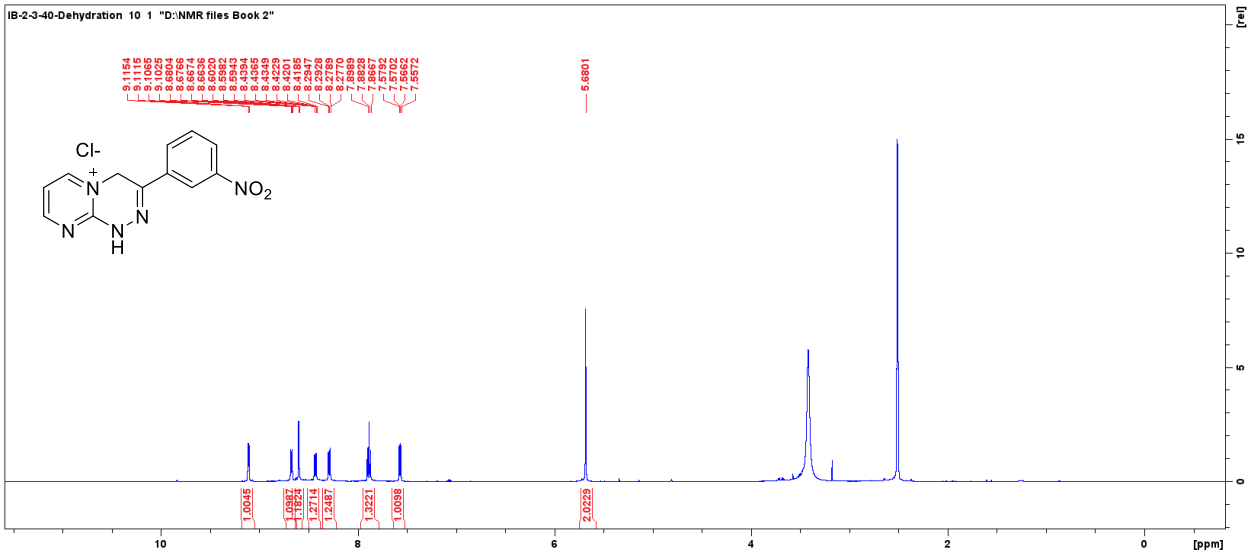

Figure 2.1.8 B: ^{1}H NMR Spectra of 3-(3-nitrophenyl)-1,4-dihydropyrimido[2,1-c][1,2,4]triazin-5-ium chloride [6d].

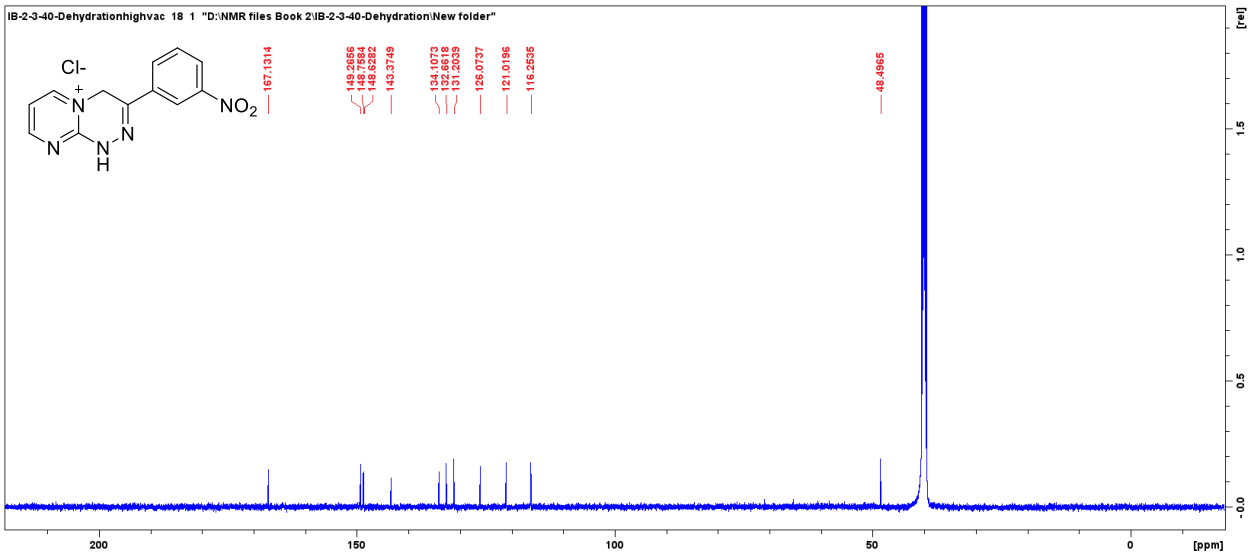

Figure 2.1.9 B: ^{13}C NMR Spectra of 3-(3-nitrophenyl)-1,4-dihydropyrimido[2,1-c][1,2,4]triazin-5-ium chloride [6d].

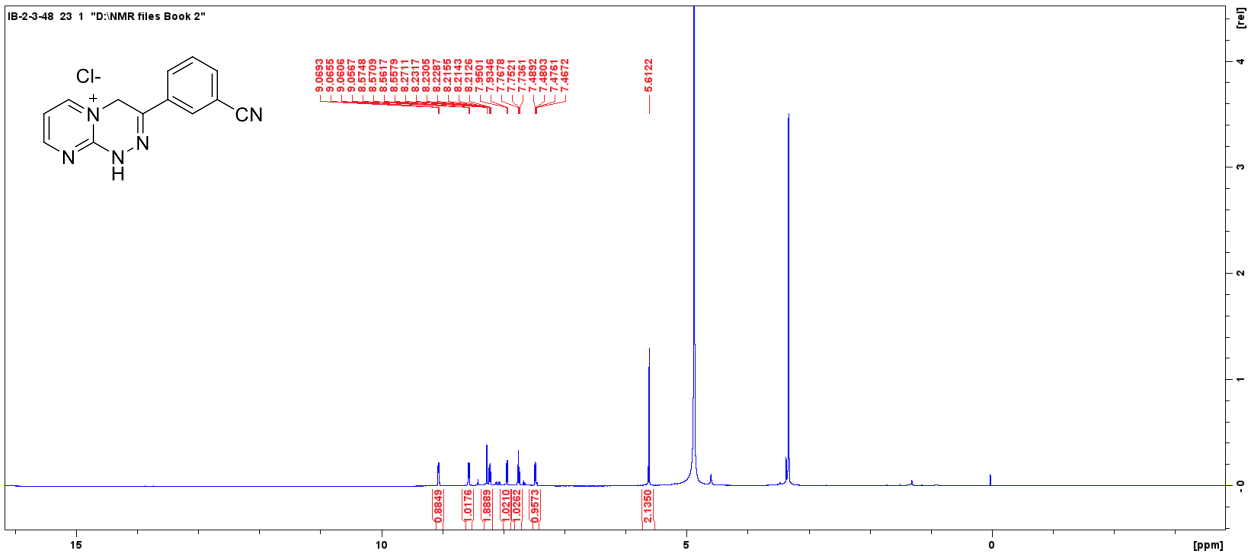

Figure 2.1.10 B: ^{1}H NMR Spectra of 3-(3-cyanophenyl)-1,4-dihydropyrimido[2,1-c][1,2,4]triazin-5-ium chloride [6e].

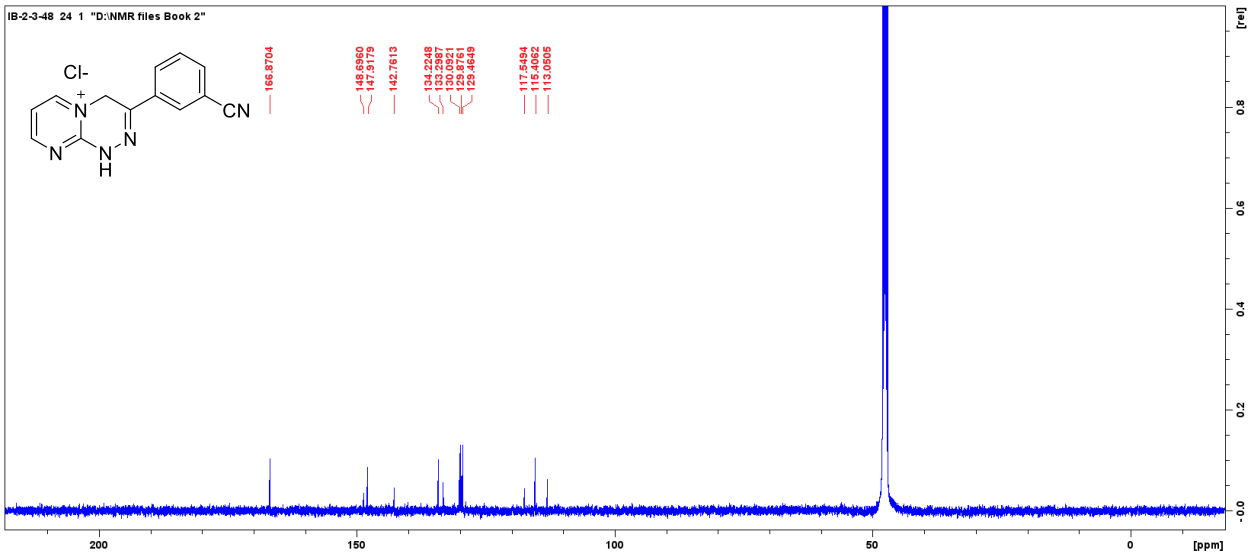

Figure 2.1.11 B: ^{13}C NMR Spectra of 3-(3-cyanophenyl)-1,4-dihydropyrimido[2,1-c][1,2,4] triazin-5-ium chloride [6e].

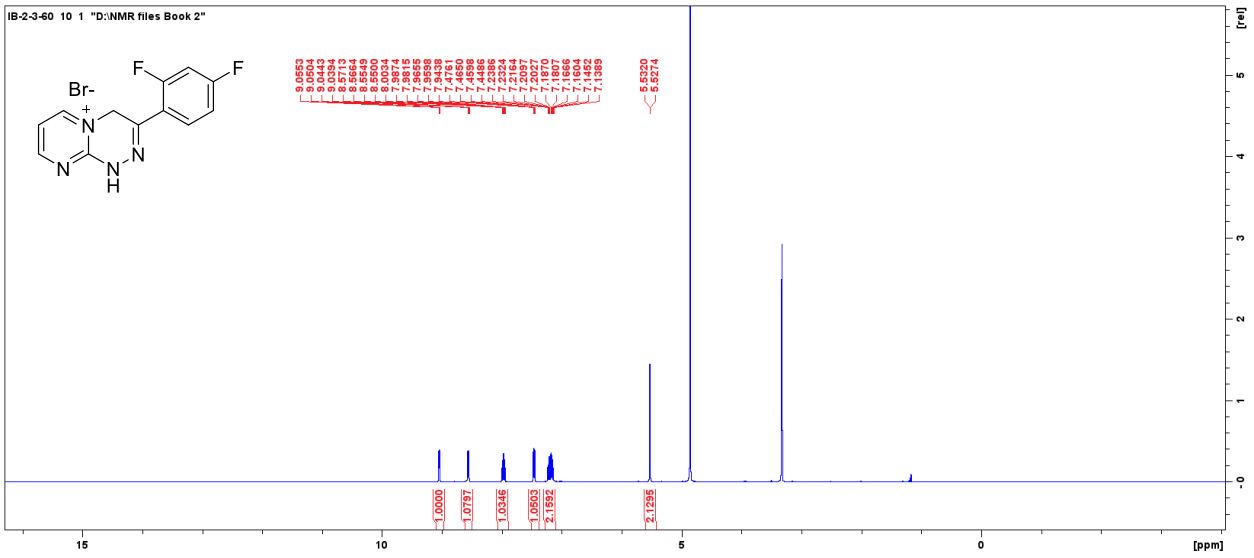

Figure 2.2.1 B: ^{1}H NMR Spectra of 3-(2,4-difluorophenyl)-1,4-dihydropyrimido[2,1-c][1,2,4] triazin-5-ium bromide [8.1a].

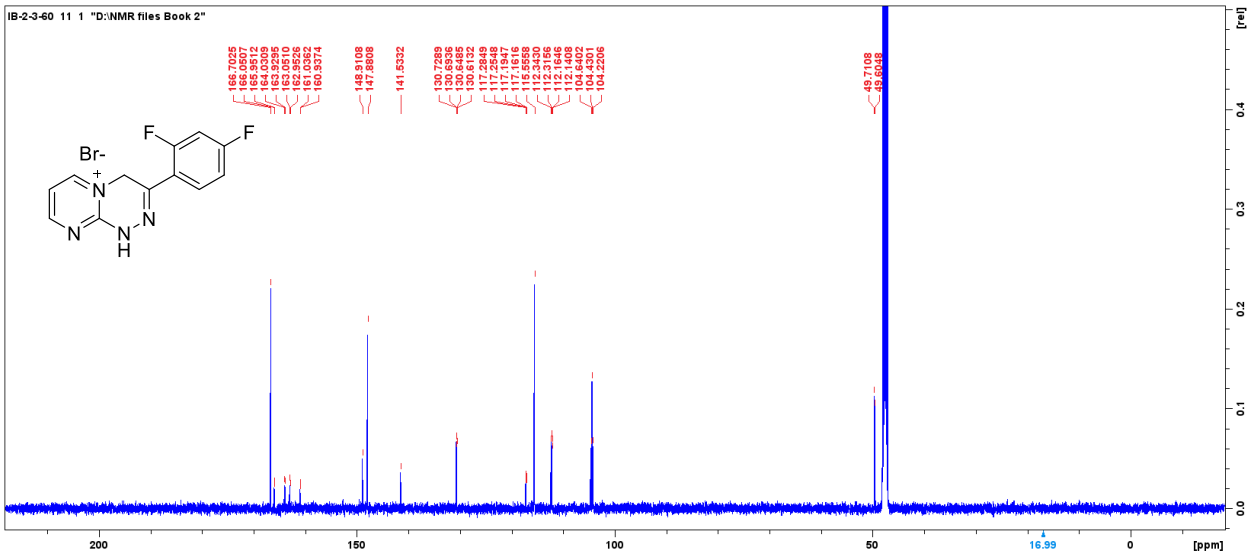

Figure 2.2.2 B: ^{13}C NMR Spectra of 3-(2,4-difluorophenyl)-1,4-dihydropyrimido[2,1-c][1,2,4] triazin-5-ium bromide [8.1a].

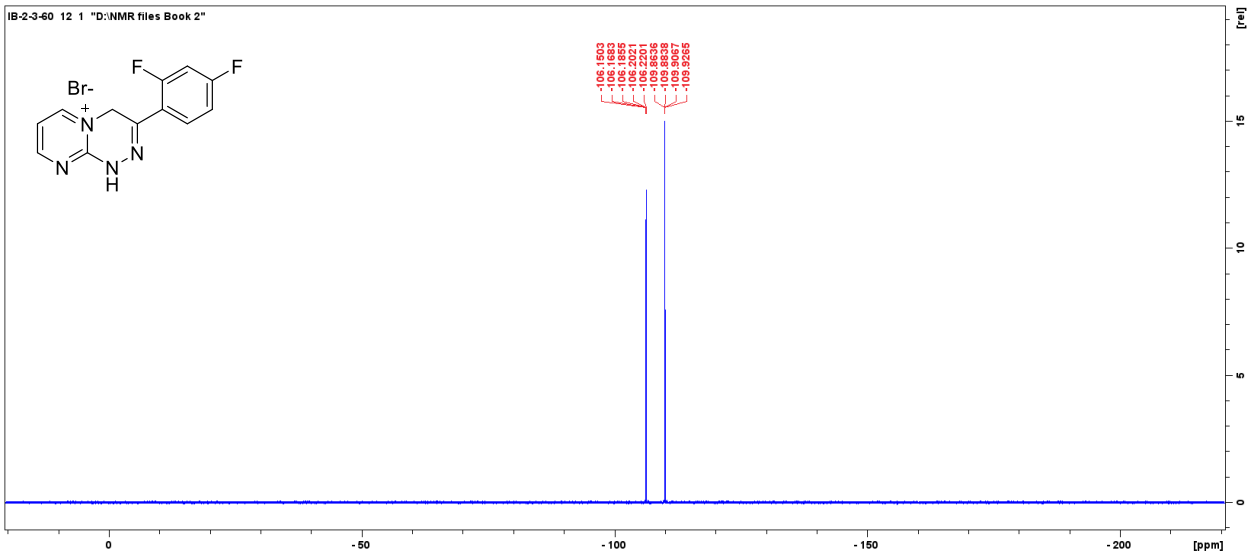

Figure 2.2.3 B: ^{19}F NMR Spectra of 3-(2,4-difluorophenyl)-1,4-dihydropyrimido[2,1-c][1,2,4] triazin-5-ium bromide [8.1a].

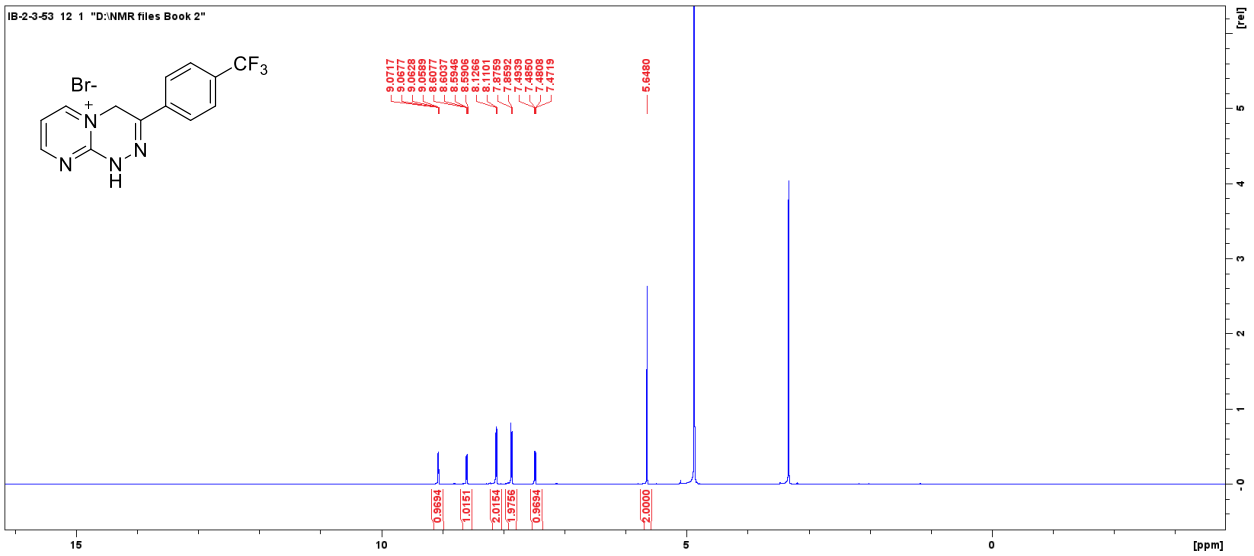

Figure 2.2.4 B: ^{1}H NMR Spectra of 3-(4-(trifluoromethyl)phenyl)-1,4-dihydropyrimido[2,1-c][1,2,4]triazin-5-ium bromide [8.1b].

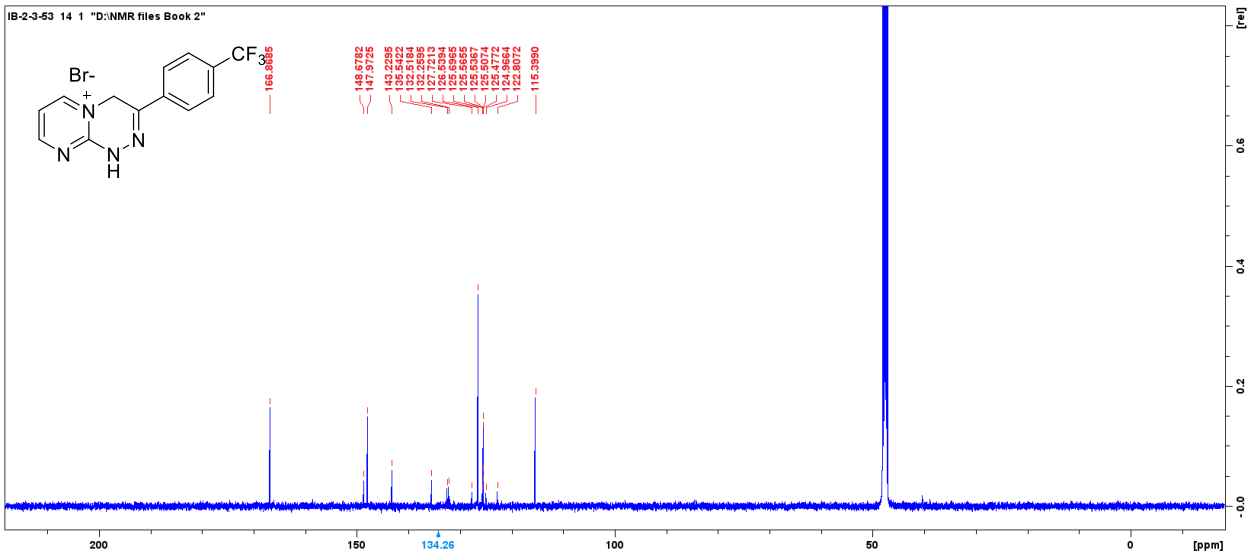

Figure 2.2.5 B: ^{13}C NMR Spectra of 3-(4-(trifluoromethyl)phenyl)-1,4-dihydropyrimido[2,1-c][1,2,4]triazin-5-ium bromide [8.1b].

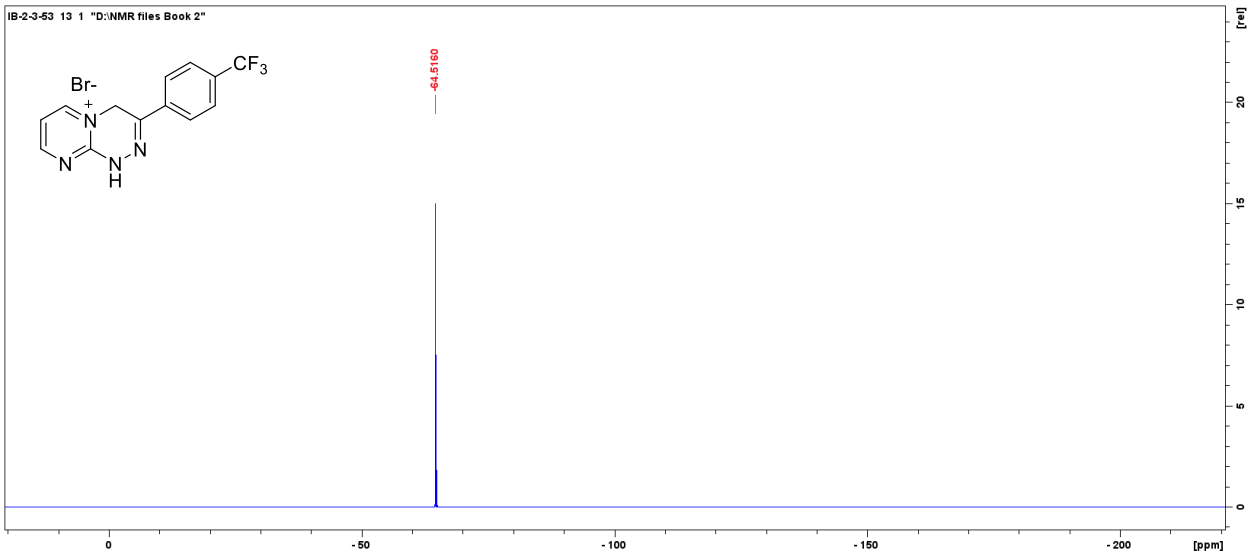

Figure 2.2.6 B: ^{19}F NMR Spectra of 3-(4-(trifluoromethyl)phenyl)-1,4-dihydropyrimido[2,1-c][1,2,4]triazin-5-ium bromide [8.1b].

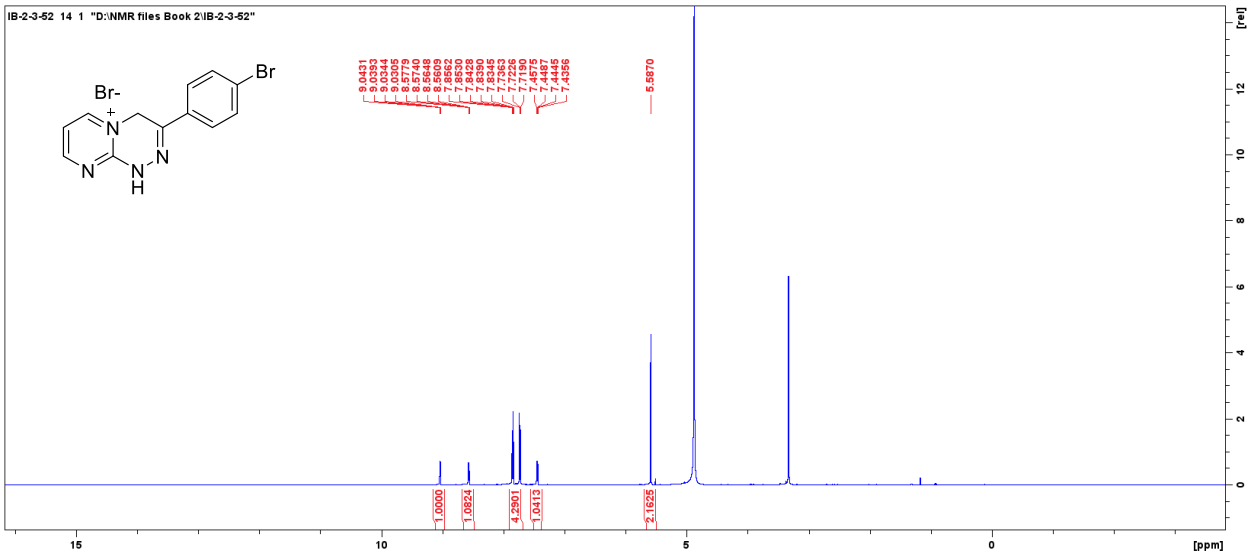

Figure 2.2.7 B: ^{1}H NMR Spectra of 3-(4-bromophenyl)-1,4-dihydropyrimido[2,1-c][1,2,4]triazin-5-ium bromide [8.1c].

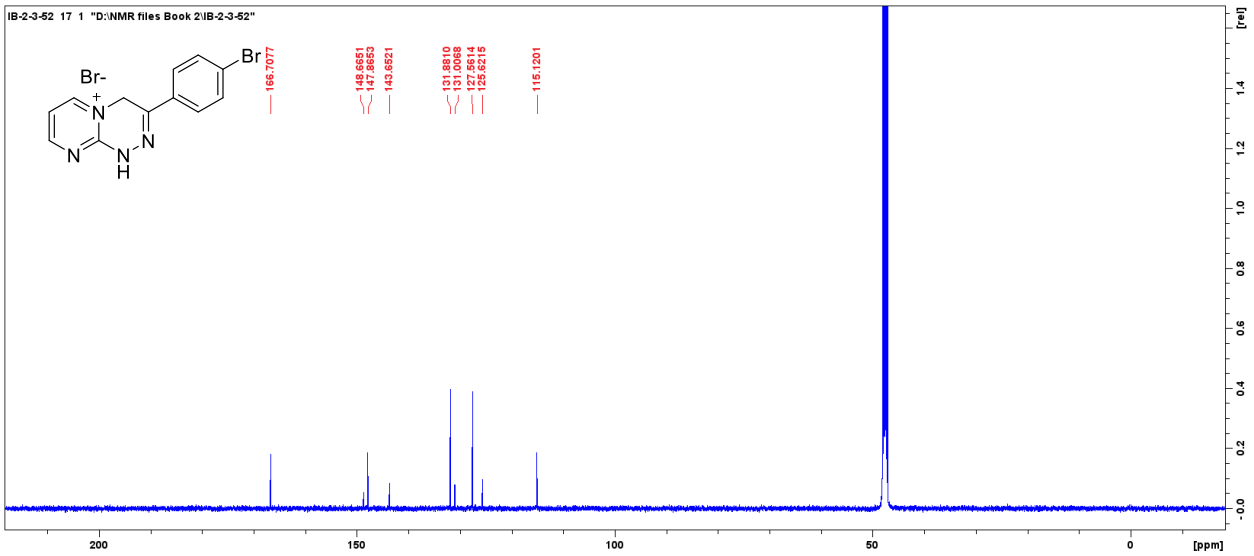

Figure 2.2.8 B: ^{13}C NMR Spectra of 3-(4-bromophenyl)-1,4-dihydropyrimido[2,1-c][1,2,4]triazin-5-ium bromide [8.1c].

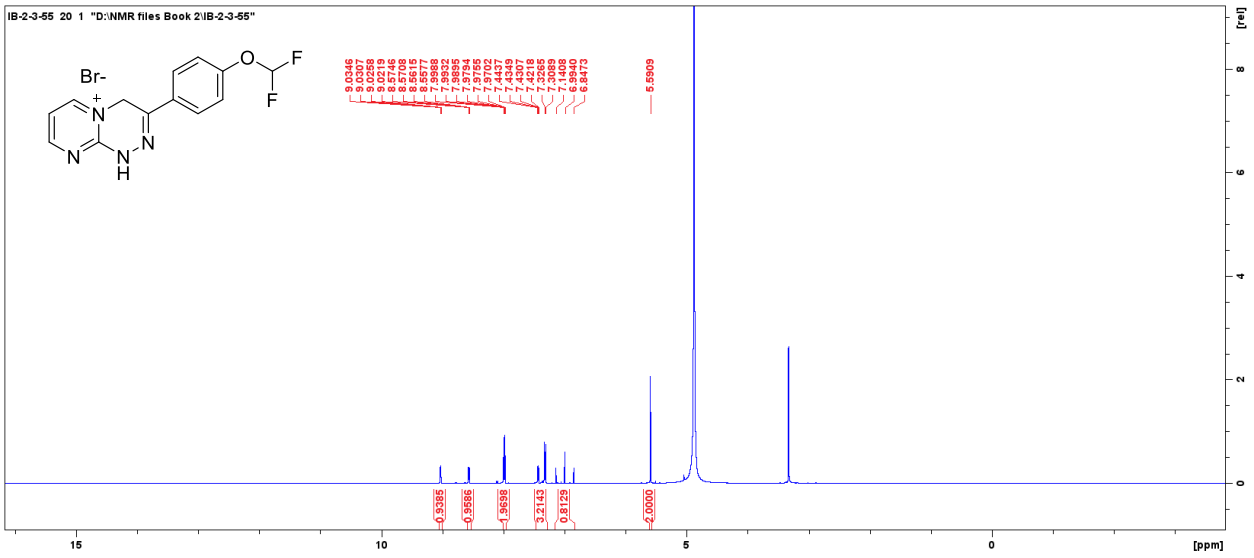

Figure 2.2.9 B: ^{1}H NMR Spectra of 3-(4-(difluoromethoxy)phenyl)-1,4-dihydropyrimido[2,1-c][1,2,4]triazin-5-ium bromide [8.1d].

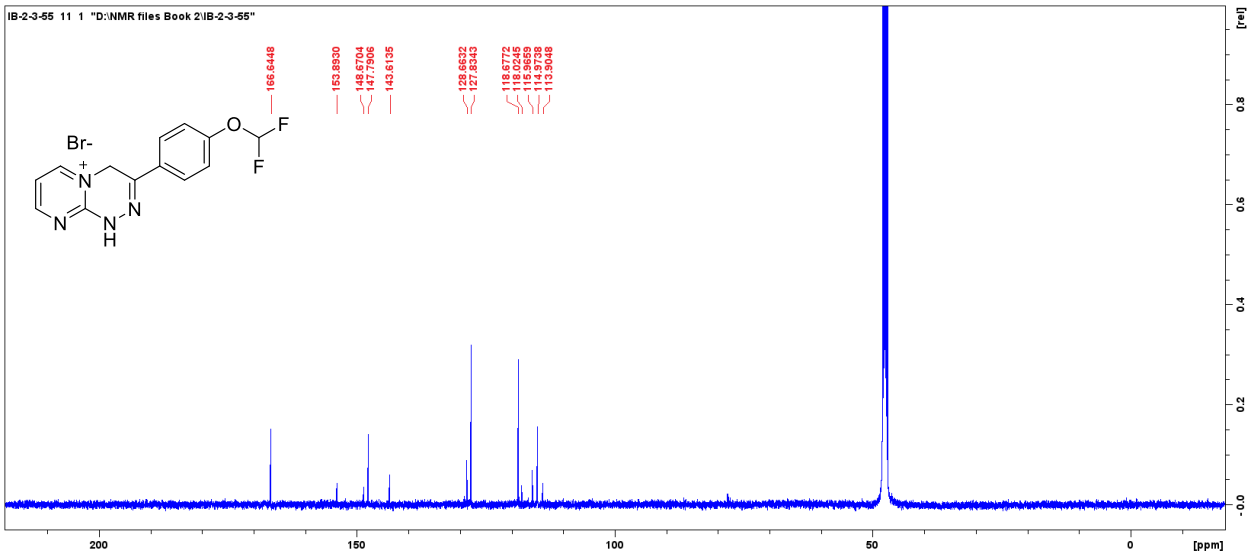

Figure 2.2.10 B: ^{13}C NMR Spectra of 3-(4-(difluoromethoxy)phenyl)-1,4-dihydropyrimido[2,1-c][1,2,4]triazin-5-ium bromide [8.1d].

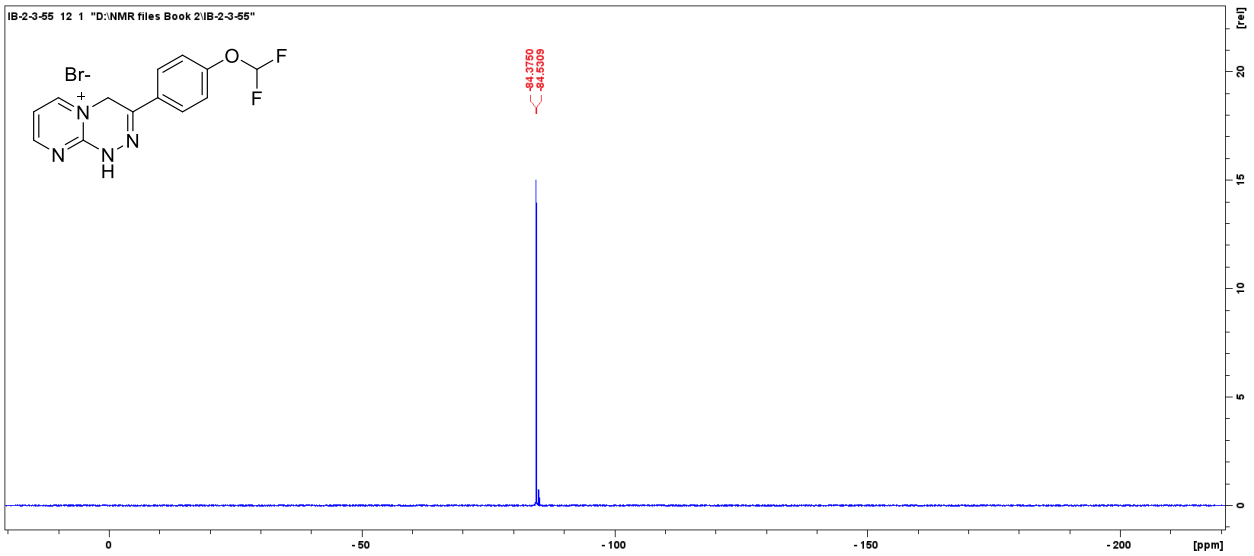

Figure 2.2.11 B: ^{19}F NMR Spectra of 3-(4-(difluoromethoxy)phenyl)-1,4-dihydropyrimido[2,1-c] [1,2,4]triazin-5-ium bromide [8.1d].

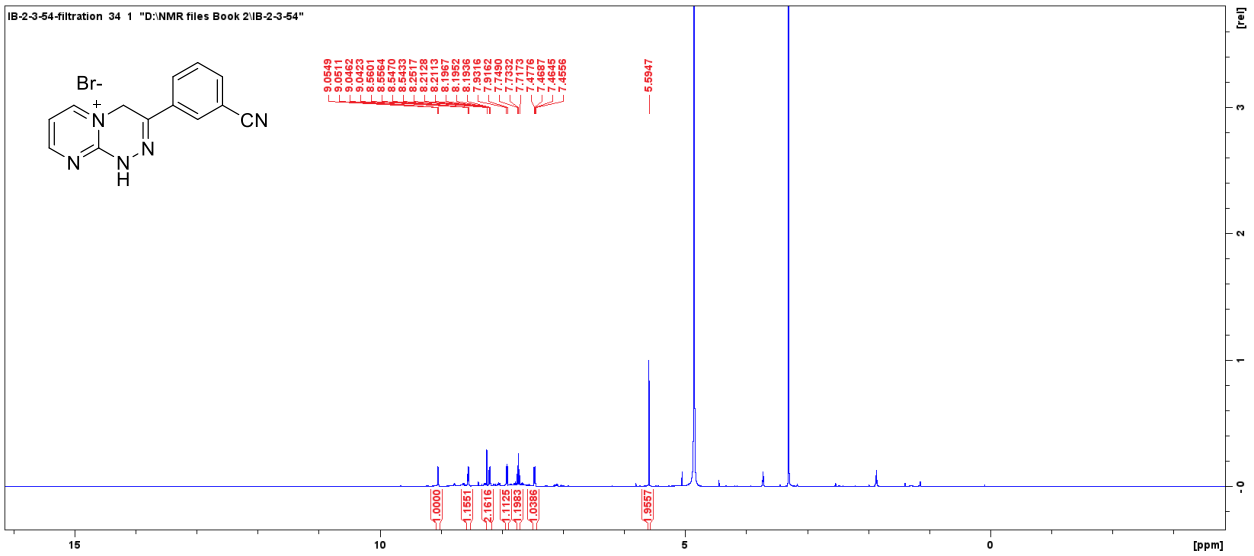

Figure 2.2.12 B: ^{1}H NMR Spectra of 3-(3-cyanophenyl)-1,4-dihydropyrimido[2,1-c][1,2,4]triazin-5-ium bromide [8.1e].

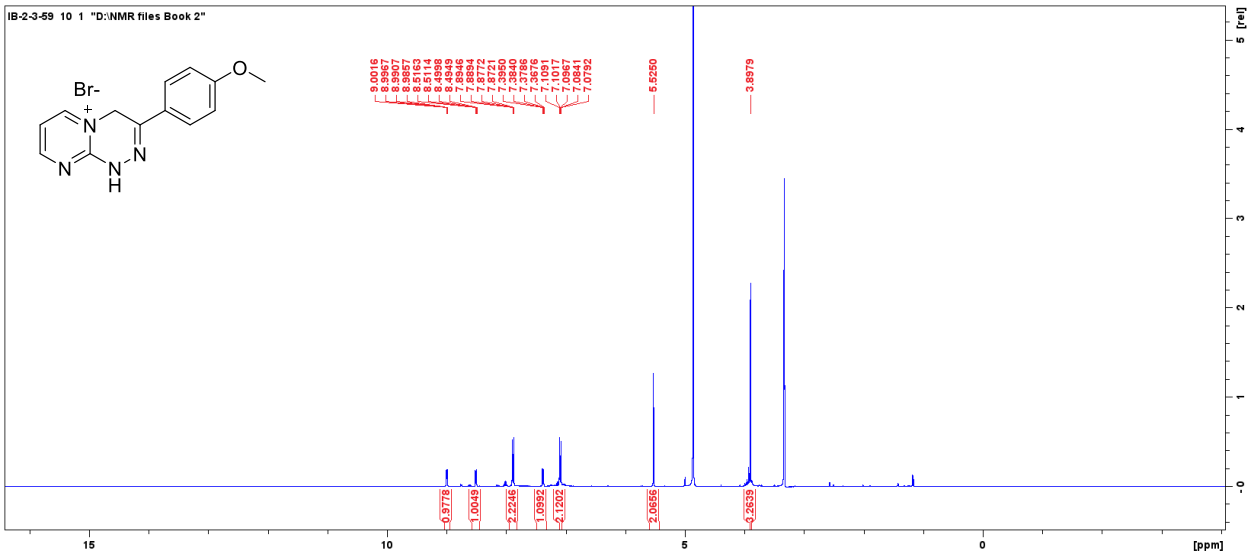

Figure 2.2.13 B: ^{1}H NMR Spectra of 3-(4-methoxyphenyl)-1,4-dihydropyrimido[2,1-c] [1,2,4] triazin-5-ium bromide [8.1f].

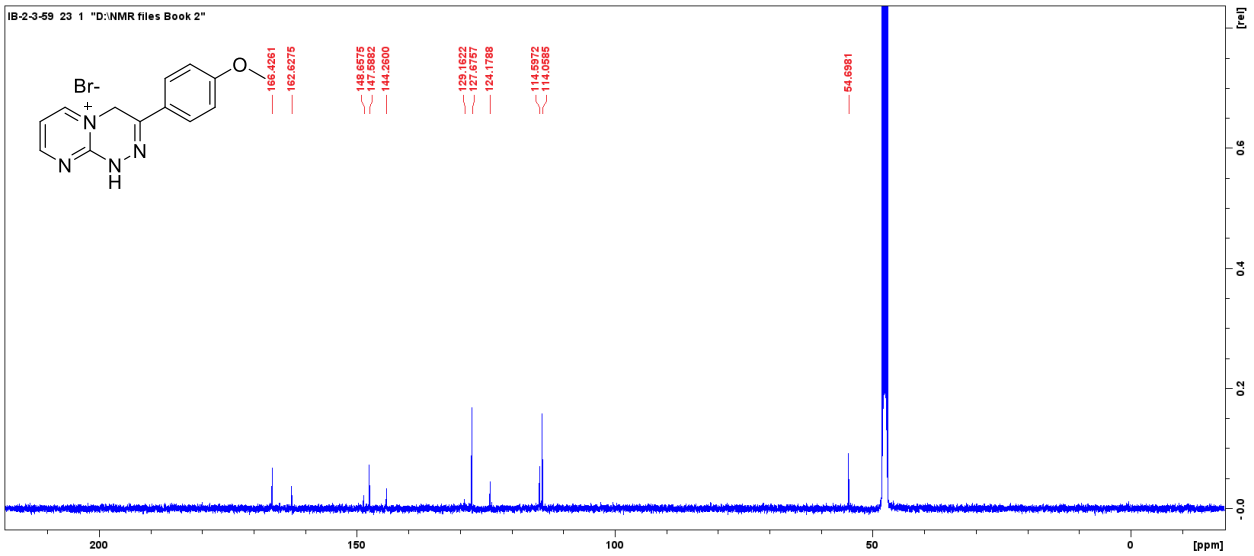

Figure 2.2.14 B: ^{13}C NMR Spectra of 3-(4-methoxyphenyl)-1,4-dihydropyrimido[2,1-c][1,2,4] triazin-5-ium bromide [8.1f].

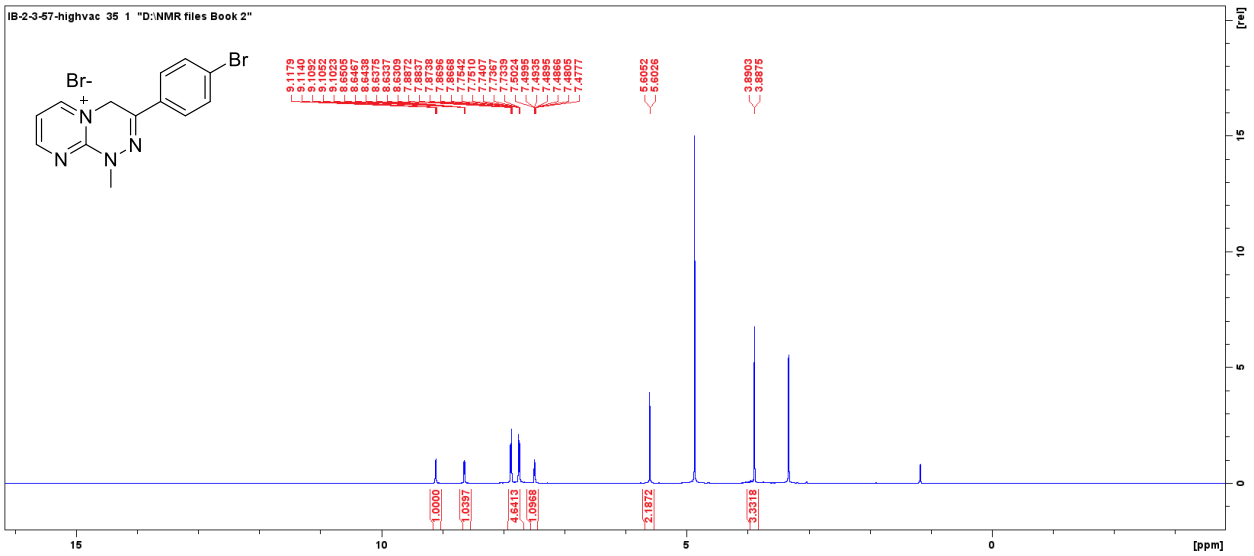

Figure 2.2.15 B: ^{1}H NMR Spectra of 3-(4-bromophenyl)-1-methyl-1,4-dihydropyrimido[2,1-c][1,2,4]triazin-5-ium bromide. [8.2c].

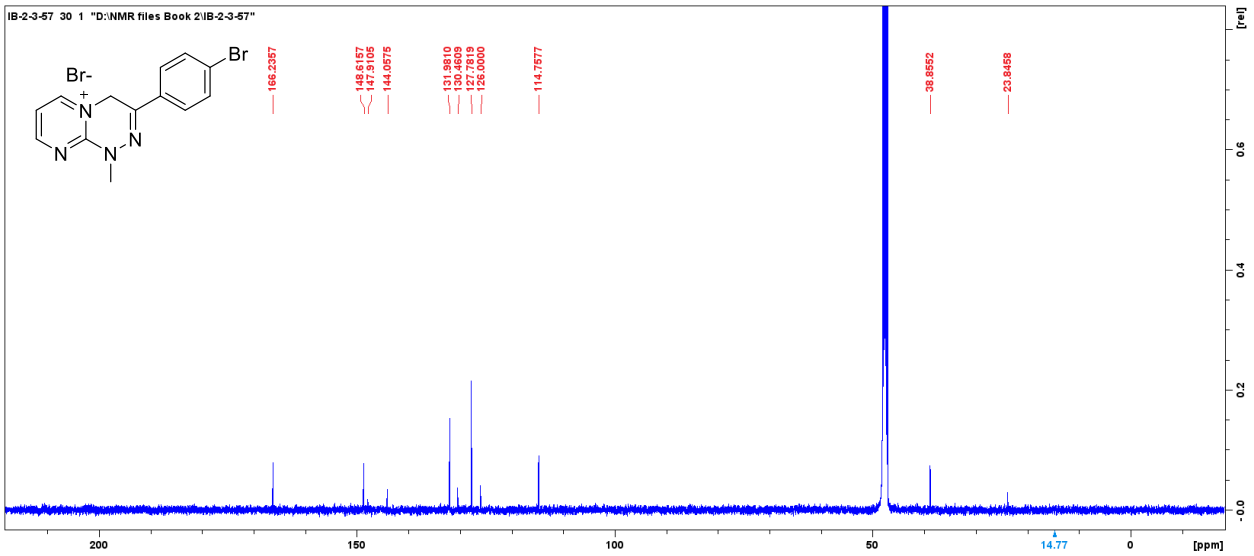

Figure 2.2.16 B: ^{13}C NMR Spectra of 3-(4-bromophenyl)-1-methyl-1,4-dihydropyrimido[2,1-c][1,2,4]triazin-5-ium bromide. [8.2c].

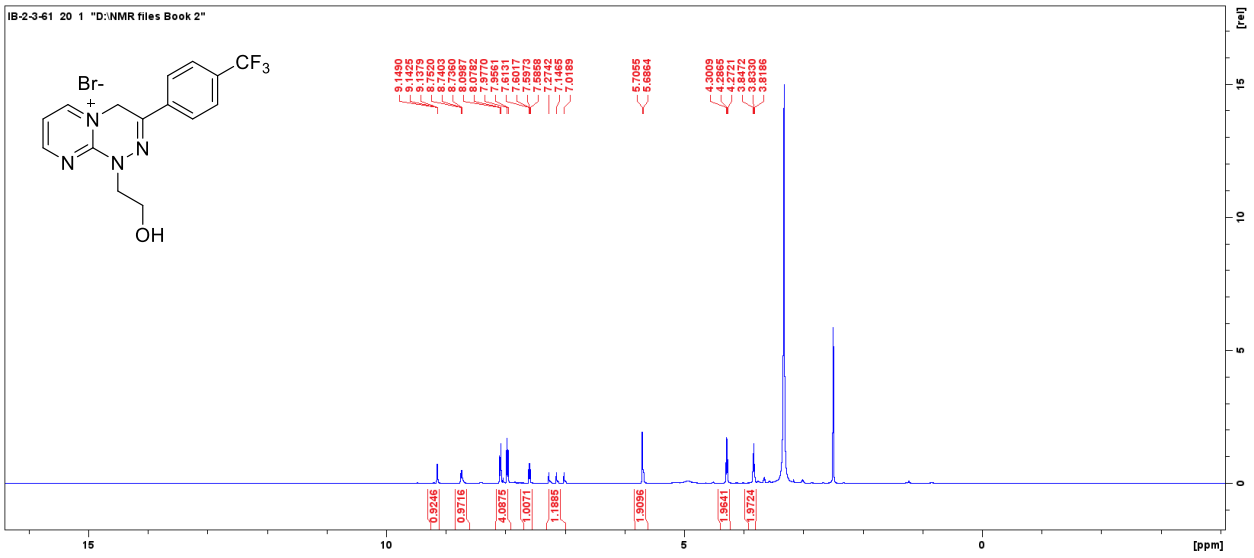

Figure 2.2.17 B: ^{1}H NMR Spectra of 1-(2-hydroxyethyl)-3-(4-(trifluoromethyl)phenyl)-1,4-dihydropyrimido[2,1-c][1,2,4]triazin-5-ium bromide [8.3b].

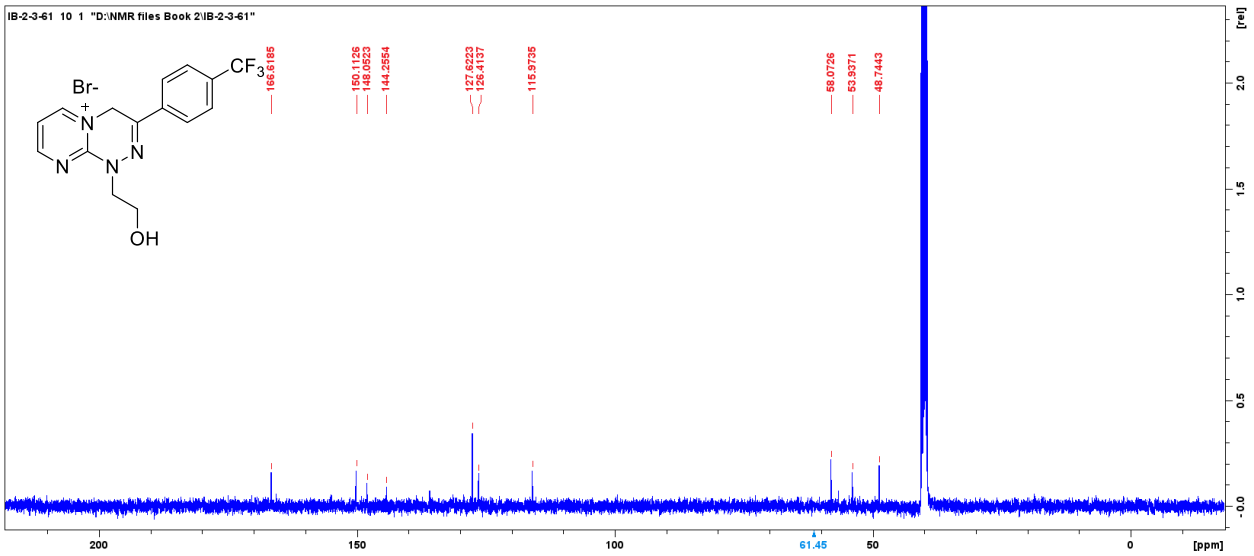

Figure 2.2.18 B: ^{13}C NMR Spectra of 1-(2-hydroxyethyl)-3-(4-(trifluoromethyl)phenyl)-1,4-dihydropyrimido[2,1-c][1,2,4]triazin-5-ium bromide [8.3b].

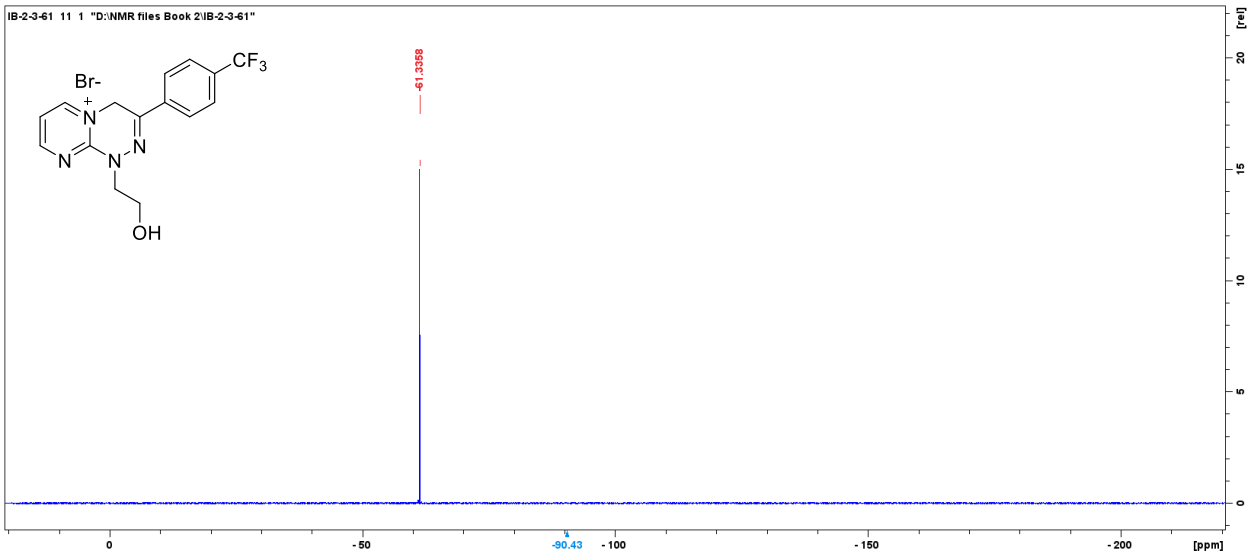

Figure 2.2.19 B: ^{19}F NMR Spectra of 1-(2-hydroxyethyl)-3-(4-(trifluoromethyl)phenyl)-1,4-dihydropyrimido[2,1-c][1,2,4]triazin-5-ium bromide [8.3b].

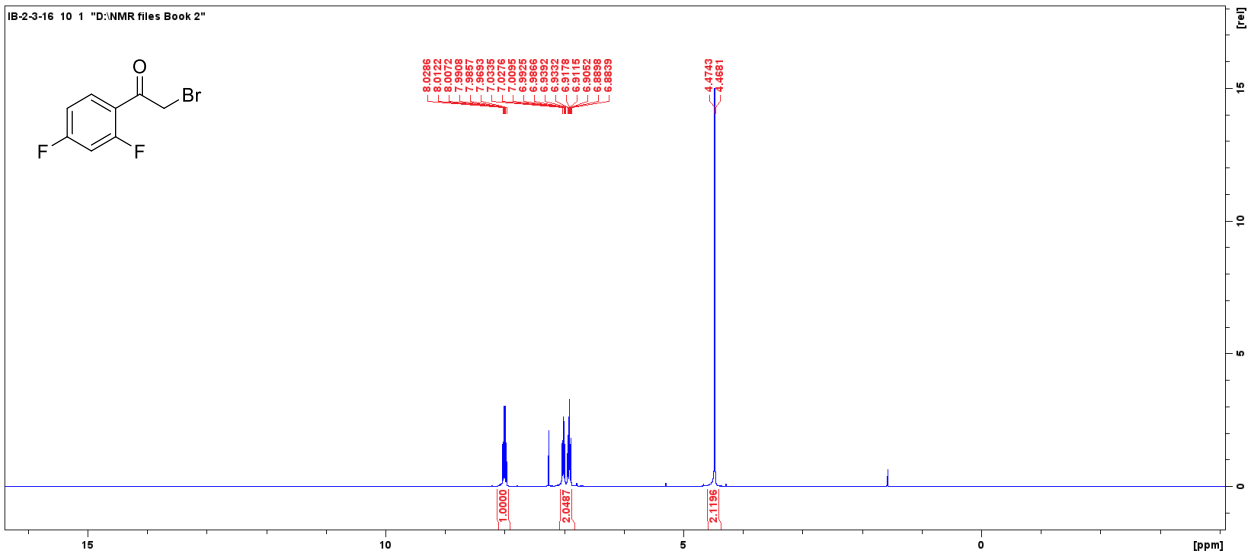

Figure 2.3.1 B: ^{1}H NMR Spectra of 2-bromo-1-(2,4-difluorophenyl)ethanone [2a].

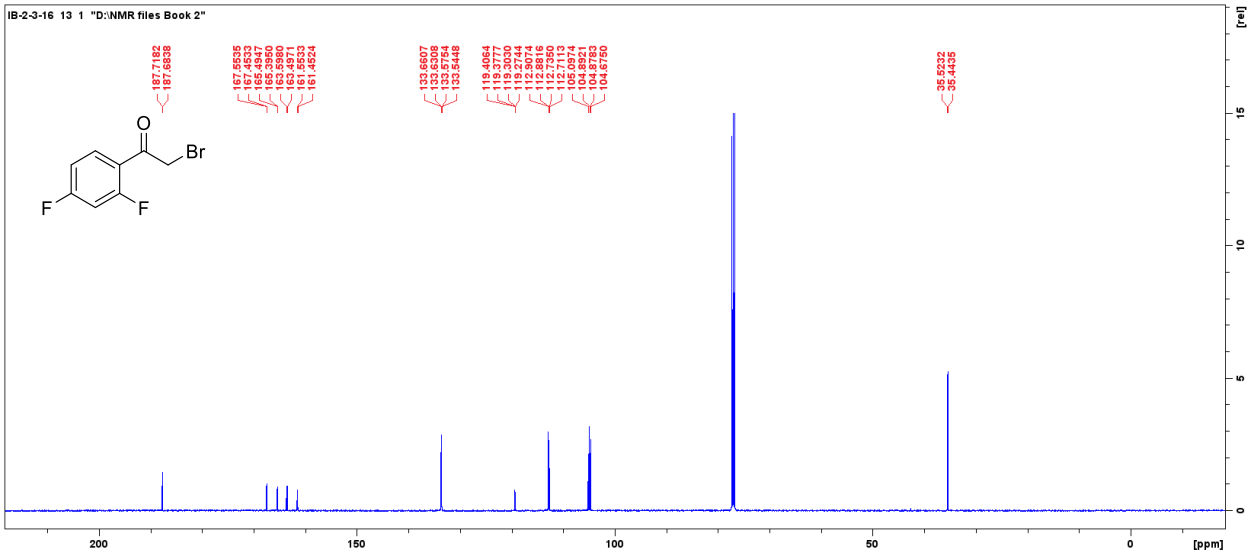

Figure 2.3.2 B: ^{13}C NMR Spectra of 2-bromo-1-(2,4-difluorophenyl)ethanone [2a].

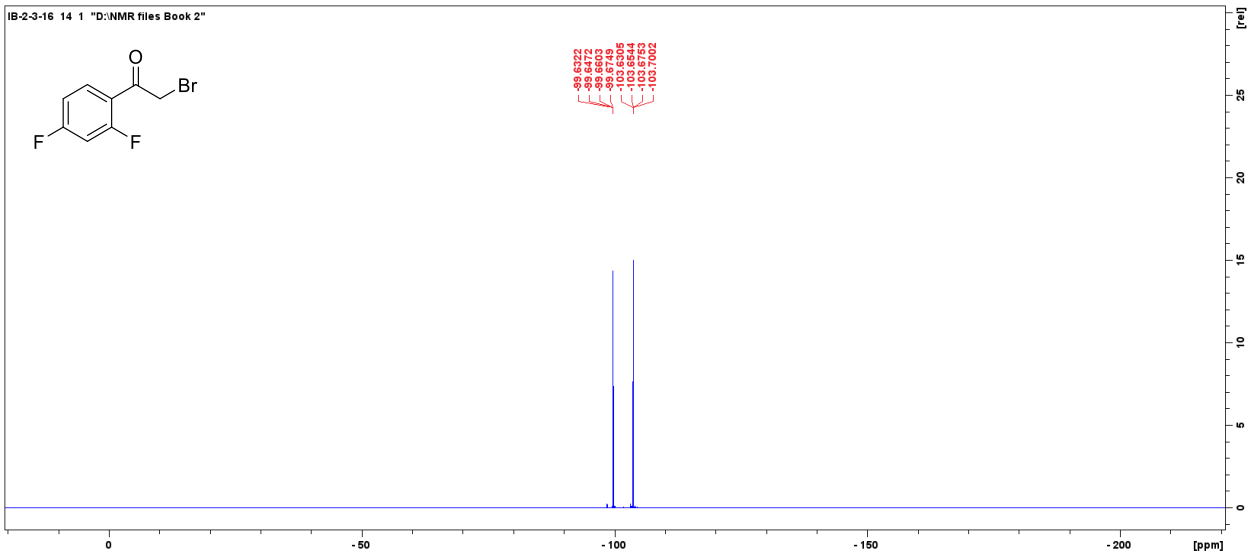

Figure 2.3.3 B: ^{19}F NMR Spectra of 2-bromo-1-(2,4-difluorophenyl)ethanone [2a].

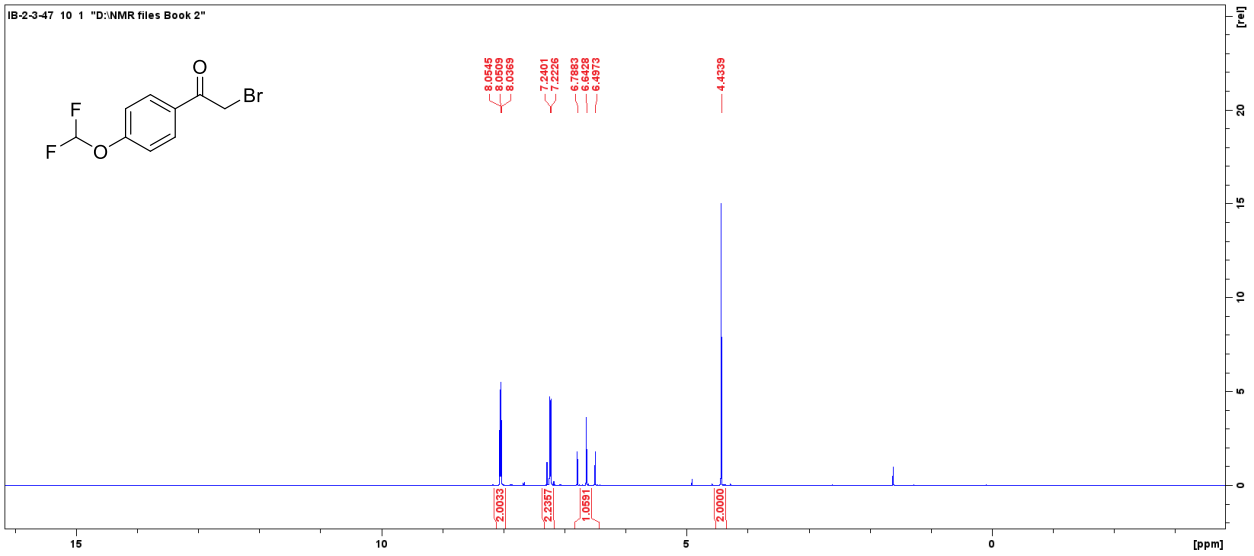

Figure 2.3.4 B: ^{1}H NMR Spectra of 2-bromo-1-(4-(difluoromethoxy)phenyl)ethanone [2d].

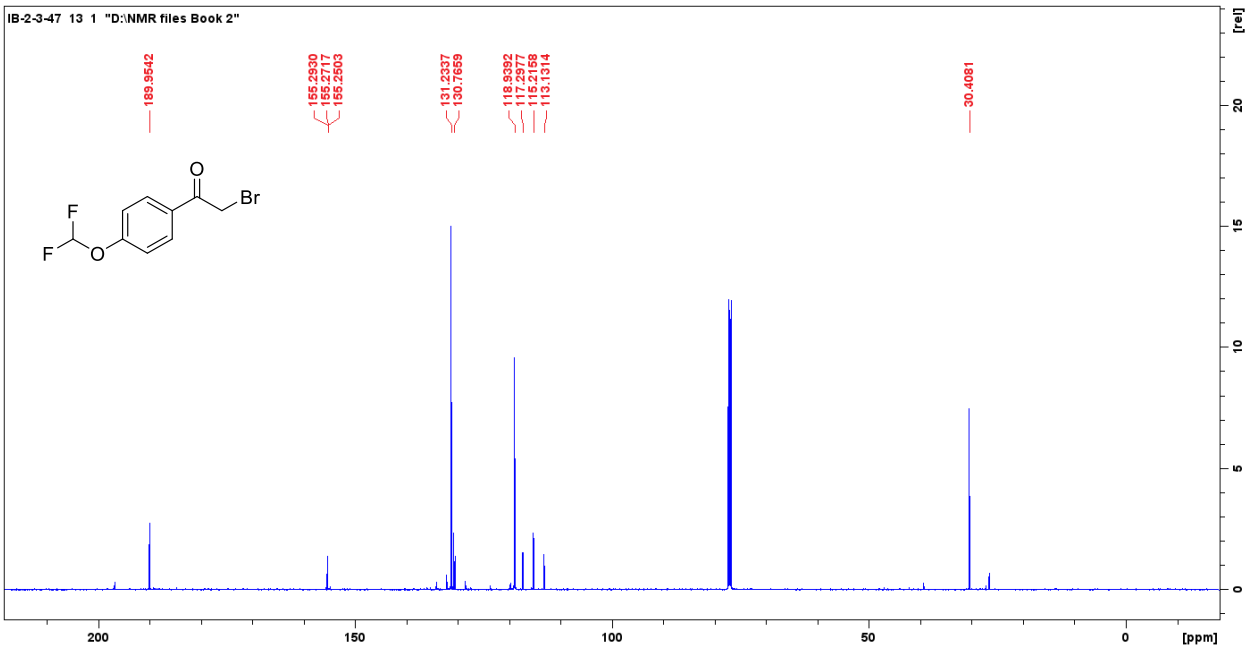

Figure 2.3.5 B: ^{13}C NMR Spectra of 2-bromo-1-(4-(difluoromethoxy)phenyl)ethanone [2d].

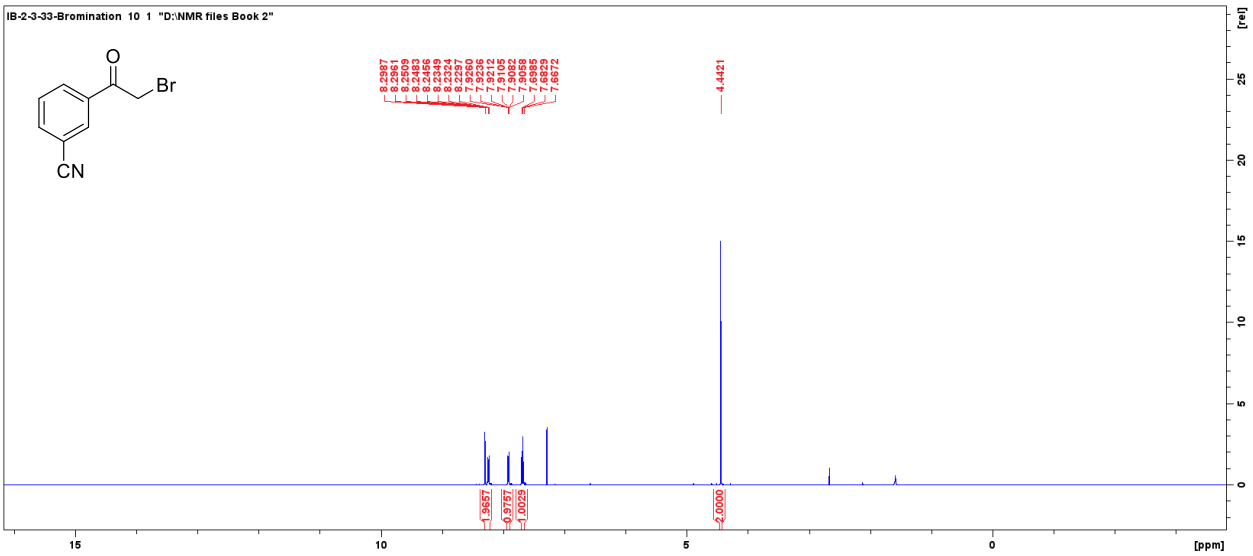

Figure 2.3.6 B: ^{1}H NMR Spectra of 3-(2-bromoacetyl)benzonitrile [2e].

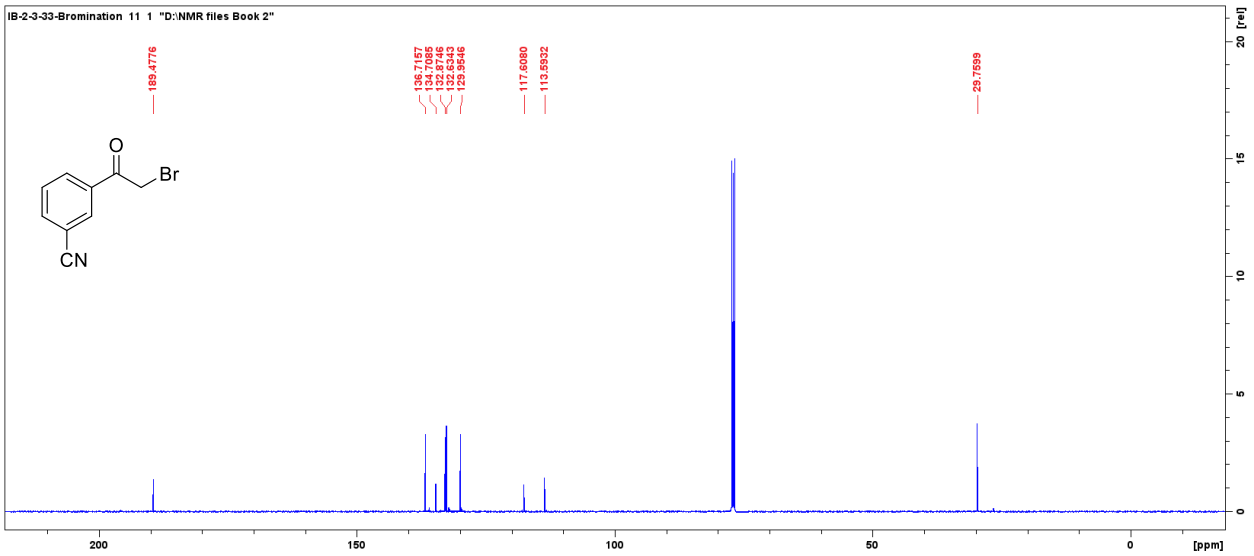

Figure 2.3.7 B: ^{13}C NMR Spectra of 3-(2-bromoacetyl)benzonitrile [2e].

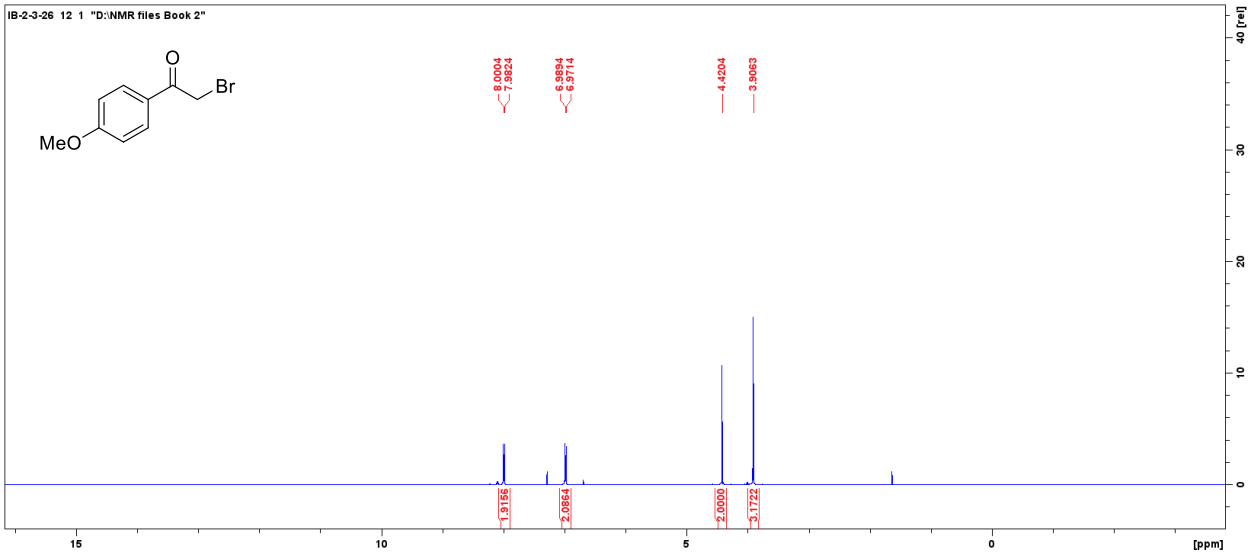

Figure 2.3.8 B: ^{1}H NMR Spectra of 2-bromo-1-(4-methoxyphenyl)ethanone [2f].

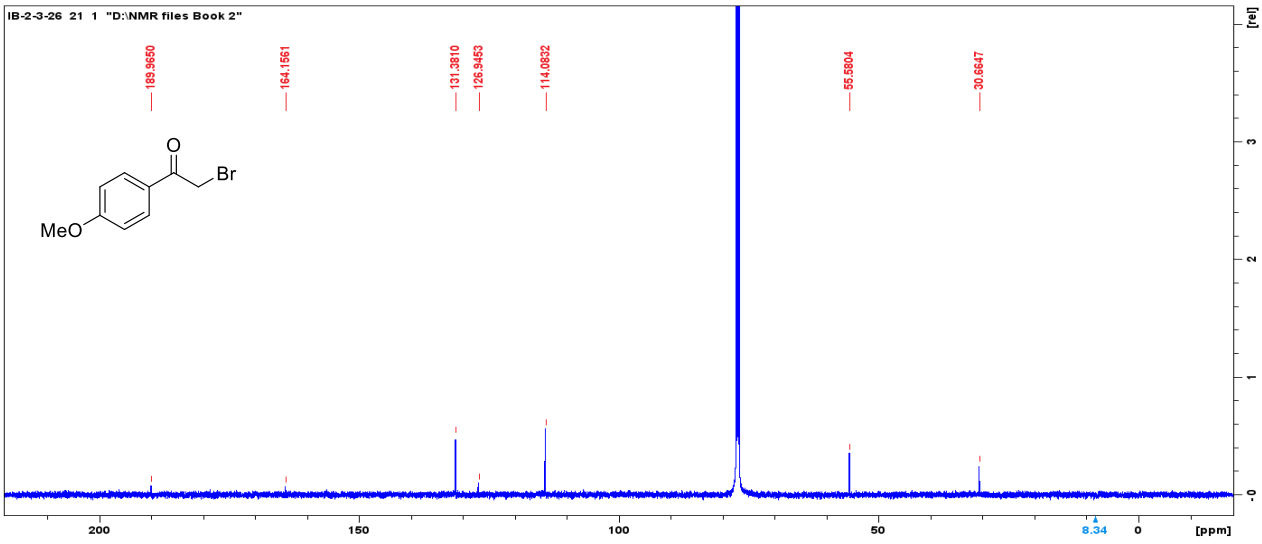

Figure 2.3.9 B: ^{13}C NMR Spectra of 2-bromo-1-(4-methoxyphenyl)ethanone [2f].

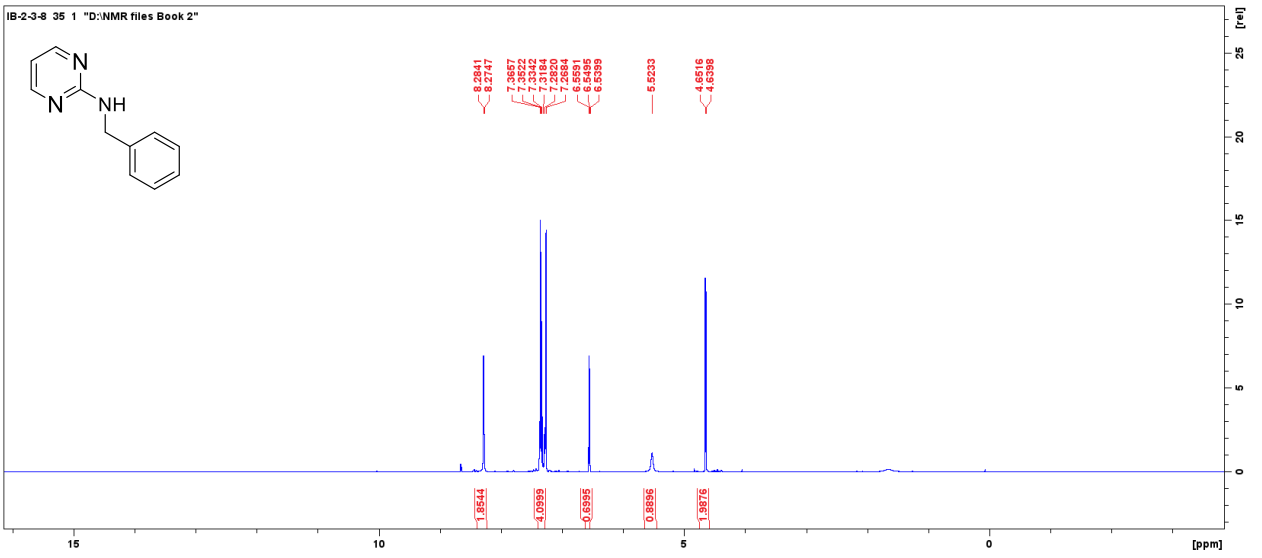

Figure 3.1.1 B: ^{1}H-NMR Spectra of N-benzylpyrimidin-2-amine [1].

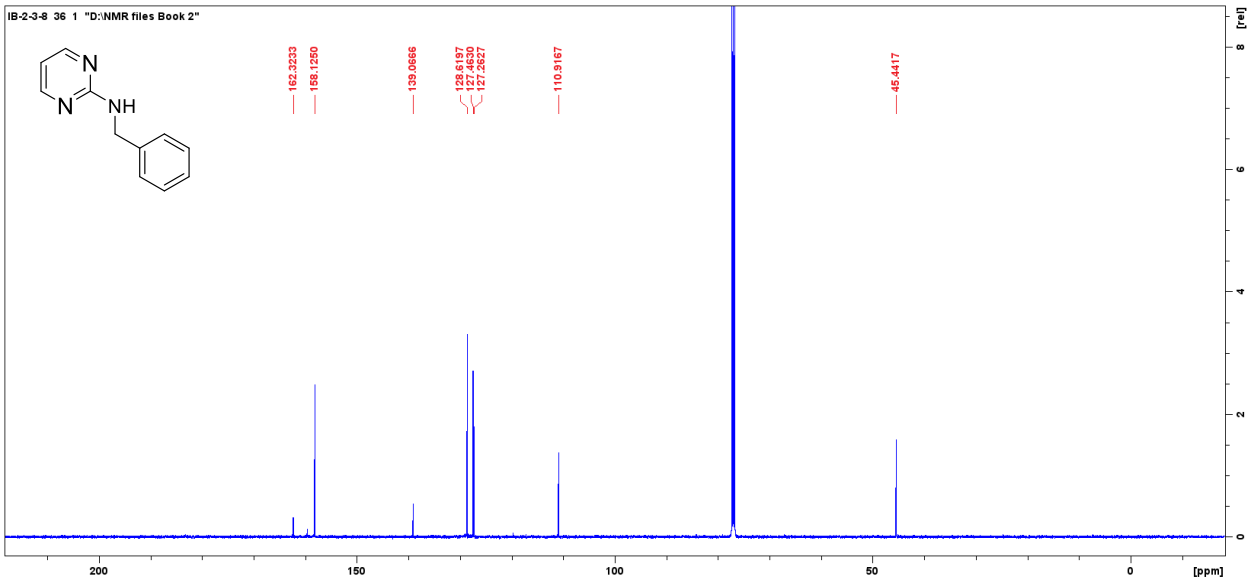

Figure 3.1.2 B: ^{13}C NMR Spectra of N-benzylpyrimidin-2-amine [1].

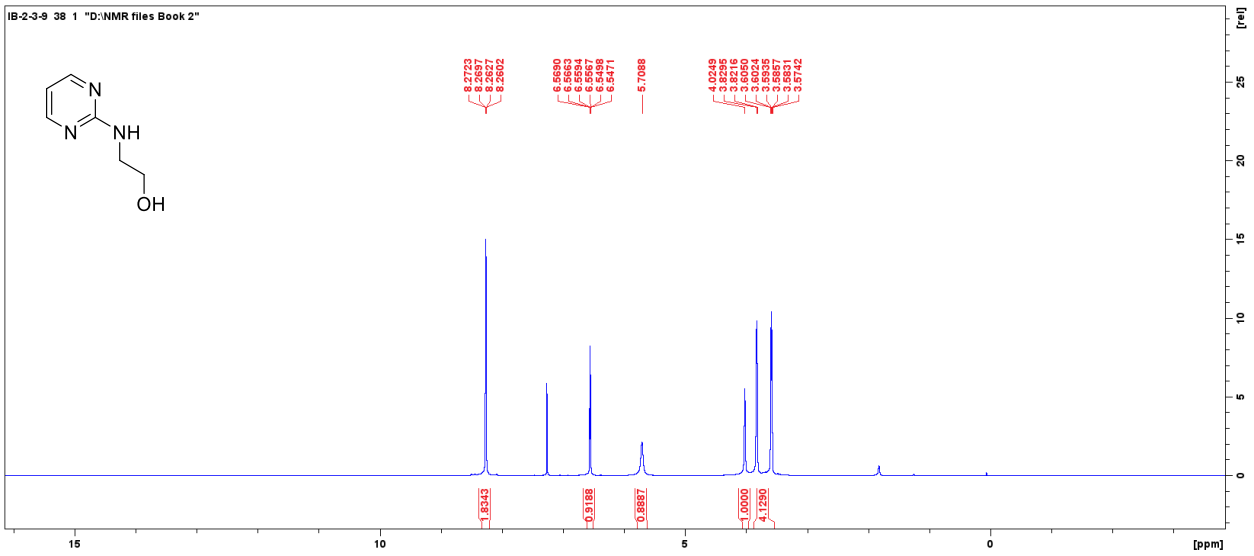

Figure 3.1.3 B: 1H-NMR Spectra of 2-(pyrimidin-2-ylamino)ethanol [2].

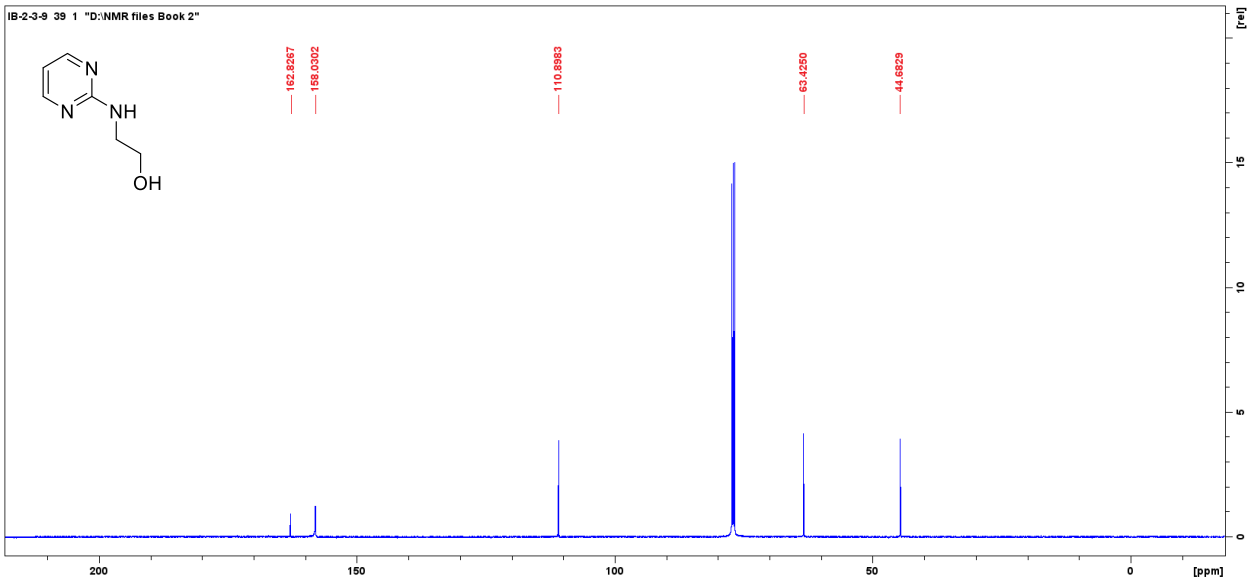

Figure 3.1.4 B: ^{13}C NMR Spectra of 2-(pyrimidin-2-ylamino)ethanol [2].

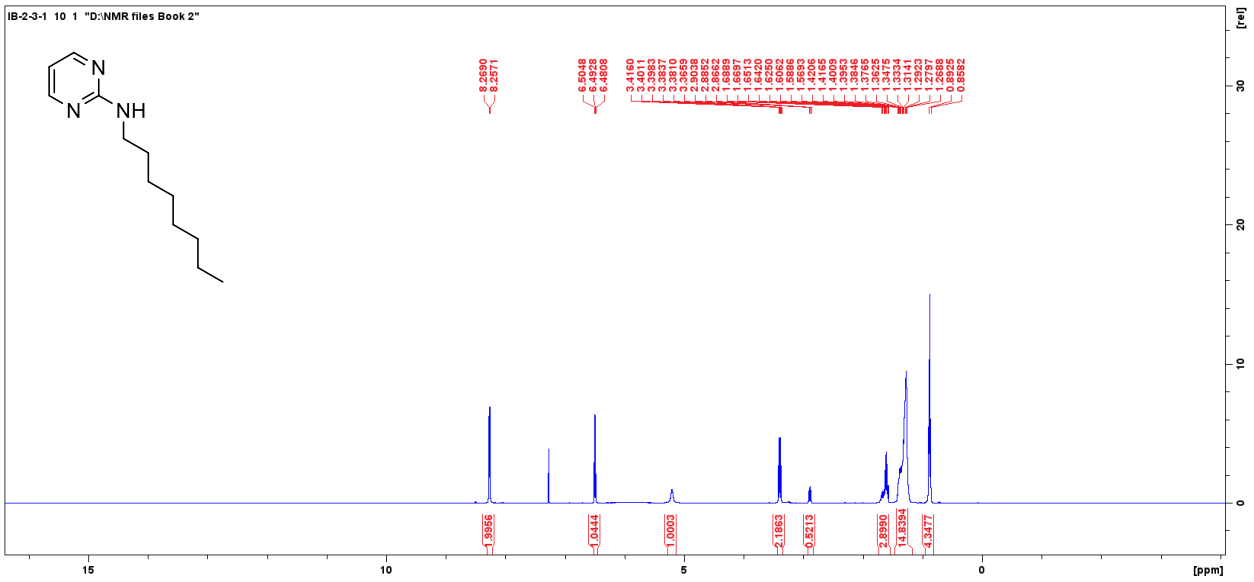

Figure 3.1.5 B: ^{1}H-NMR Spectra of N-octylpyrimidin-2-amine [6].

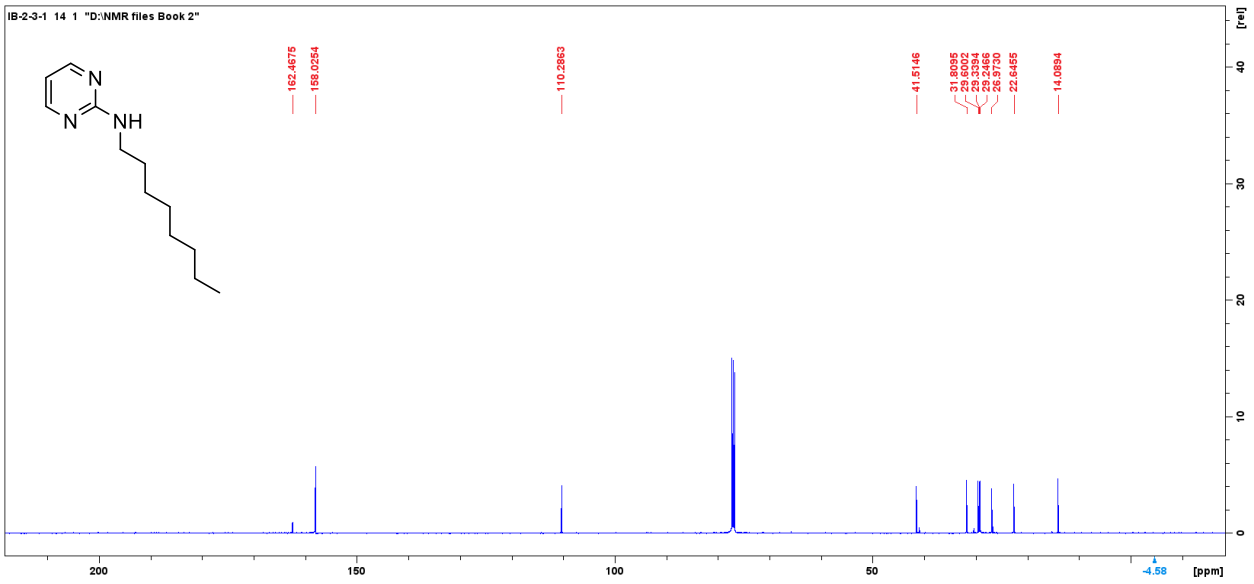

Figure 3.1.6 B: ^{13}C NMR Spectra of N-octylpyrimidin-2-amine [6].

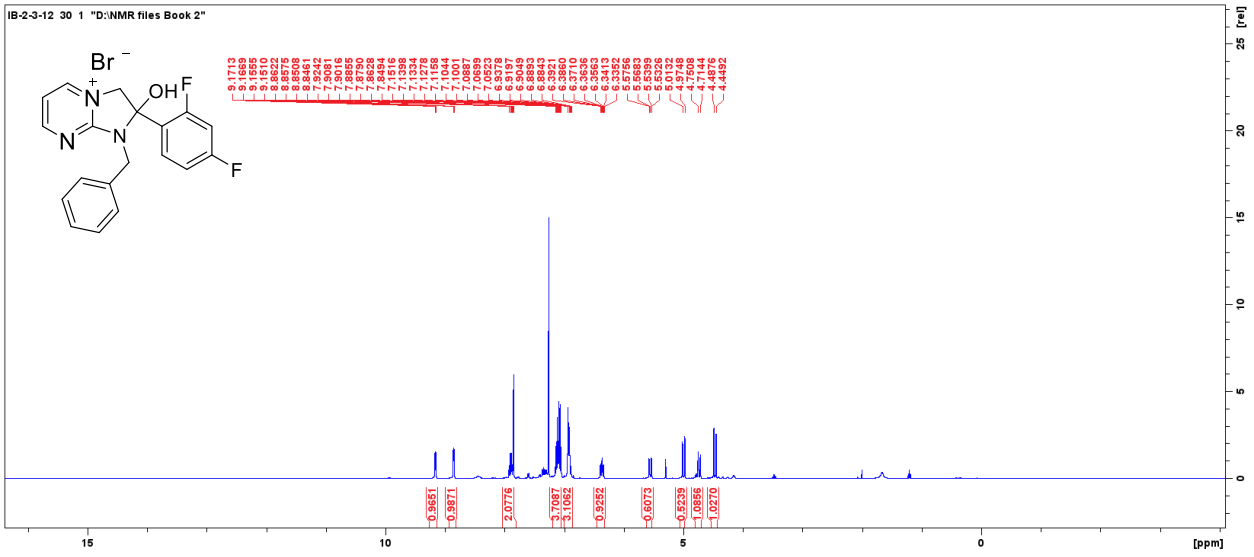

Figure 3.2.1 B: 1H-NMR Spectra of 1-benzyl-2-(2,4-difluorophenyl)-2-hydroxy-2,3-dihydro-1H-imidazo[1,2-a]pyrimidin-4-ium bromide [1a′].

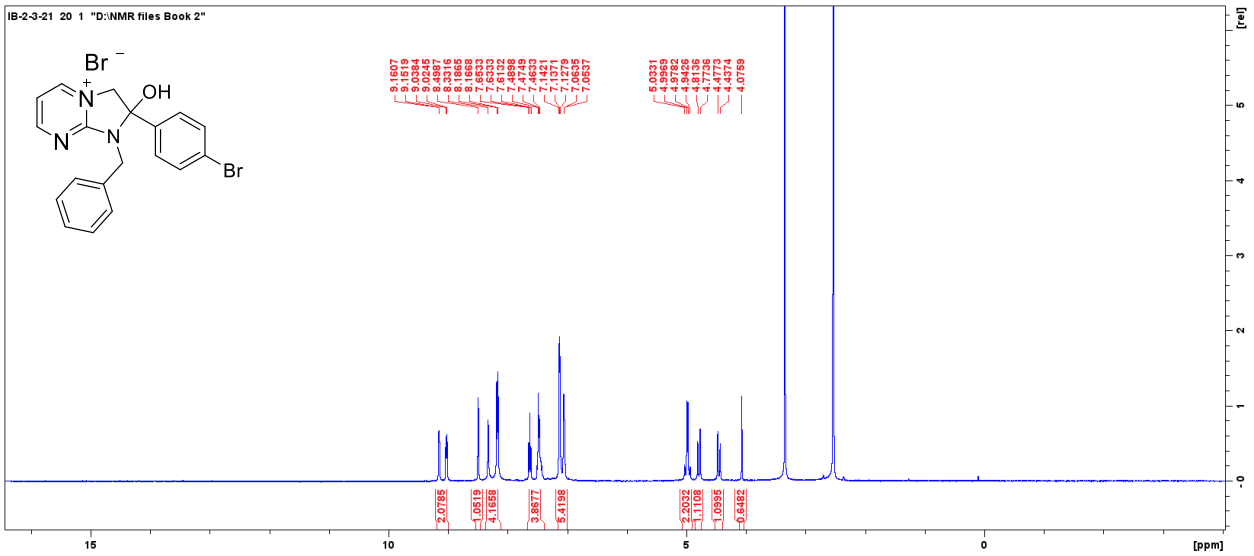

Figure 3.2.2 B: ^{1}H-NMR Spectra of 1-benzyl-2-(4-bromophenyl)-2-hydroxy-2,3-dihydro-1H-imidazo[1,2-a]pyrimidin-4-ium bromide [1c′].

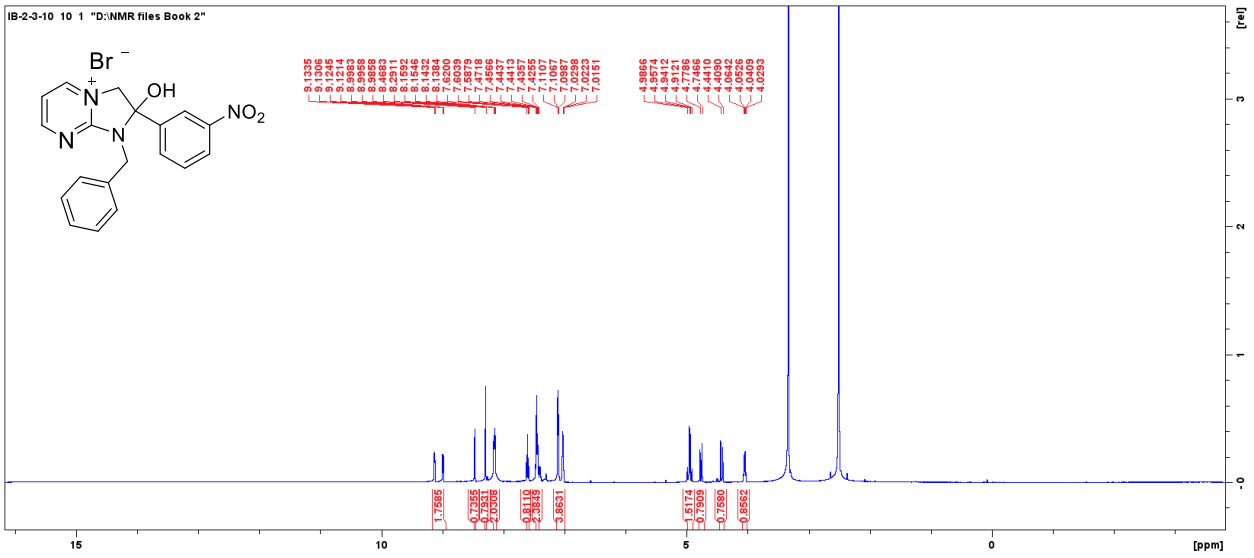

Figure 3.2.3 B: ^{1}H-NMR Spectra of 1-benzyl-2-hydroxy-2-(3-nitrophenyl)-2,3-dihydro-1H-imidazo[1,2-a]pyrimidin-4-ium bromide [1d′].

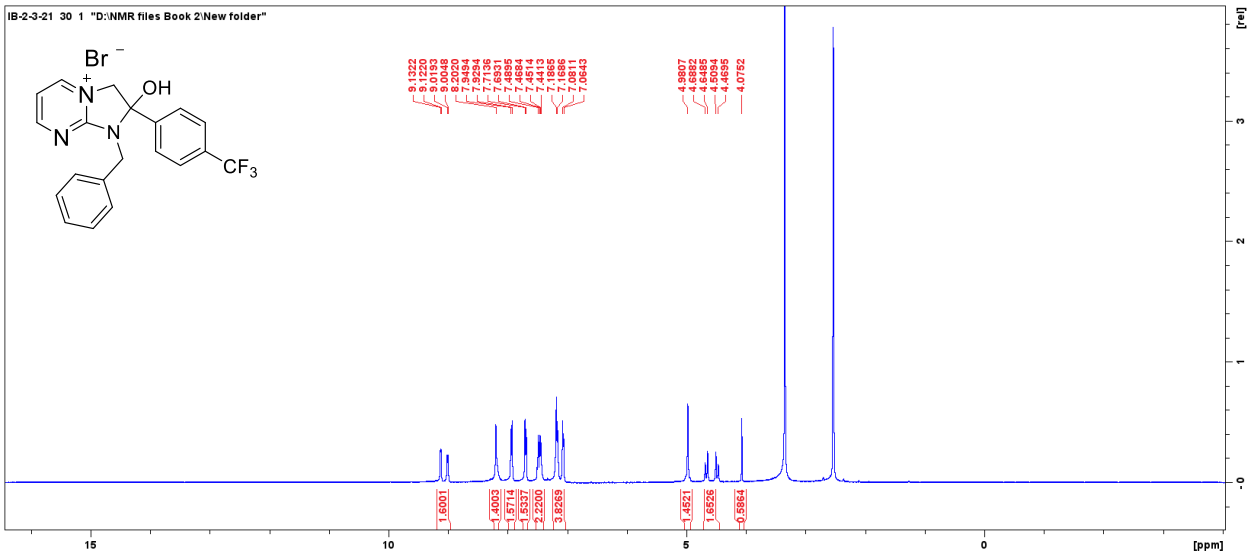

Figure 3.2.4 B: 1H-NMR Spectra of 2-hydroxy-1-(2-hydroxyethyl)-2-(4-(trifluoromethyl)phenyl)-2,3-dihydro-1H-imidazo[1,2-a]pyrimidin-4-ium bromide [1e′].

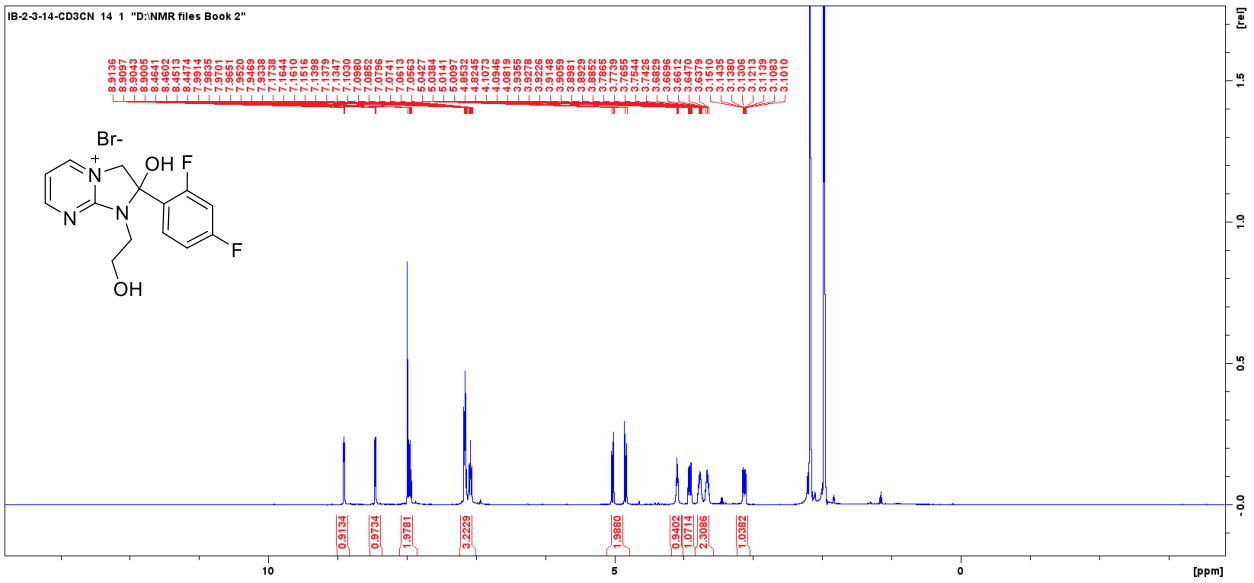

Figure 3.2.5 B: 1H-NMR Spectra of 2-(2,4-difluorophenyl)-2-hydroxy-1-(2-hydroxyethyl)-2,3-dihydro-1H-imidazo[1,2-a]pyrimidin-4-ium bromide [2a′].

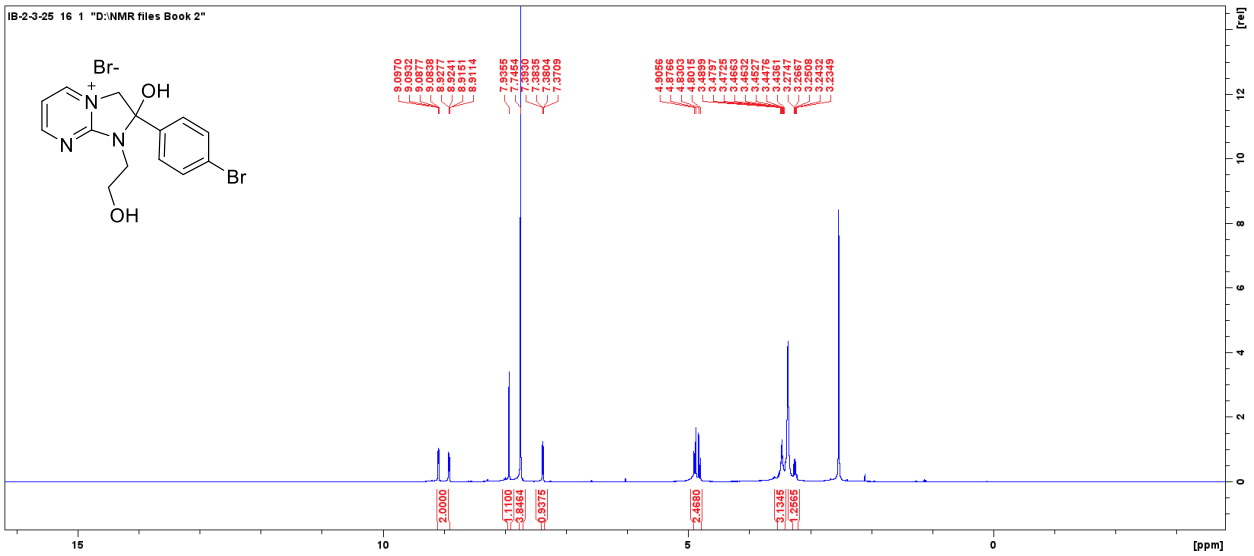

Figure 3.2.6 B: 1H-NMR Spectra of 2-(4-bromophenyl)-2-hydroxy-1-(2-hydroxyethyl)-2,3-dihydro-1H-imidazo[1,2-a]pyrimidin-4-ium bromide [2c′].

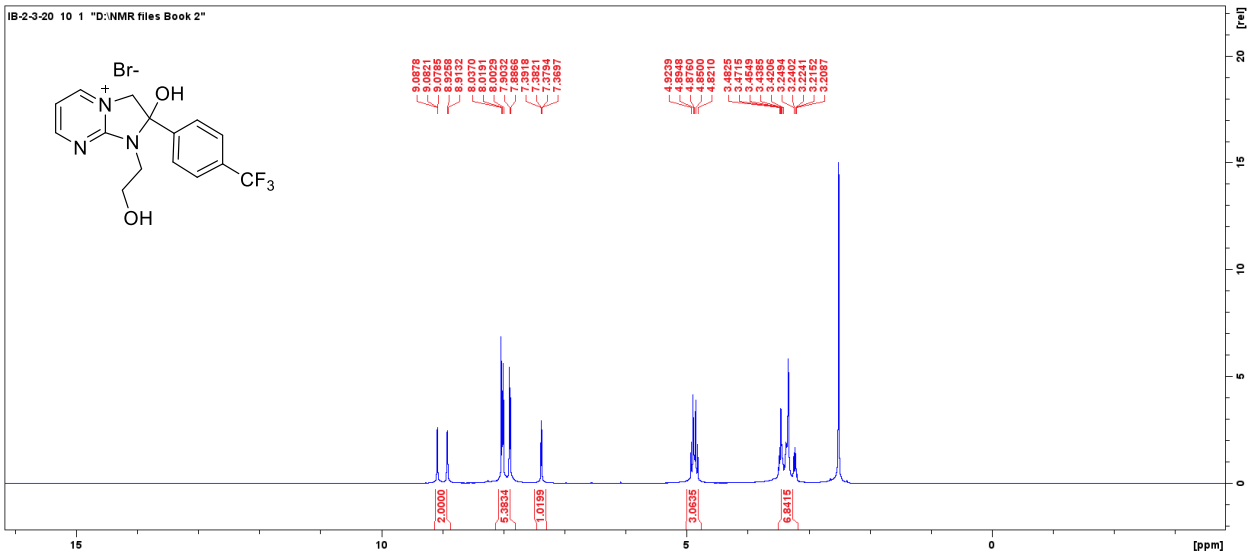

Figure 3.2.7 B: 1H-NMR Spectra of 2-hydroxy-1-(2-hydroxyethyl)-2-(4-(trifluoromethyl)phenyl)-2,3-dihydro-1H-imidazo[1,2-a]pyrimidin-4-ium bromide [2d’].

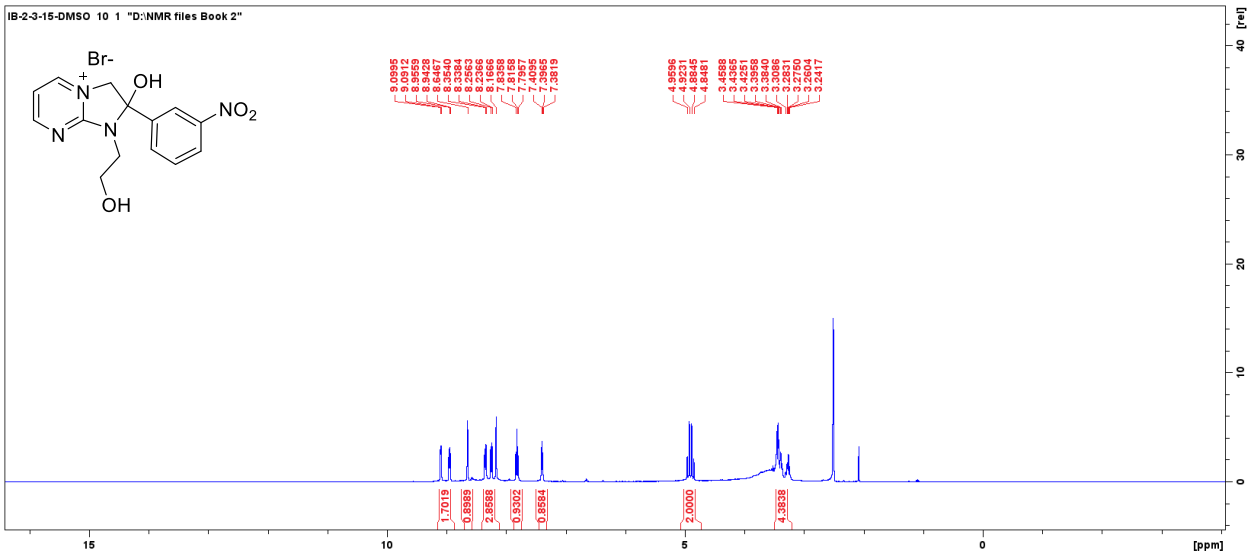

Figure 3.2.8 B: ^{1}H-NMR Spectra of 2-hydroxy-1-(2-hydroxyethyl)-2-(3-nitrophenyl)-2,3-dihydro-1H-imidazo[1,2-a]pyrimidin-4-ium bromide [2e'].

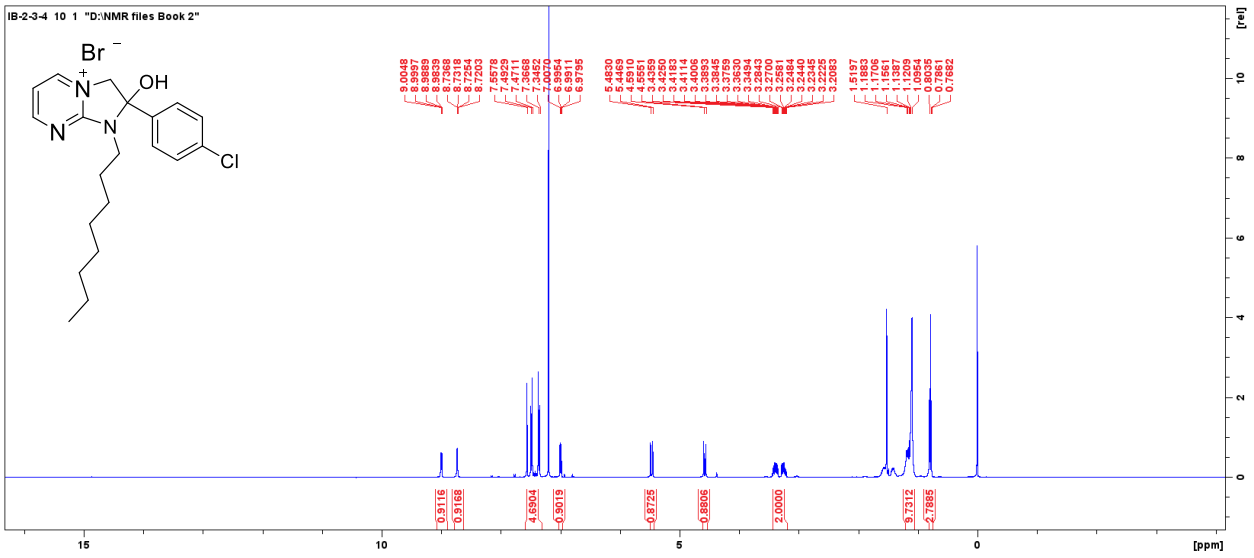

Figure 3.2.9 B: ^{1}H-NMR Spectra of 2-(4-chlorophenyl)-2-hydroxy-1-octyl-2,3-dihydro-1H-imidazo[1,2-a]pyrimidin-4-ium bromide [6a'].

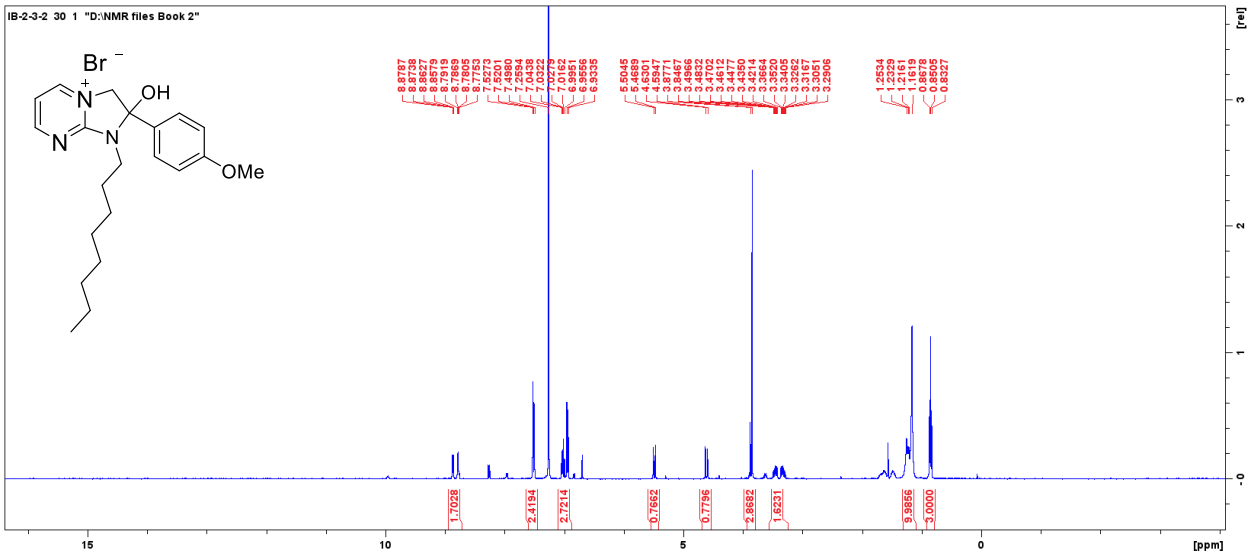

Figure 3.2.10 B: [1]H-NMR Spectra of 2-hydroxy-2-(4-methoxyphenyl)-1-octyl-2,3-dihydro-1H-imidazo[1,2-a]pyrimidin-4-ium bromide [6b']

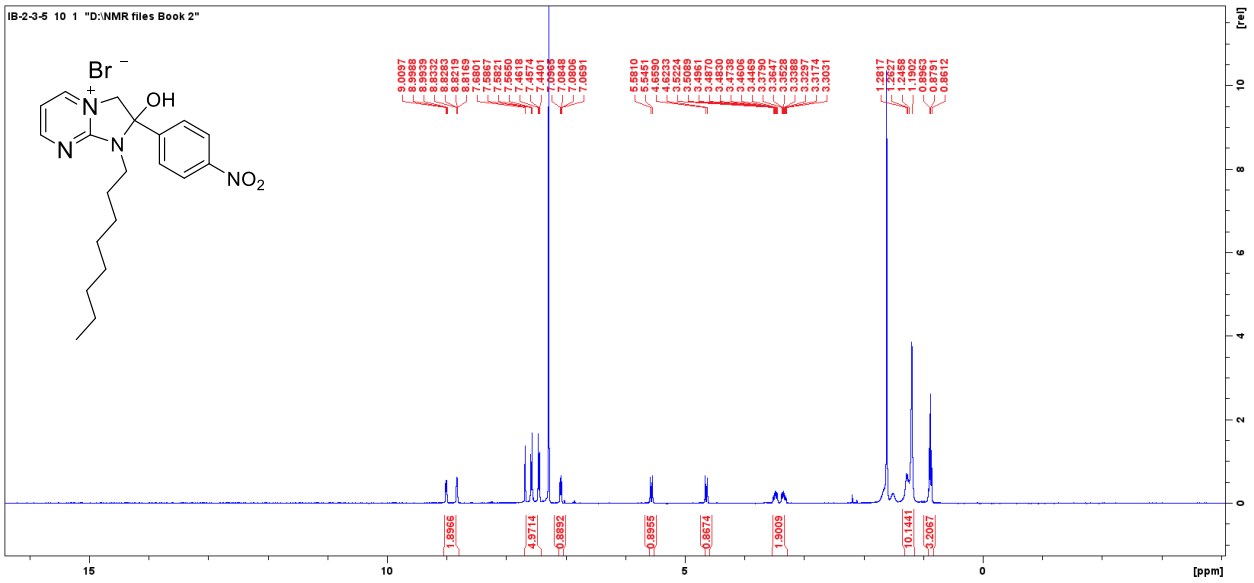

Figure 3.2.11 B: [1]H-NMR Spectra of 2-hydroxy-2-(4-nitrophenyl)-1-octyl-2,3-dihydro-1H-imidazo[1,2-a]pyrimidin-4-ium bromide [6c'].

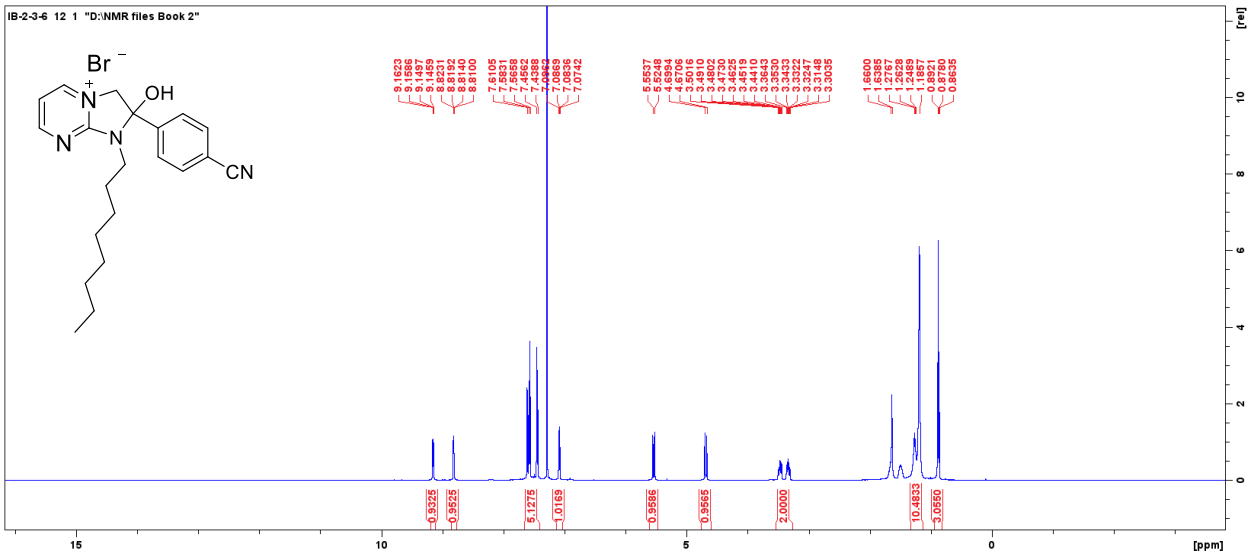

Figure 3.2.12 B: ^{1}H-NMR Spectra of 2-(4-cyanophenyl)-2-hydroxy-1-octyl-2,3-dihydro-1H-imidazo[1,2-a]pyrimidin-4-ium bromide [6d'].

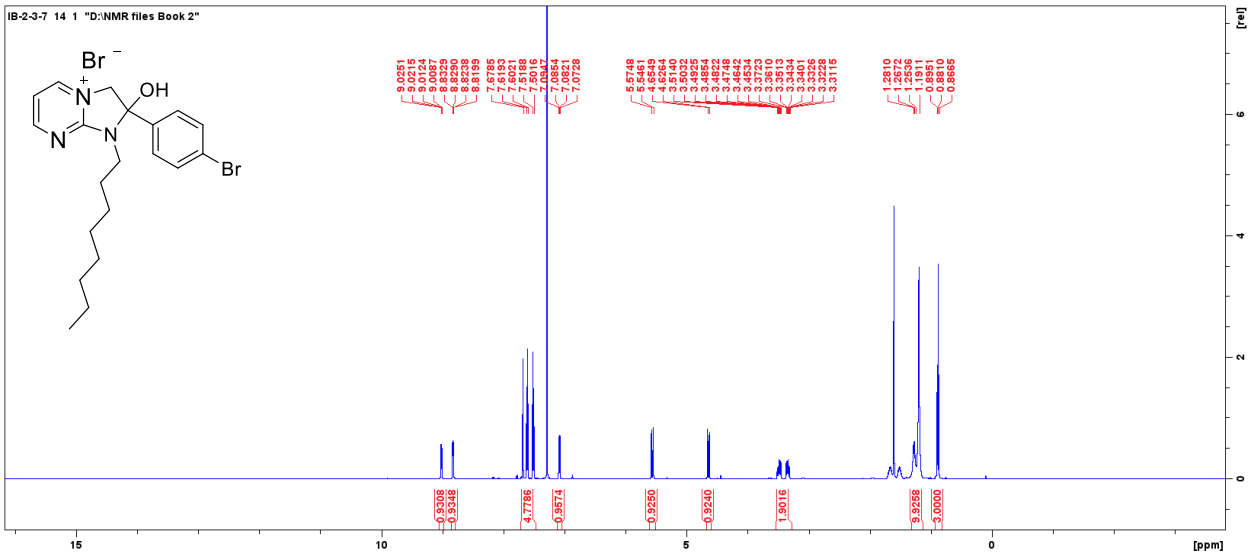

Figure 3.2.13 B: ^{1}H-NMR Spectra of 2-(4-bromophenyl)-2-hydroxy-1-octyl-2,3-dihydro-1H-imidazo[1,2-a]pyrimidin-4-ium bromide [6e'].

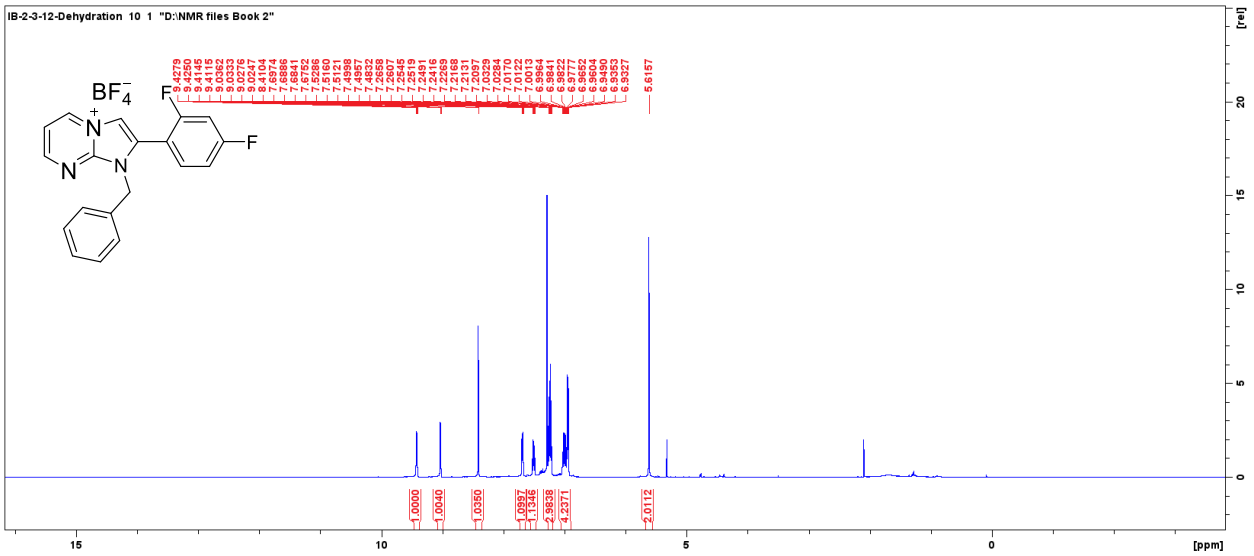

Figure 3.3.1 B: ^{1}H-NMR Spectra of 1-benzyl-2-(2,4-difluorophenyl)-1H-imidazo[1,2-a]pyrimidin-4-ium tetrafluoroborate [1a].

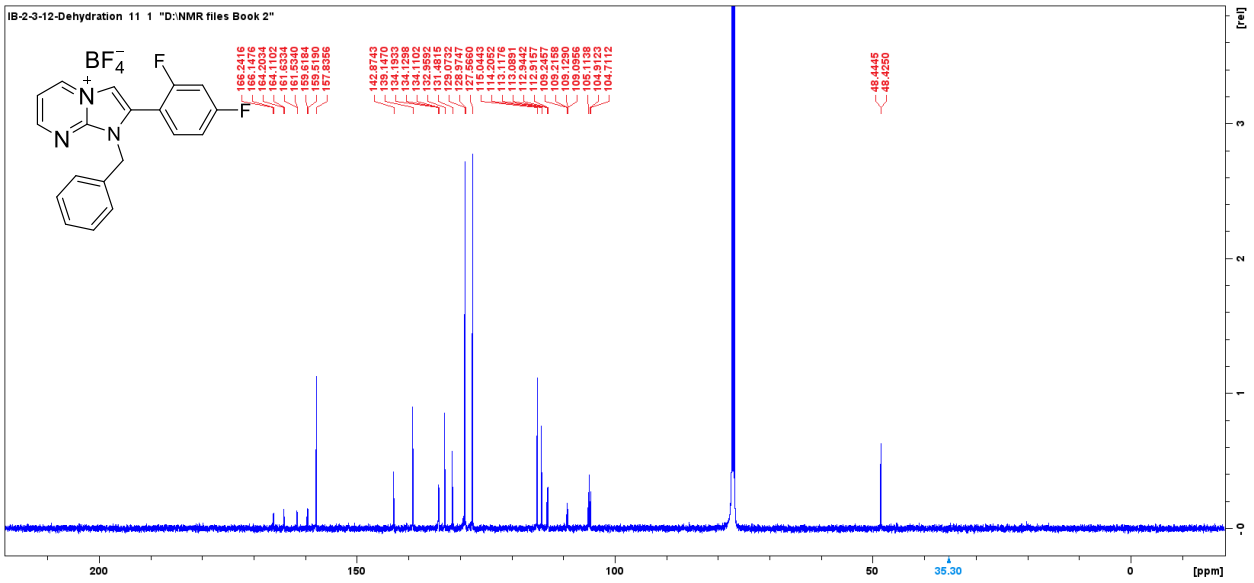

Figure 3.3.2 B: ^{13}C NMR Spectra of 1-benzyl-2-(2,4-difluorophenyl)-1H-imidazo[1,2-a]pyrimidin-4-ium tetrafluoroborate [1a].

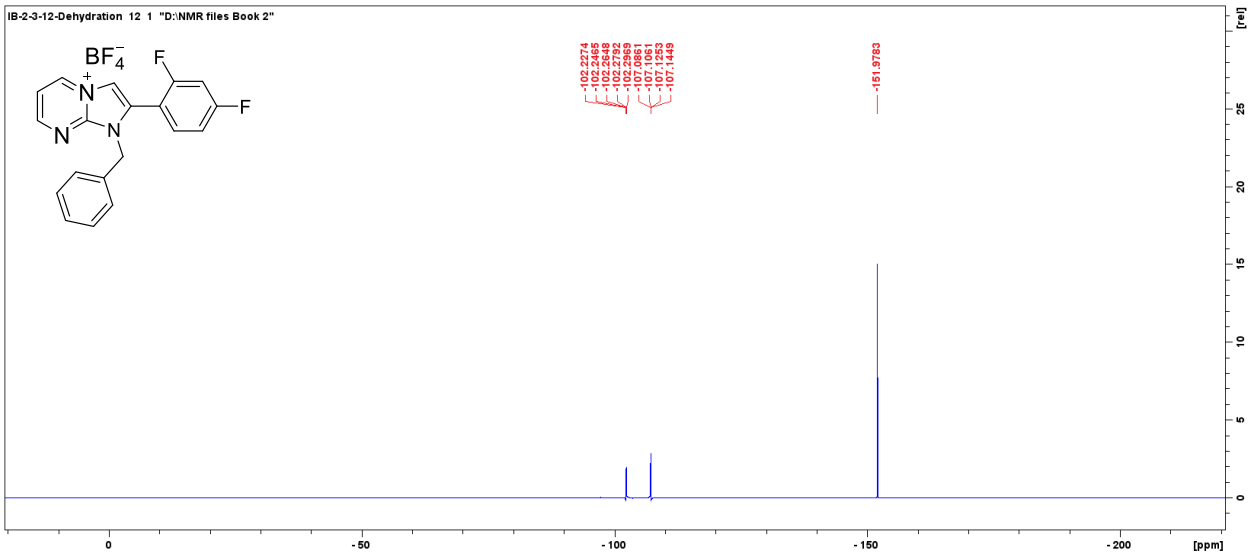

Figure 3.3.3 B: ^{19}F NMR Spectra of 1-benzyl-2-(2,4-difluorophenyl)-1H-imidazo[1,2-a]pyrimidin-4-ium tetrafluoroborate [1a].

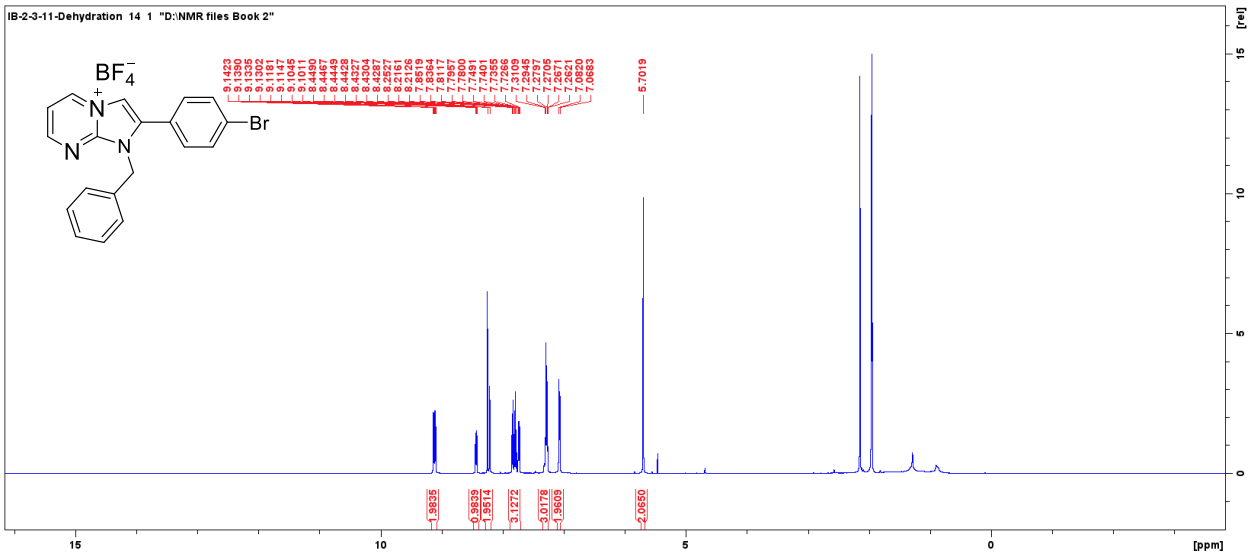

Figure 3.3.4 B: ^{1}H-NMR Spectra of 1-benzyl-2-(4-bromophenyl)-1H-imidazo[1,2-a]pyrimidin-4-ium tetrafluoroborate [1c].

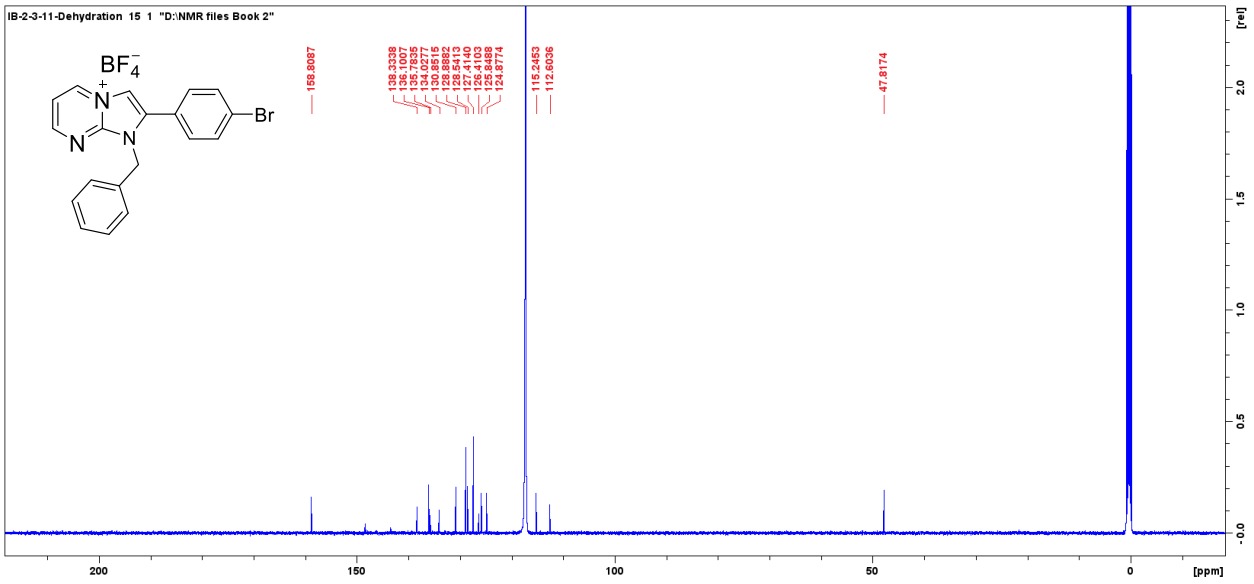

Figure 3.3.5 B: ^{13}C NMR Spectra of 1-benzyl-2-(4-bromophenyl)-1H-imidazo[1,2-a]pyrimidin-4-ium tetrafluoroborate [1c].

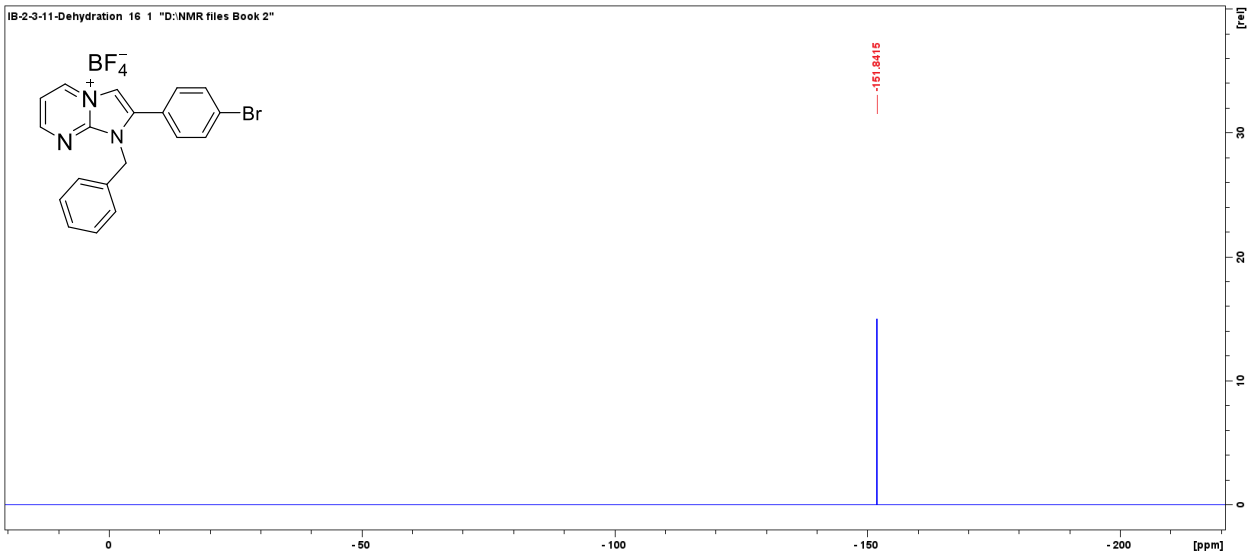

Figure 3.3.6 B: ^{19}F NMR Spectra of 1-benzyl-2-(4-bromophenyl)-1H-imidazo[1,2-a]pyrimidin-4-ium tetrafluoroborate [1c].

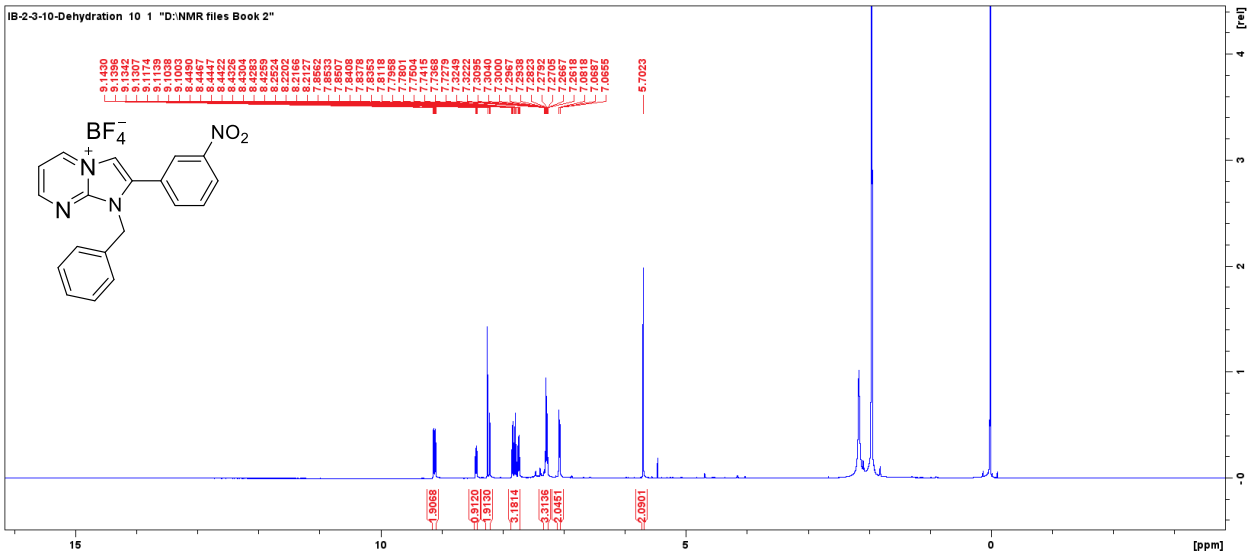

Figure 3.3.7 B: ^{1}H-NMR Spectra of 1-benzyl-2-(3-nitrophenyl)-1H-imidazo[1,2-a]pyrimidin-4-ium tetrafluoroborate [1d].

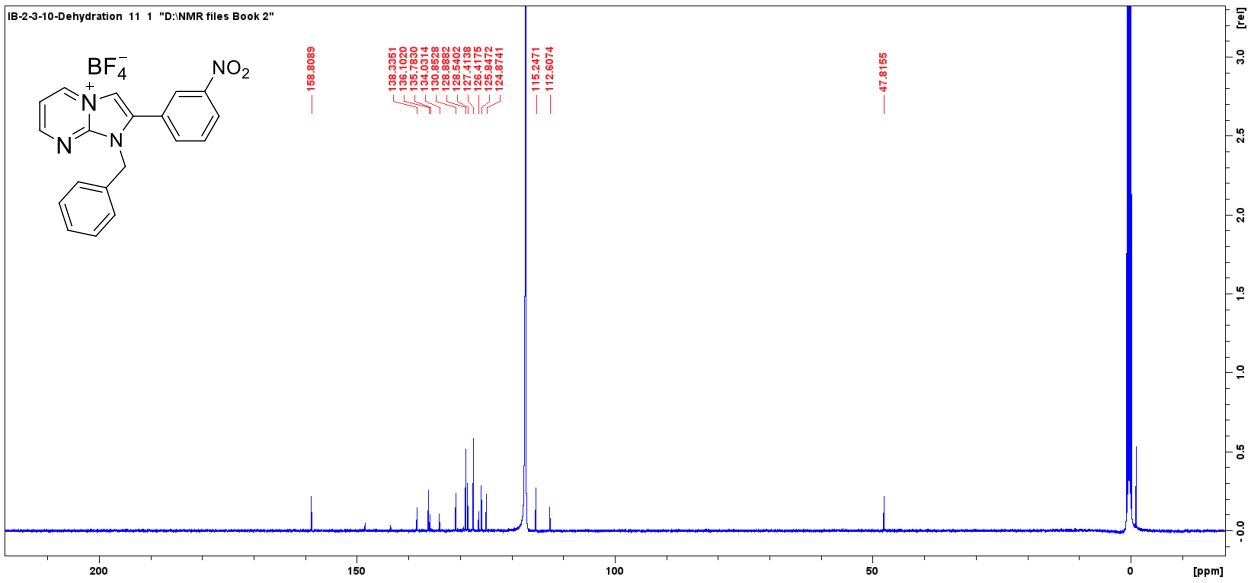

Figure 3.3.8 B: ^{13}C NMR Spectra of 1-benzyl-2-(3-nitrophenyl)-1H-imidazo[1,2-a]pyrimidin-4-ium tetrafluoroborate [1d].

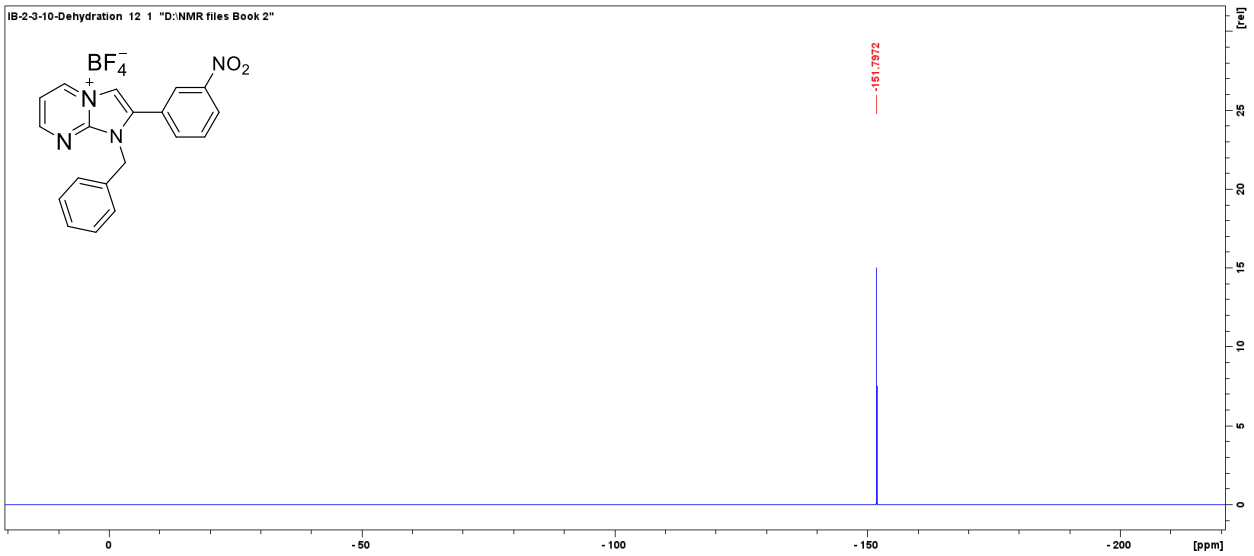

Figure 3.3.9 B: ^{19}F NMR Spectra of 1-benzyl-2-(3-nitrophenyl)-1H-imidazo[1,2-a]pyrimidin-4-ium tetrafluoroborate [1d].

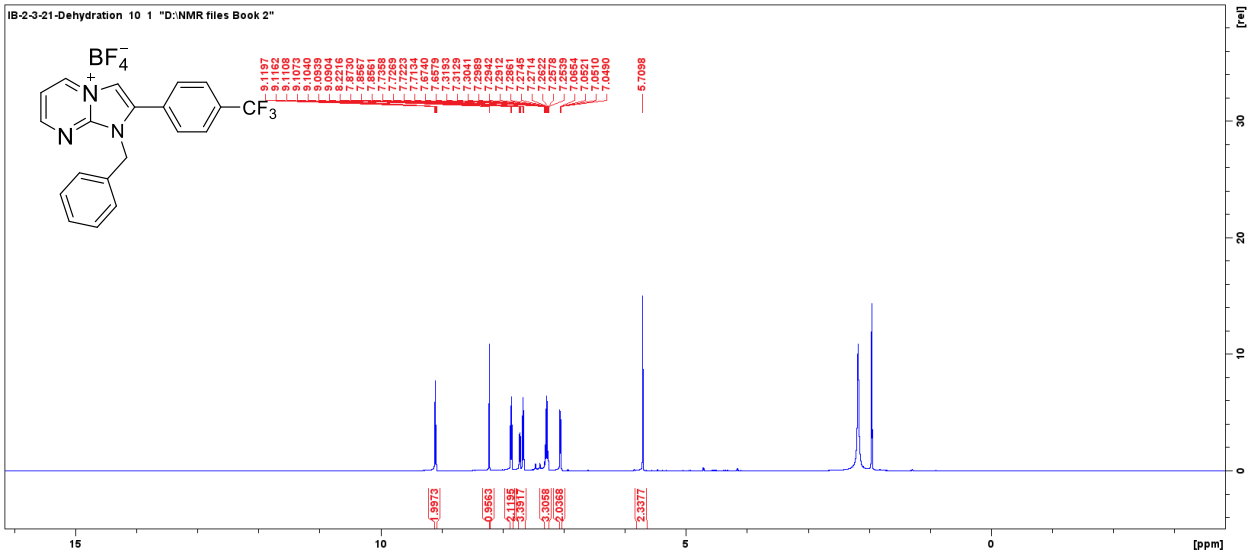

Figure 3.3.10 B: ^{1}H-NMR Spectra of 1-benzyl-2-(4-(trifluoromethyl)phenyl)-1H-imidazo[1,2-a]pyrimidin-4-ium tetrafluoroborate [1e].

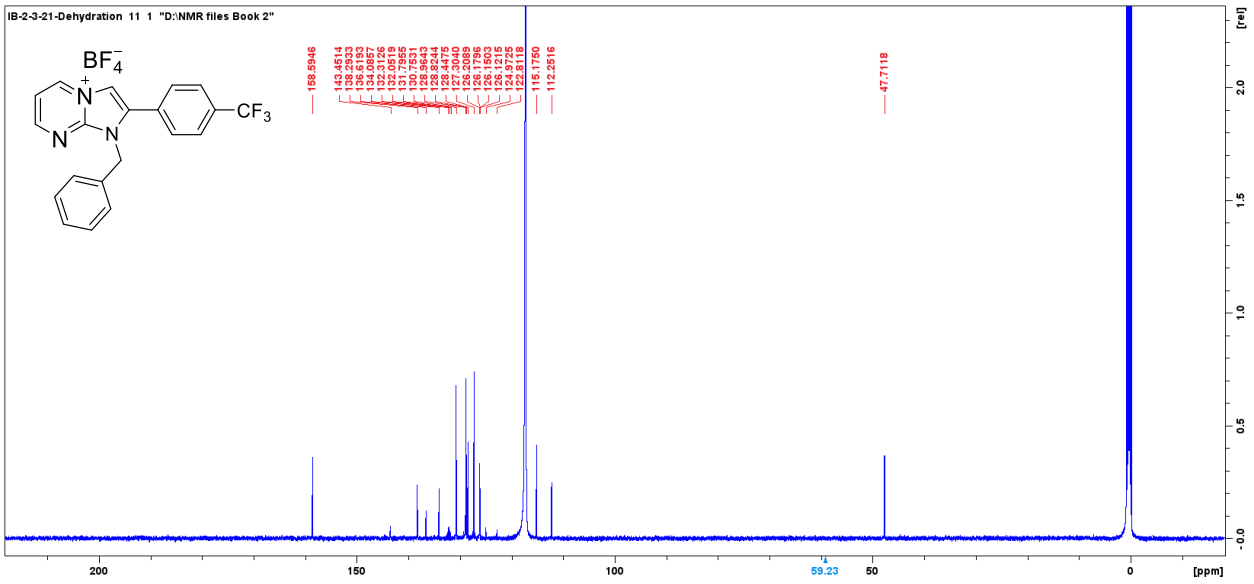

Figure 3.3.11 B: ^{13}C NMR Spectra of 1-benzyl-2-(4-(trifluoromethyl)phenyl)-1H-imidazo[1,2-a]pyrimidin-4-ium tetrafluoroborate [1e].

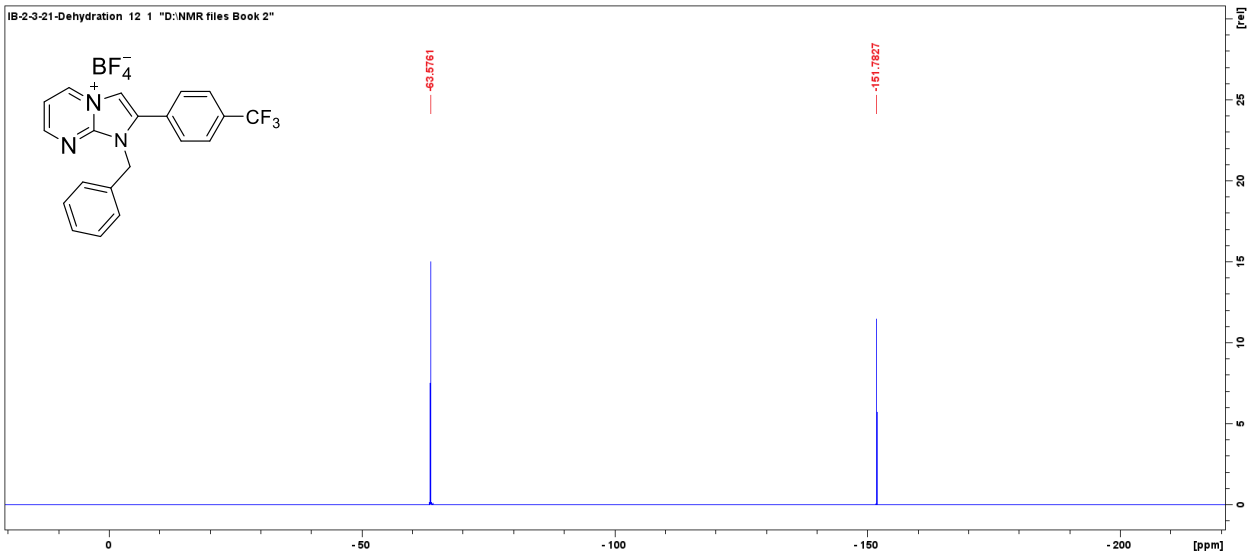

Figure 3.3.12 B: ^{19}F NMR Spectra of 1-benzyl-2-(4-(trifluoromethyl)phenyl)-1H-imidazo[1,2-a]pyrimidin-4-ium tetrafluoroborate [1e].

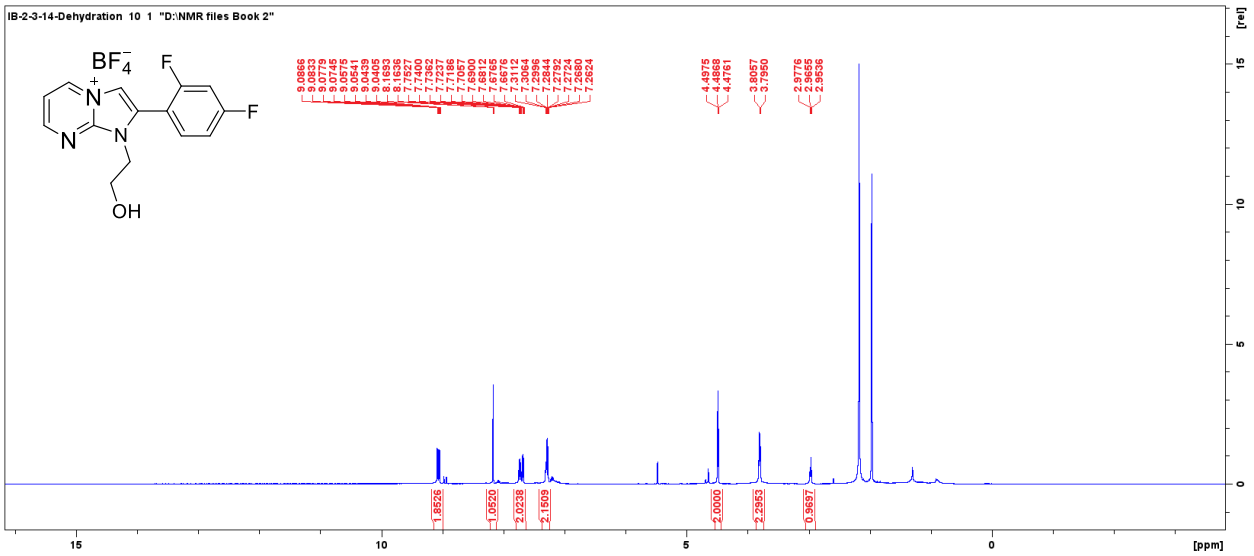

Figure 3.3.13 B: ^{1}H-NMR Spectra of 2-(2,4-difluorophenyl)-1-(2-hydroxyethyl)-1H-imidazo[1,2-a]pyrimidin-4-ium tetrafluoroborate [2a].

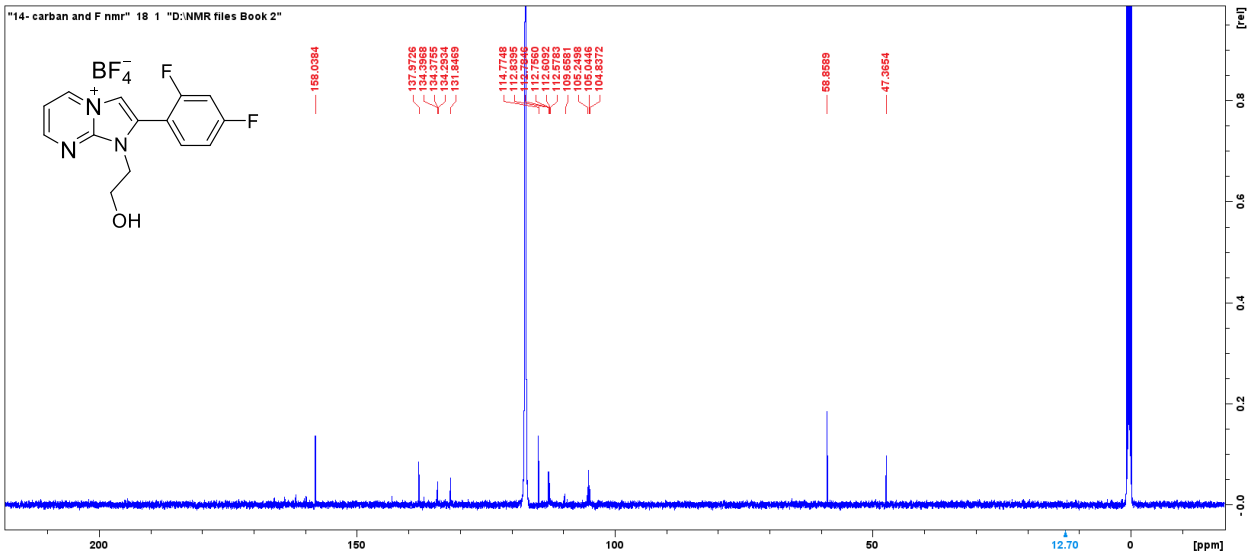

Figure 3.3.14 B: ^{13}C NMR Spectra of 2-(2,4-difluorophenyl)-1-(2-hydroxyethyl)-1H-imidazo[1,2-a]pyrimidin-4-ium tetrafluoroborate [2a].

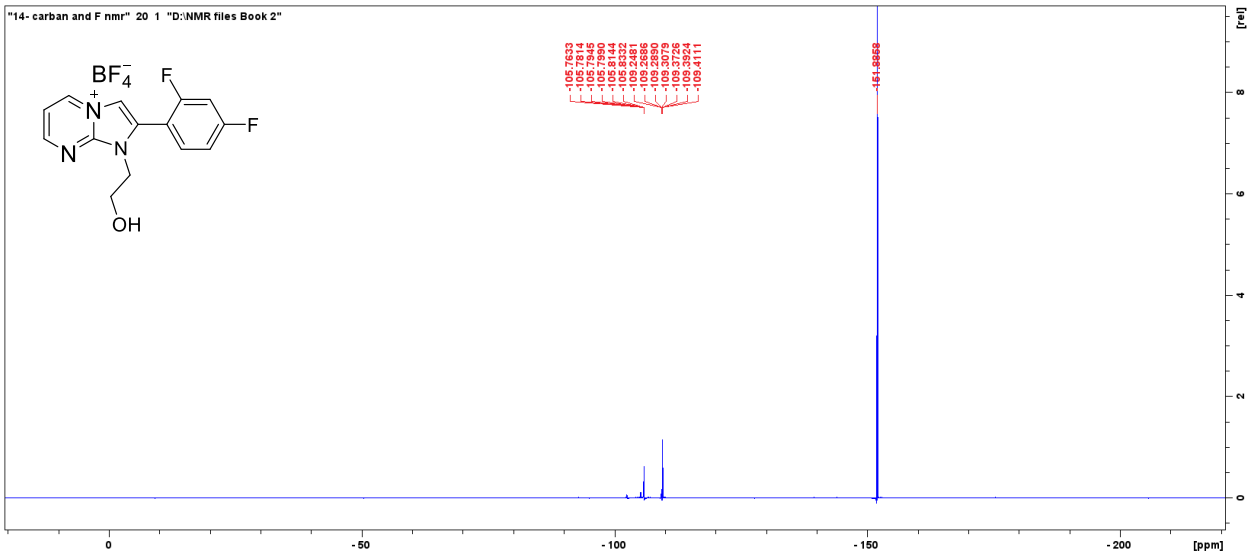

Figure 3.3.15 B: ^{19}F NMR Spectra of 2-(2,4-difluorophenyl)-1-(2-hydroxyethyl)-1H-imidazo[1,2-a]pyrimidin-4-ium tetrafluoroborate [2a].

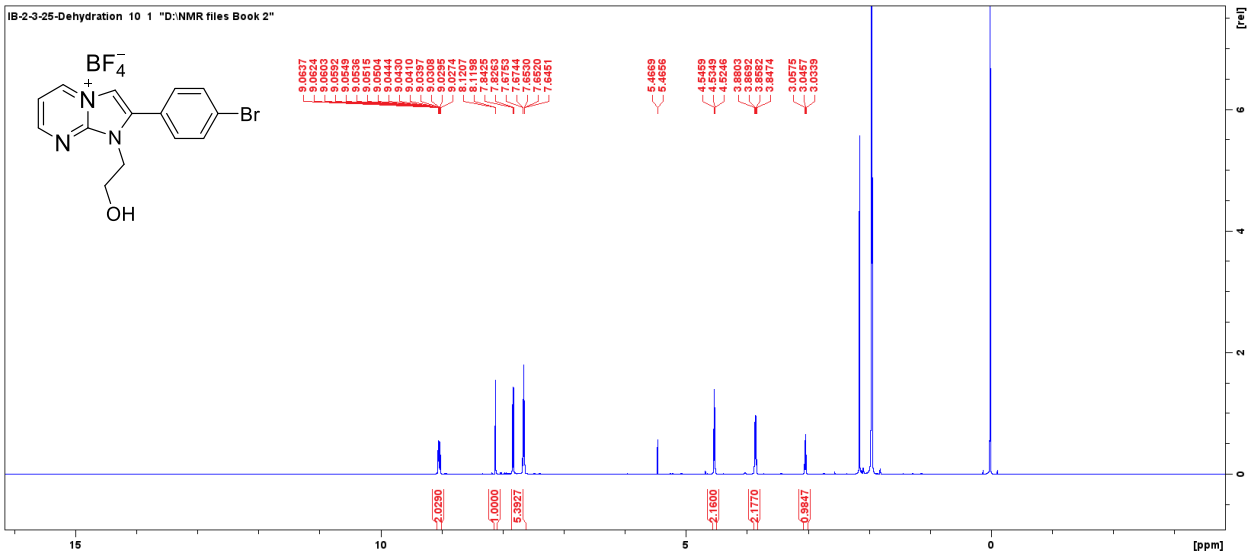

Figure 3.3.16 B: ^{1}H-NMR Spectra of 2-(4-bromophenyl)-1-(2-hydroxyethyl)-1H-imidazo[1,2-a]pyrimidin-4-ium tetrafluoroborate [2c].

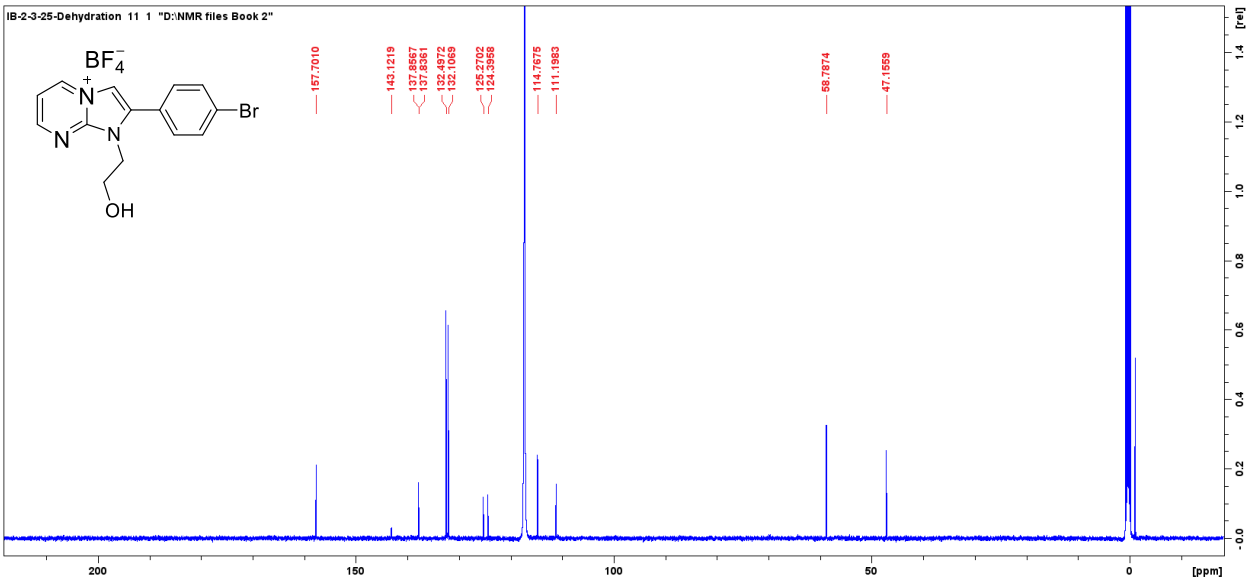

Figure 3.3.17 B: ^{13}C NMR Spectra of 2-(4-bromophenyl)-1-(2-hydroxyethyl)-1H-imidazo[1,2-a]pyrimidin-4-ium tetrafluoroborate [2c].

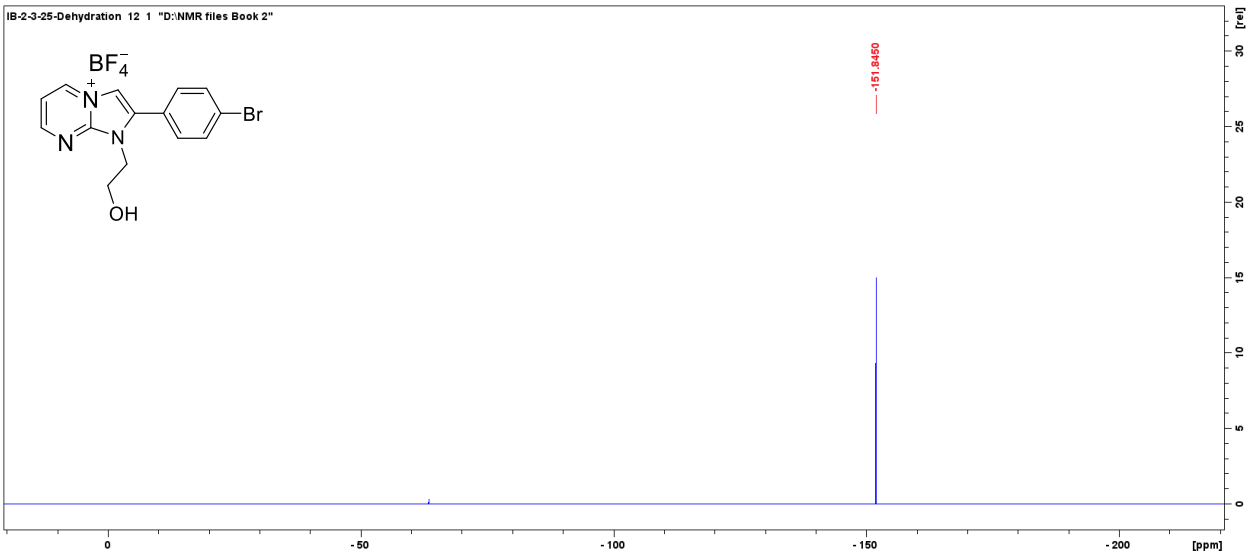

Figure 3.3.18 B: ^{19}F NMR Spectra of 2-(4-bromophenyl)-1-(2-hydroxyethyl)-1H-imidazo[1,2-a]pyrimidin-4-ium tetrafluoroborate [2c].

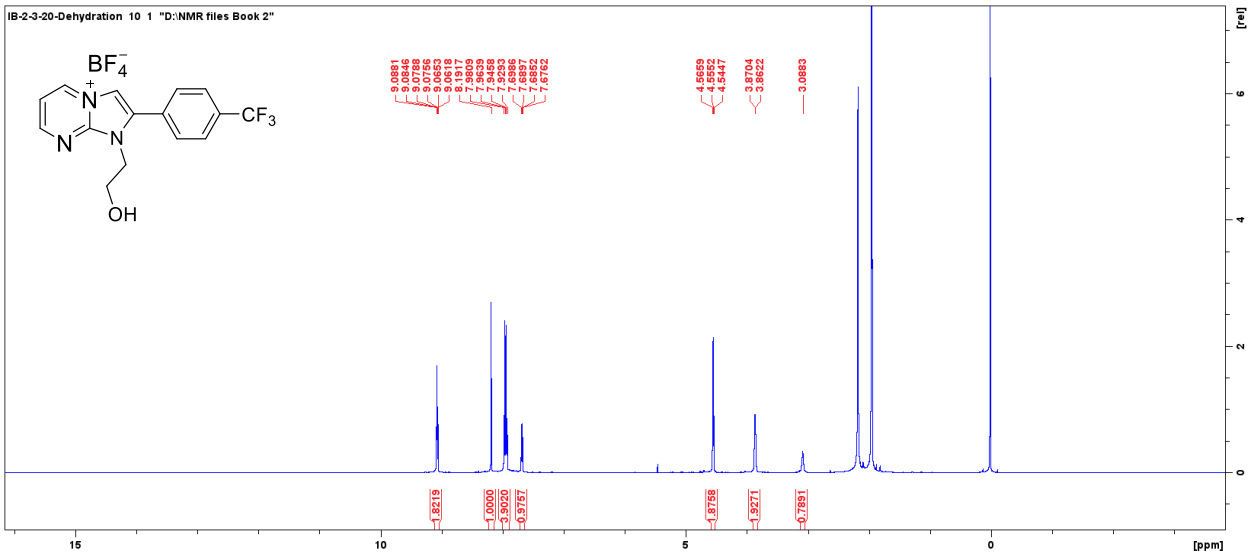

Figure 3.3.19 B: ^{1}H-NMR Spectra of 1-(2-hydroxyethyl)-2-(4-(trifluoromethyl)phenyl)-1H-imidazo[1,2-a]pyrimidin-4-ium tetrafluoroborate [2d].

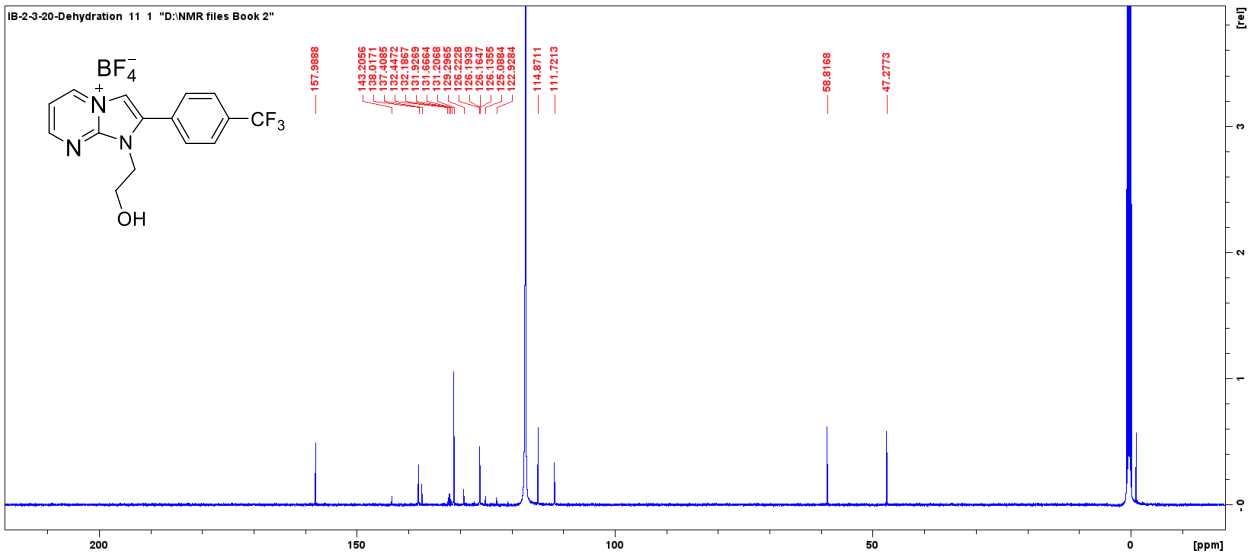

Figure 3.3.20 B: ^{13}C NMR Spectra of 1-(2-hydroxyethyl)-2-(4-(trifluoromethyl)phenyl)-1H-imidazo[1,2-a]pyrimidin-4-ium tetrafluoroborate [2d].

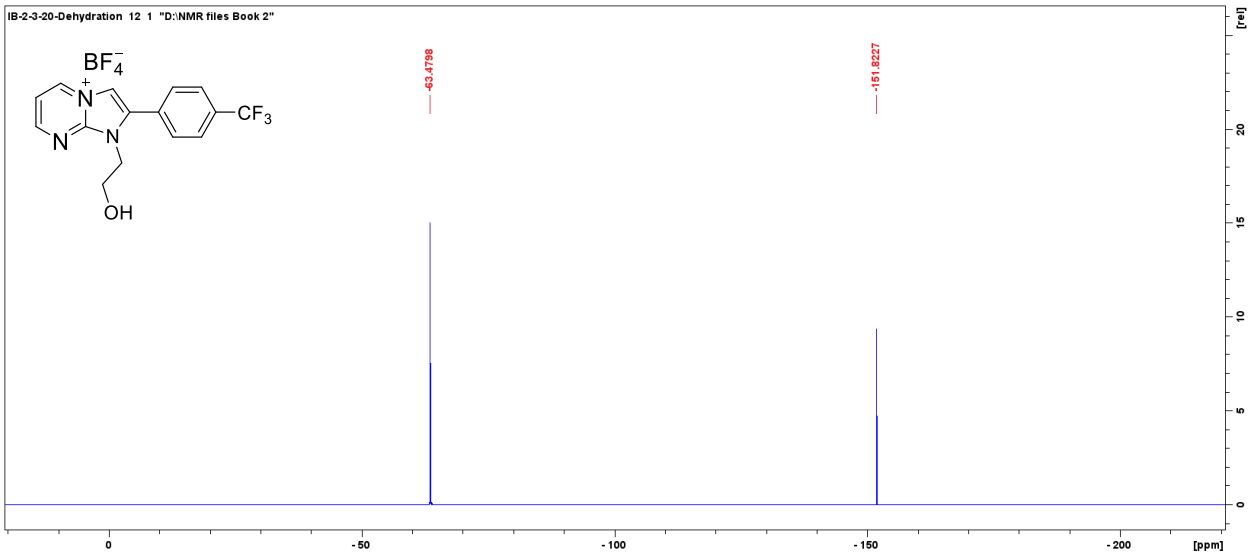

Figure 3.3.21 B: ^{19}F NMR Spectra of 1-(2-hydroxyethyl)-2-(4-(trifluoromethyl)phenyl)-1H-imidazo[1,2-a]pyrimidin-4-ium tetrafluoroborate [2d].

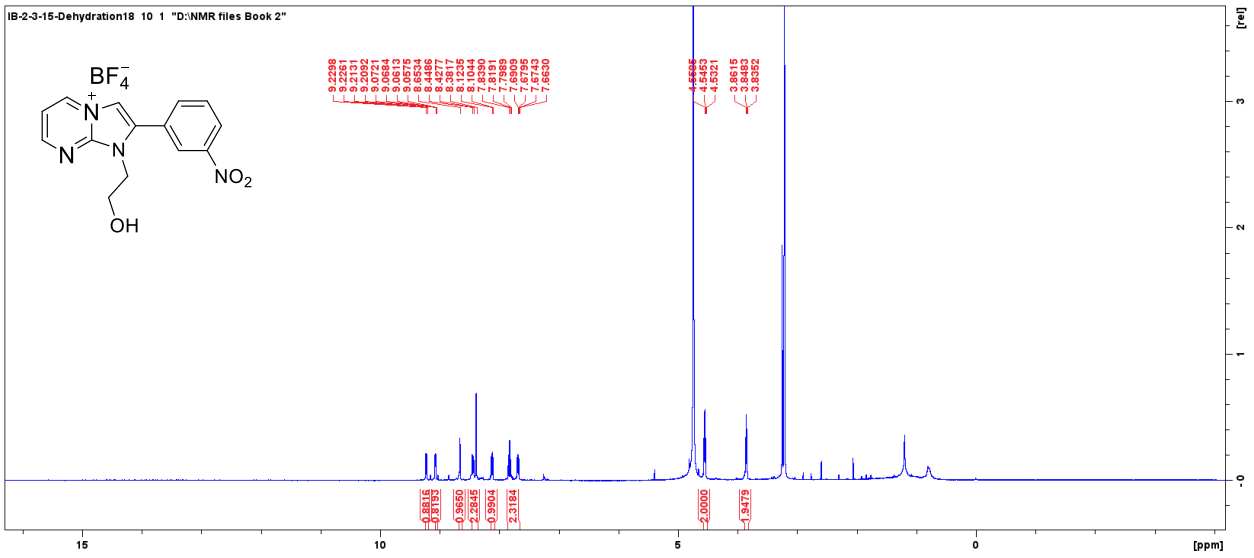

Figure 3.3.22 B: 1H-NMR Spectra of 1-(2-hydroxyethyl)-2-(3-nitrophenyl)-1H-imidazo[1,2-a]pyrimidin-4-ium tetrafluoroborate [2e].

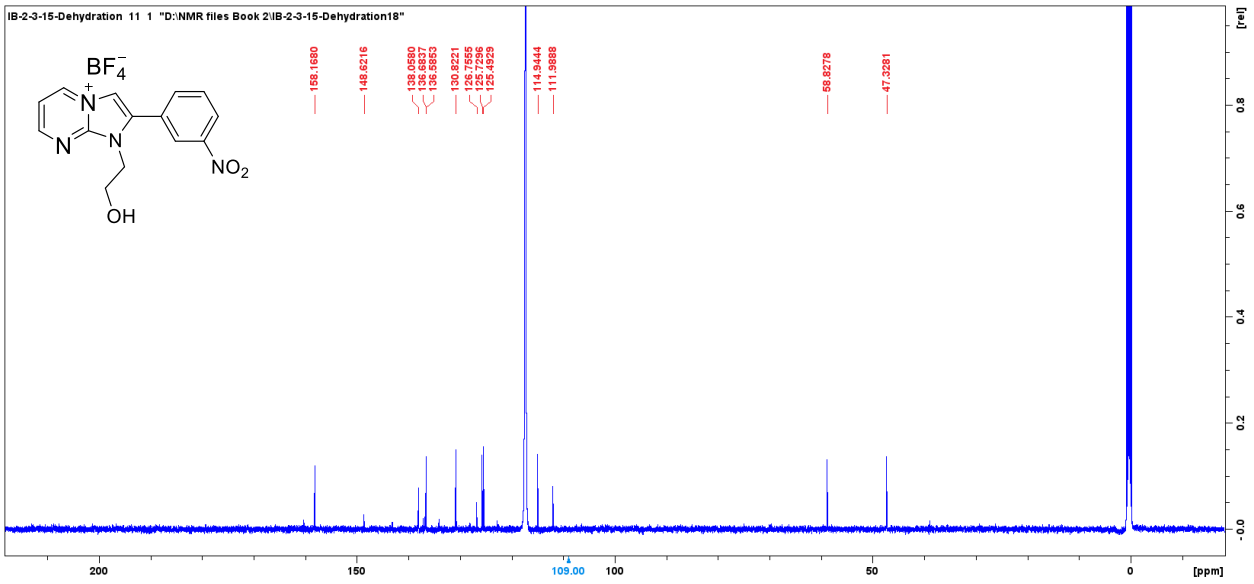

Figure 3.3.23 B: ^{13}C NMR Spectra of 1-(2-hydroxyethyl)-2-(3-nitrophenyl)-1H-imidazo[1,2-a]pyrimidin-4-ium tetrafluoroborate [2e].

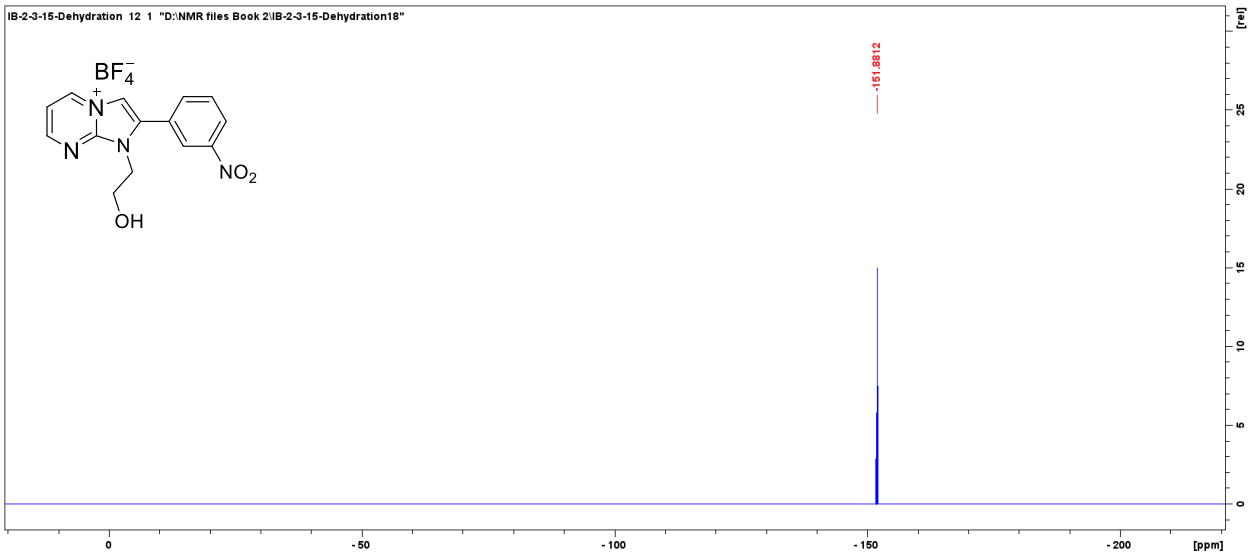

Figure 3.3.24 B: 19F NMR Spectra of 1-(2-hydroxyethyl)-2-(3-nitrophenyl)-1H-imidazo[1,2-a]pyrimidin-4-ium tetrafluoroborate [2e].

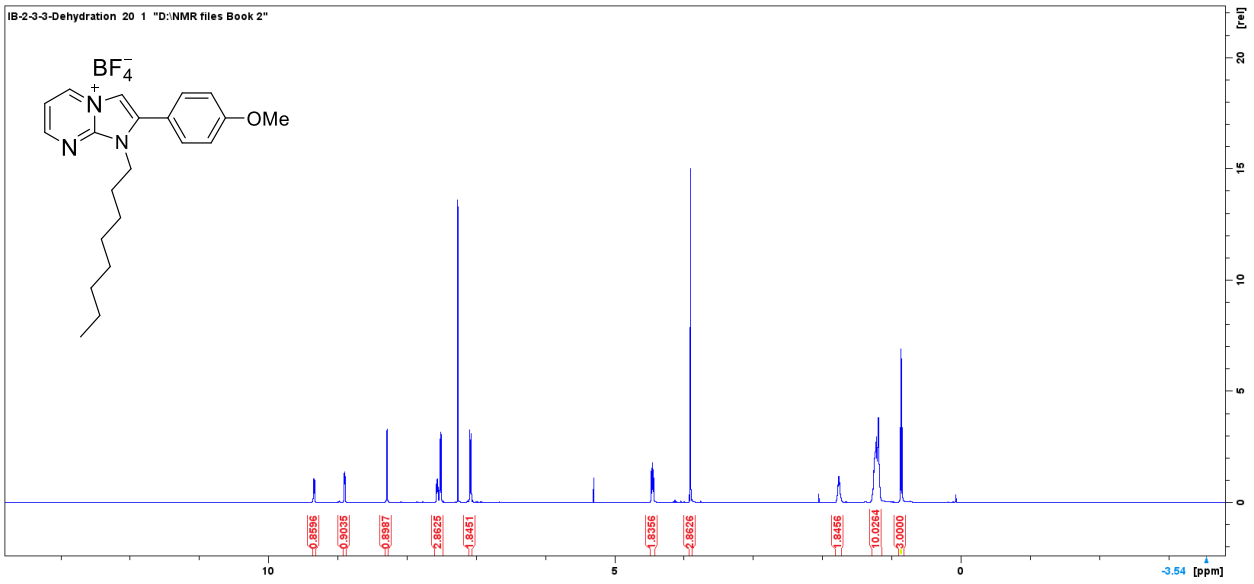

Figure 3.3.25 B: ^{1}H-NMR Spectra of 2-(4-methoxyphenyl)-1-octyl-1H-imidazo[1,2-a]pyrimidin-4-ium tetrafluoroborate [6a].

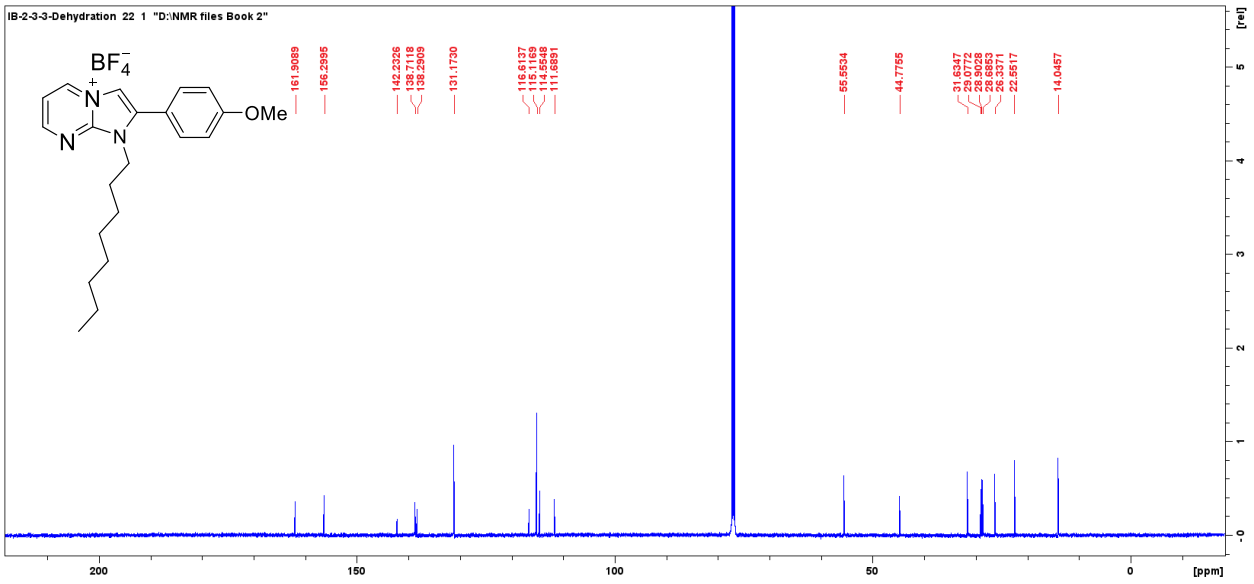

Figure 3.3.26 B: ^{13}C NMR Spectra of 2-(4-methoxyphenyl)-1-octyl-1H-imidazo[1,2-a]pyrimidin-4-ium tetrafluoroborate [6a].

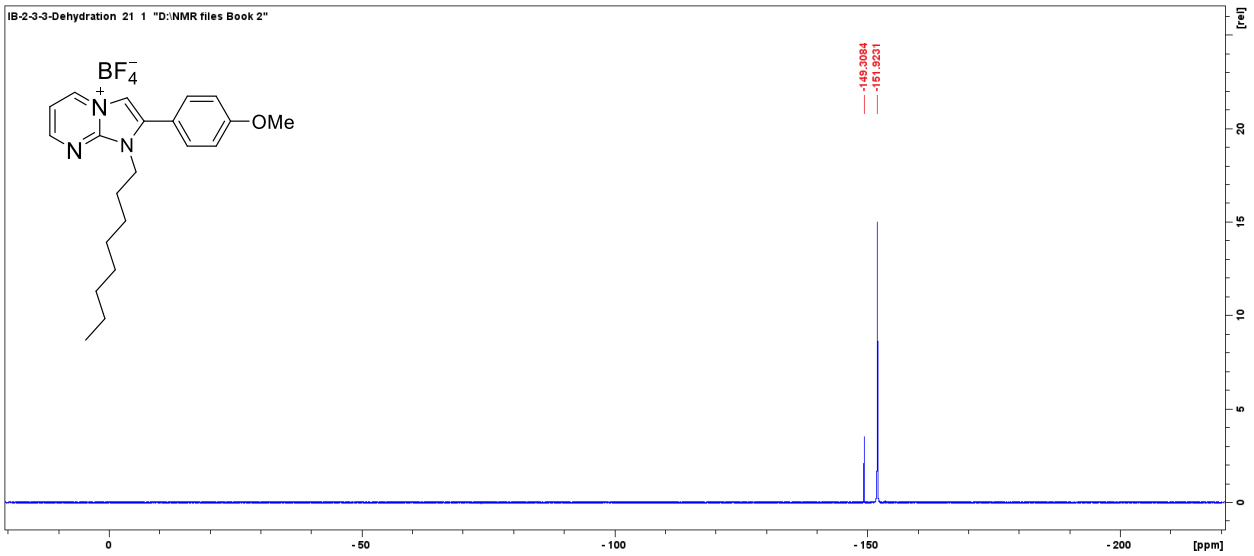

Figure 3.3.27 B: ^{19}F NMR Spectra of 2-(4-methoxyphenyl)-1-octyl-1H-imidazo[1,2-a]pyrimidin-4-ium tetrafluoroborate [6a].

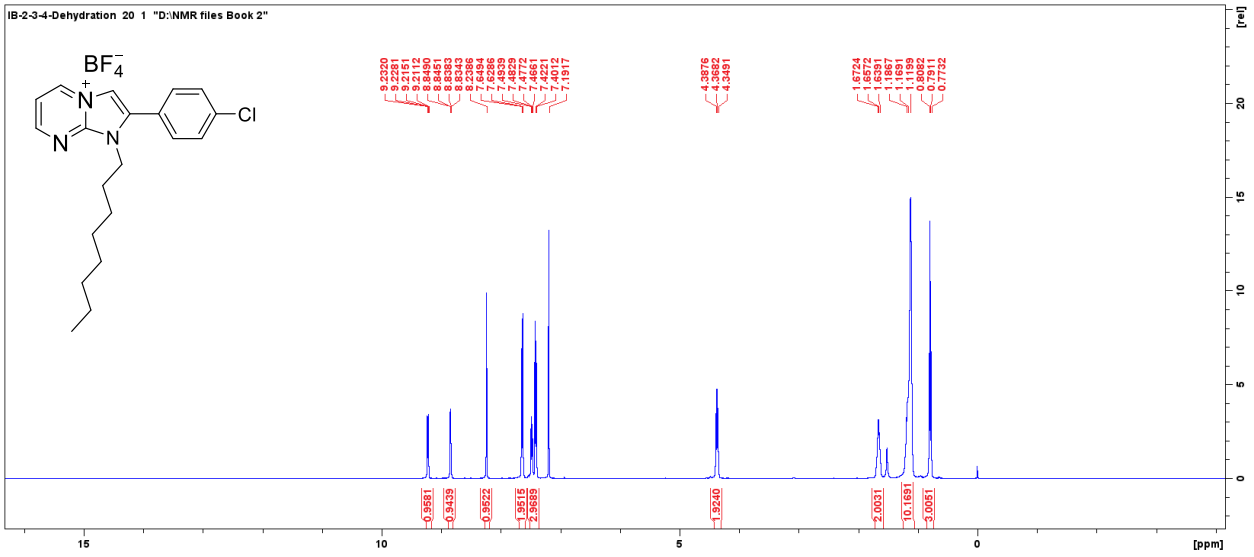

Figure 3.3.28 B: ^{1}H-NMR Spectra of 2-(4-chlorophenyl)-1-octyl-1H-imidazo[1,2-a]pyrimidin-4-ium tetrafluoroborate [6b].

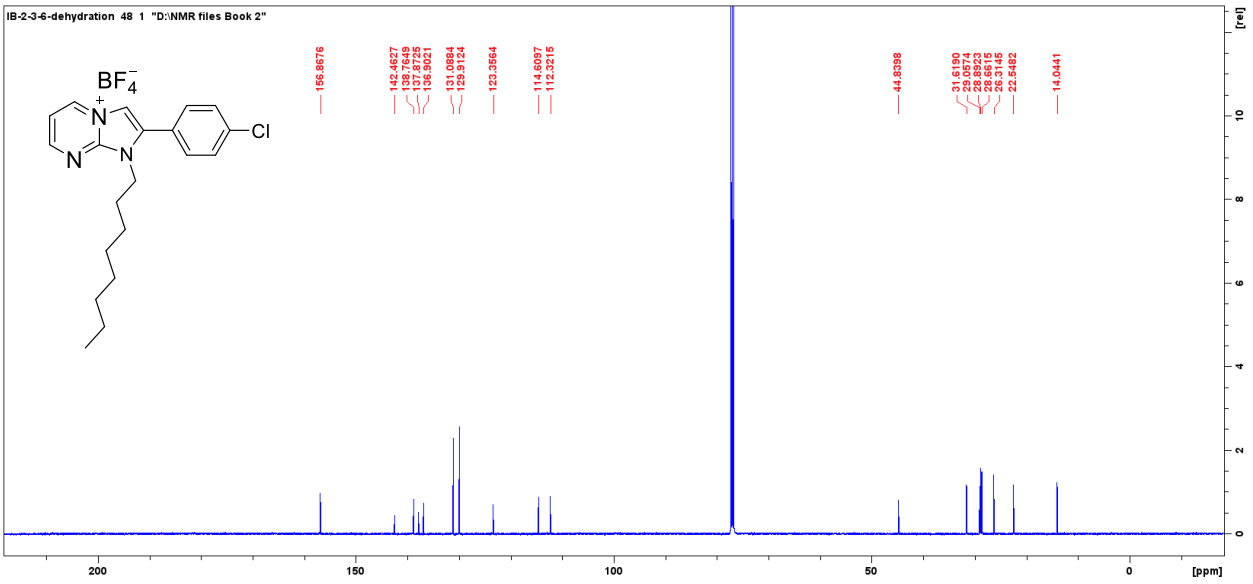

Figure 3.3.29 B: ^{13}C NMR Spectra of 2-(4-chlorophenyl)-1-octyl-1H-imidazo[1,2-a]pyrimidin-4-ium tetrafluoroborate [6b].

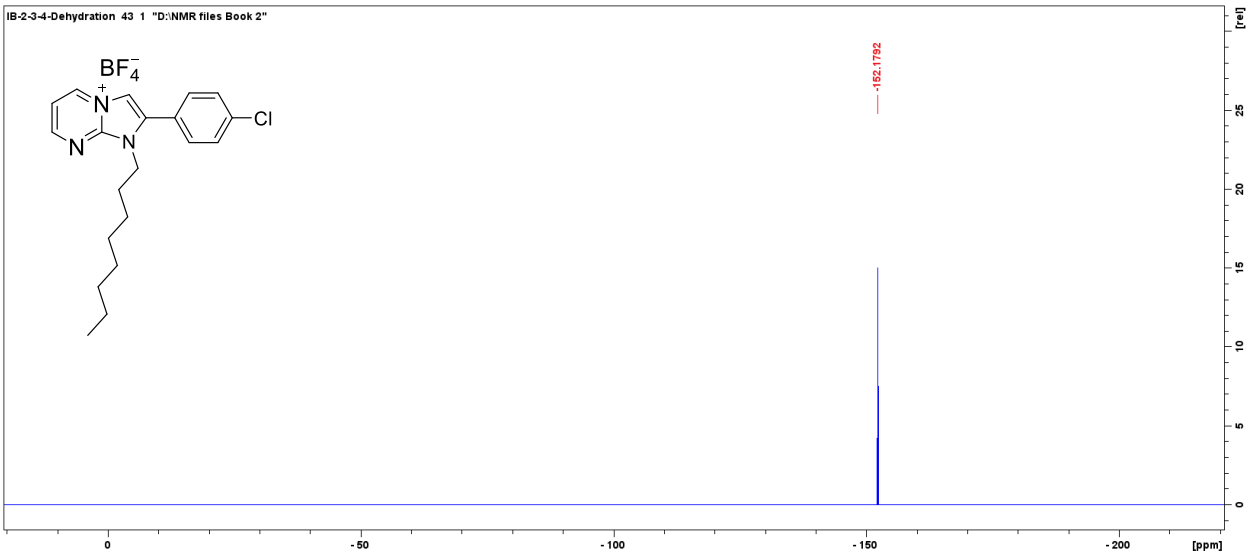

Figure 3.3.30 B: ^{19}F NMR Spectra of 2-(4-chlorophenyl)-1-octyl-1H-imidazo[1,2-a]pyrimidin-4-ium tetrafluoroborate [6b].

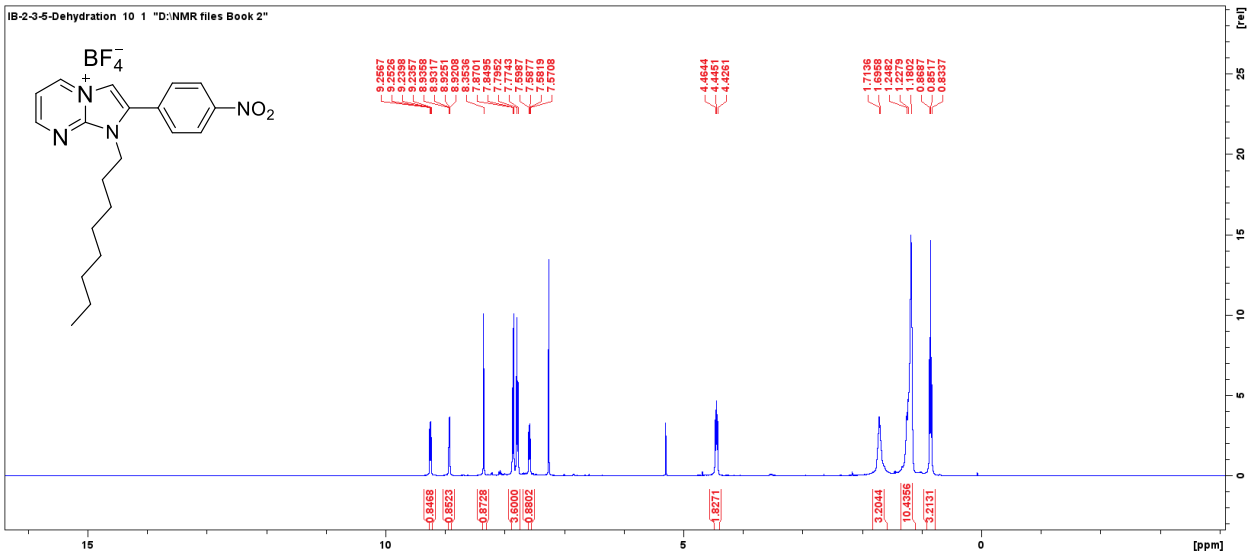

Figure 3.3.31 B: ^{1}H-NMR Spectra of 2-(4-nitrophenyl)-1-octyl-1H-imidazo[1,2-a]pyrimidin-4-ium tetrafluoroborate [6c].

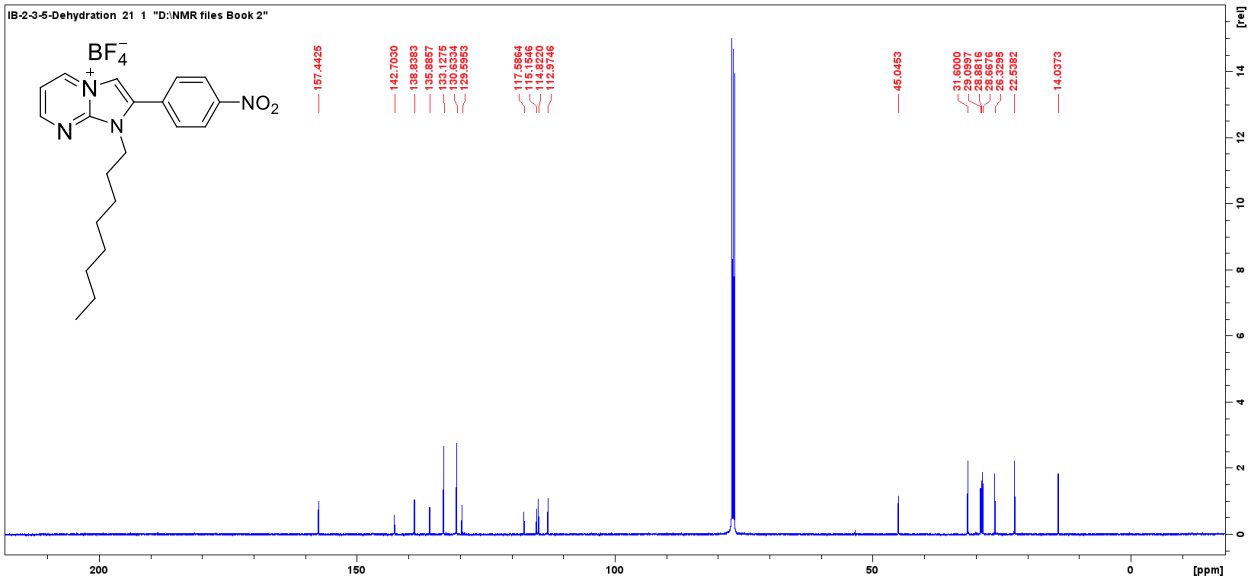

Figure 3.3.32 B: ^{13}C NMR Spectra of 2-(4-nitrophenyl)-1-octyl-1H-imidazo[1,2-a]pyrimidin-4-ium tetrafluoroborate [6c].

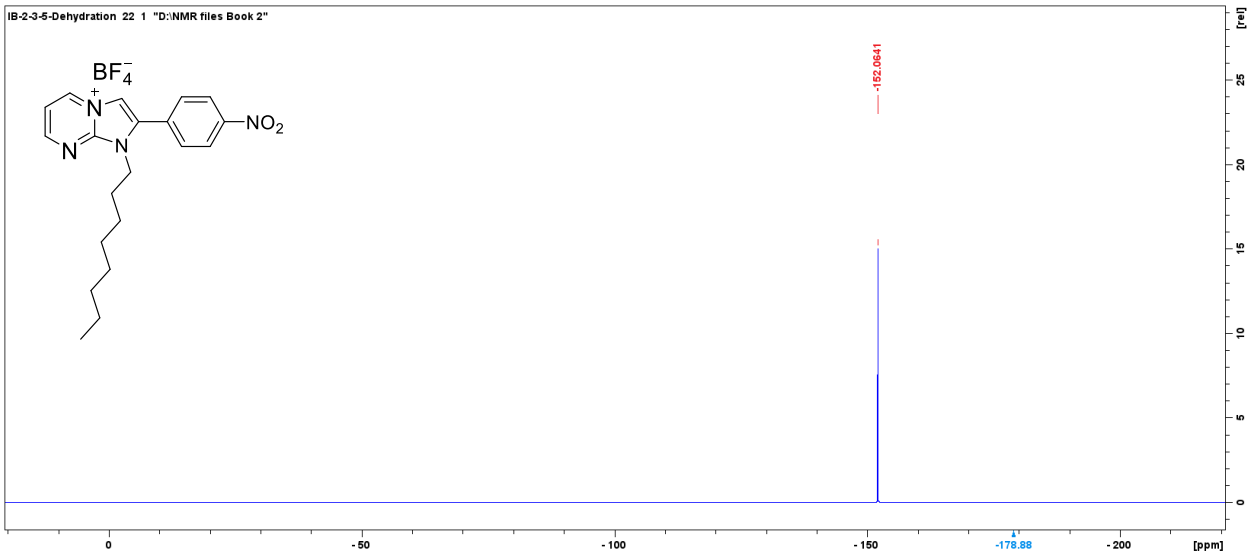

Figure 3.3.33 B: ^{19}F NMR Spectra of 2-(4-nitrophenyl)-1-octyl-1H-imidazo[1,2-a]pyrimidin-4-ium tetrafluoroborate [6c].

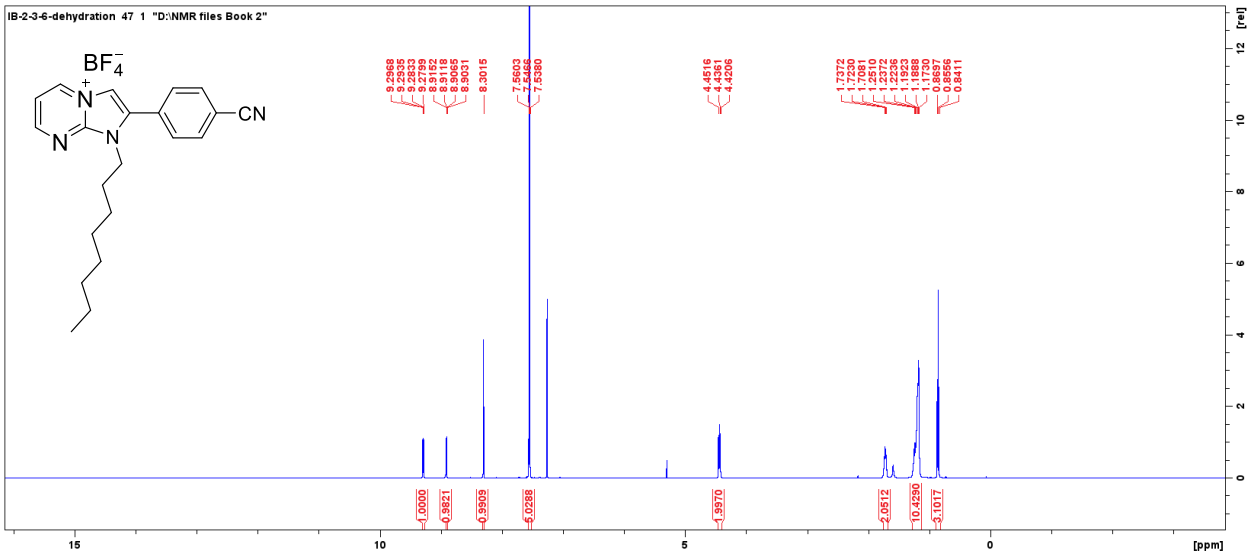

Figure 3.3.34 B: ^{1}H-NMR Spectra of 2-(4-cyanophenyl)-1-octyl-1H-imidazo[1,2-a]pyrimidin-4-ium tetrafluoroborate[6d].

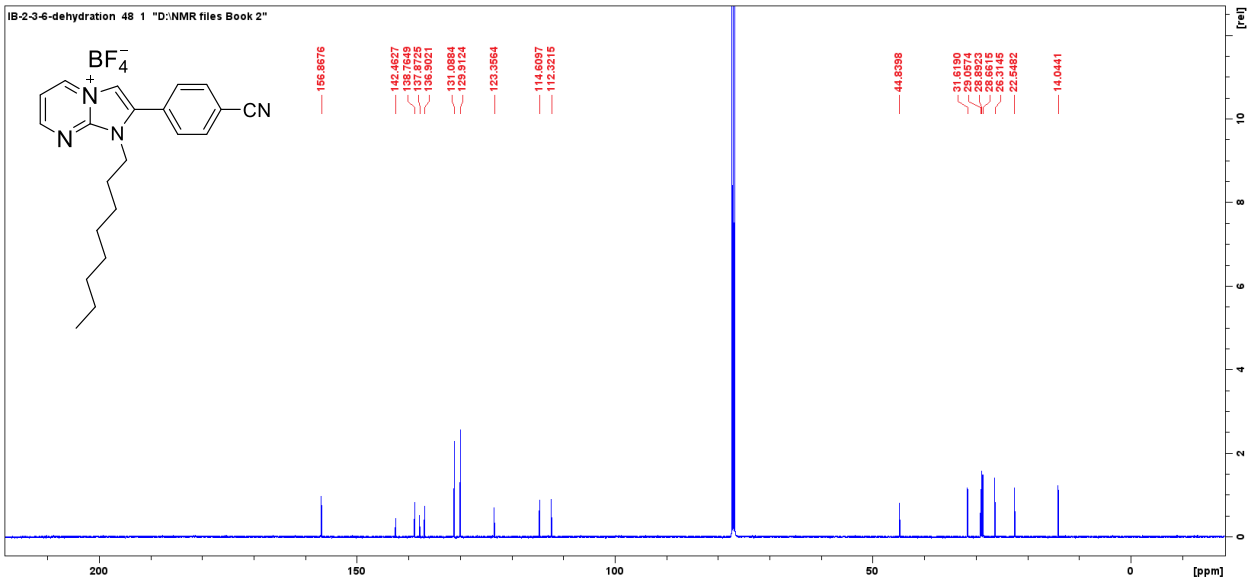

Figure 3.3.35 B: ^{13}C NMR Spectra of 2-(4-cyanophenyl)-1-octyl-1H-imidazo[1,2-a]pyrimidin-4-ium tetrafluoroborate[6d].

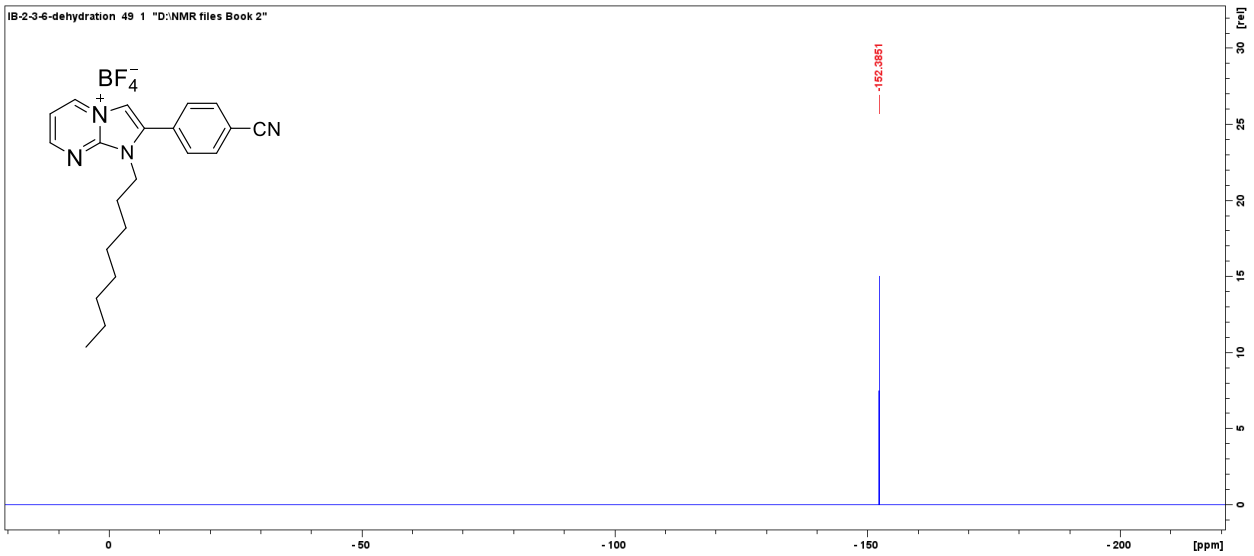

Figure 3.3.36 B: ^{19}F NMR Spectra of 2-(4-cyanophenyl)-1-octyl-1H-imidazo[1,2-a]pyrimidin-4-ium tetrafluoroborate[6d].

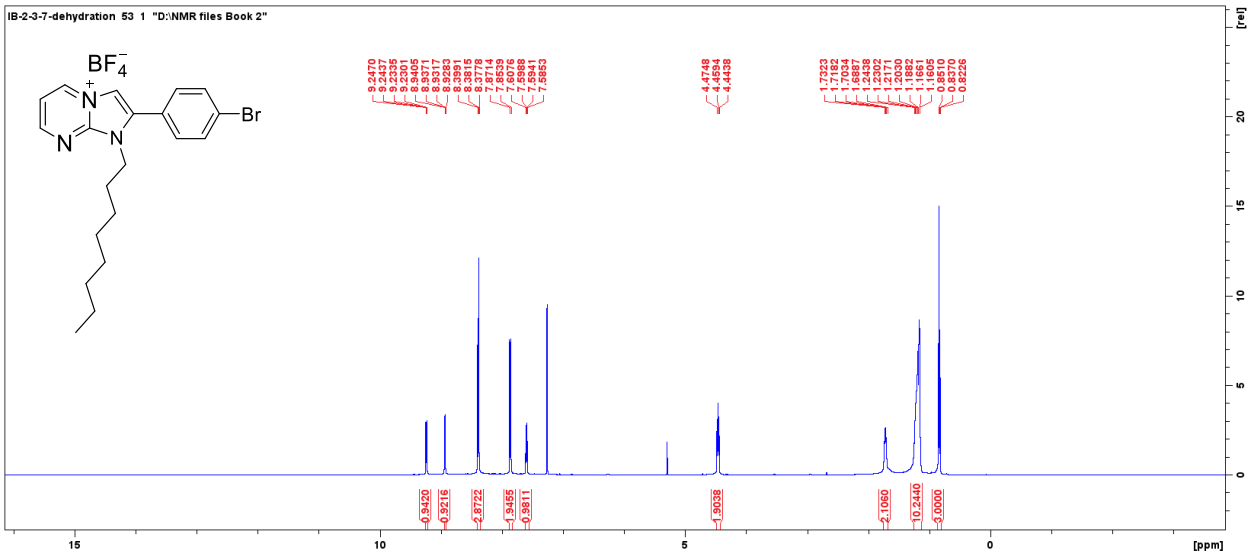

Figure 3.3.37 B: ^{1}H-NMR Spectra of 2-(4-bromophenyl)-1-octyl-1H-imidazo[1,2-a]pyrimidin-4-ium tetrafluoroborate [6e].

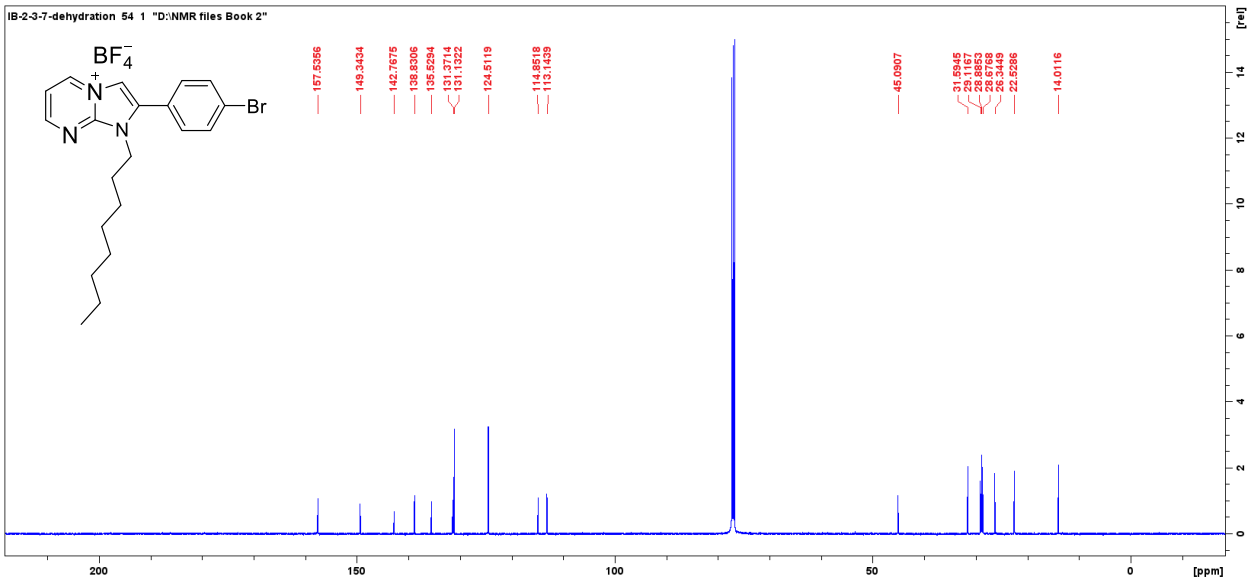

Figure 3.3.38 B: 13C NMR Spectra of 2-(4-bromophenyl)-1-octyl-1H-imidazo[1,2-a]pyrimidin-4-ium tetrafluoroborate [6e].

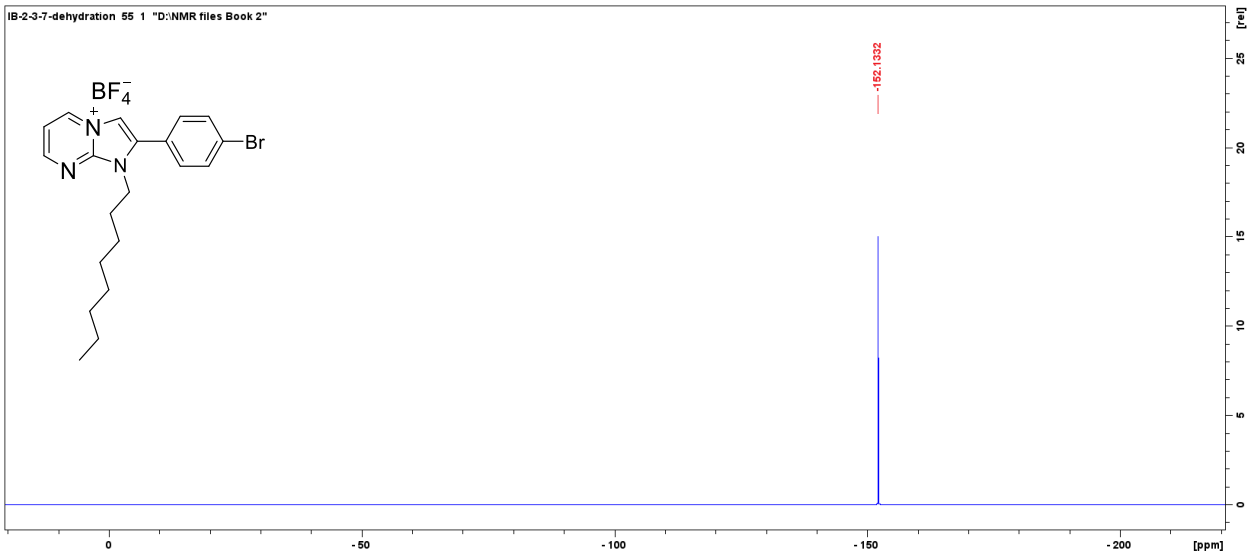

Figure 3.3.39 B: ^{19}F NMR Spectra of 2-(4-bromophenyl)-1-octyl-1H-imidazo[1,2-a]pyrimidin-4-ium tetrafluoroborate [6e].